UNIVERSITY OF SOUTHAMPTON

Faculty of Physical Science and Engineering

Optoelectronics Research Centre

Development of Multi-element Fibres for Applications in Space-Division Multiplexing

by

Saurabh Jain

A thesis submitted for a degree of

Doctor of Philosophy

October 2015

University of Southampton

Abstract

Faculty of Physical Science and Engineering
Optoelectronics Research Centre

Doctor of Philosophy

Development of Multi-element Fibre for Applications in Space-Division Multiplexing

by Saurabh Jain

This thesis presents a novel multi-element fibre (MEF) technology for implementing space-division multiplexing (SDM) in optical fibres. MEF comprises multiple fibre-elements that are drawn and coated together using a common polymer coating. In MEF, the fibre-elements are compatible with current technology i. e. the fibre-elements can be directly fusion spliced to standard single mode pigtail fibre. Thus, a smooth upgrade from WDM based systems to SDM system is possible. In this work, MEF technology has been implemented for both, passive SDM fibres and SDM amplifiers.

Erbium-doped Core-pump MEF amplifiers have been demonstrated exhibiting similar gain and noise figure performance to conventional Er-doped fibre amplifier while maintaining ultralow crosstalk levels. In addition, an Erbium/Ytterbium-doped cladding-pumped MEF amplifier has been developed, and a novel technique to achieve a broadband gain has been demonstrated which could cover wavelength region of 1536nm-1615nm using a single multimode pump. Furthermore, MEF technology has been combined with mode-division multiplexing to show that higher spatial multiplicity could be achieved by implementing the MEF with other SDM technologies.

In passive MEFs, the fabricated fibres have been characterised for their loss and transmission properties, showing low loss and error-free transmission. Also, the MEFs are proof-tested showing high strength. The compatibility of MEF fibres have been tested in a concatenated SDM system demonstrating their flexibility in the telecom network.

Table of Contents

List of Tables

List of Figures

Declaration of Authorship

I, Saurabh Jain, declare that thesis entitled, “Multi-Element Fibres for Applications in Space-Division Multiplexing” and the work presented in this thesis are my own. I confirm that:

1. This work was done wholly or mainly while in candidature for a research degree at this University;

2. Where any part of this thesis has previously been submitted for a degree or any other qualification at this University or any other institution, this has been clearly stated;

3. Where I have consulted the published work of others, this is always clearly attributed;

4. Where I have quoted from the work of others, the source is always given. With the exception of such quotations, this thesis is entirely my own work;

5. I have acknowledged all main sources of help;

6. Where the thesis is based on work done by myself jointly with others, I have made clear exactly what was done by others and what I have contributed myself;

7. Parts of this work has been published in journal articles and conference proceedings reported in the List of Publications

Signed: Saurabh Jain

Date: October 2015

Acknowledgements

Firstly, I would like to express my sincere gratitude to my advisor Prof. Jayanta Sahu for the continuous support of my Ph.D study and related research, for his patience, motivation, and support. His guidance helped me in all the time of research and writing of this thesis. Special thanks to Dr. Timothy May-Smith for his providing me a constant helping hand throughout my PhD. I would also like extend sincere thanks to Silica Group members especially Dr. Pranabesh Barua, Rob Standish and Naresh Thipparapu for their help on many occasions.

I thank my fellow lab mates and friends, in particular Dr. Victor Rancano and Reza Sandoghchi for sharing their expertise, testing my fibres and providing me with good advices from time-to-time. I wish to thank Dr. Yongmin Jung for sharing his expertise in multimode amplifier, and Dr. Ming Ding, Rand Ismaeel and Imran Khudus for tapering the pump fibres on numerous occasions.

I am also thankful to the ORC administration staff for providing their outstanding support. I thank EPSRC sponsors for giving me the opportunity to study at ORC and gain invaluable experience. I also wish to thank the collaborators at LPMC, Prof. Mourad Benabedesslam and Dr. Mady Franck for their hospitality, guidance and expertise during the visit for TSL measurements.

Finally, thanks to all my friends at ORC and outside who supported and encouraged me through the years. Without their precious support it would not have been possible to conduct this research.

Last but not the least, I would like to thank my family: my parents and to my brother and sister for supporting me throughout PhD, writing this thesis and my life in general.

Abbreviations

Abbreviation	Meaning
WDM	Wavelength division multiplexing
SSMF	Single mode fibres
C-band	Conventional band
L-band	Long band
SDM	Space-division multiplexing
Er	Erbium
ROADM	Reconfigurable optical add drop multiplexer
MCF	Multicore Fibre
MMF	Multimode Fibre
MEF	Multi-element Fibre
MIMO	Multiple-input-multiple-output
FMF	Few-mode Fibre
DMGD	Differential mode group delay
MDL	Mode dependent loss
DMG	Differential mode gain
OAM	Orbital angular momentum
CC-MCF	Coupled core multicore fibre
TMC	Tapered multicore connector
ME-EDFA	Multi-element Erbium doped fibre amplifiers
ME-EYDFA	Multi-element Erbium/Ytterbium doped fibre amplifiers
MEFA	Multi-element Fibre Amplifier
Bi	Bismuth
GWL	Glass working lathe
MCVD	Modified chemical vapour deposition
OSA	Optical Spectrum Analyser
TLS	Tuneable laser source
NF	Noise figure
ASE	Amplified spontaneous emission
MEFA	Multi-element fibre amplifier
LD	Laser diode
RIP	Refractive index profile
3M-MEFA	3-moded multi-element fibre amplifier
3MF	3-moded fibre
CCD	Charged coupled device
OSNR	Optical signal to noise ratio
CFQ	Clear fused quartz
NA	Numerical aperture
Ge	Germanium
OTDR	Optical time domain reflectometer
XCT	X-ray coherence tomographic
OOK	On/Off Keying
BPSK	Binary Phase-Shift Keying
QPSK	Quadrature Phase-Shift Keying
DCF	Dispersion compensating fibre
BER	Bit-error rate
MVOA	Manual variable optical attenuator
OCT	Optical coherence tomography
P	Phosphorous

List of Publications

Journals

[1] N. K. Thipparapu, **S. Jain**, A. A. Umnikov, P. Barua, and J. K. Sahu, "1120nm diode-pumped Bi-doped fiber amplifier," Opt. Lett., **40**(10), 2441-2444, (2015)

[2] **S. Jain**, N. K. Thipparapu, P. Barua, and J. K. Sahu, "Cladding-Pumped Er/Yb-Doped Multi-Element Fiber Amplifier for Wideband Applications," IEEE Photonics Technology Letters, 27 (4), 356 - 358 (2015)

[3] S. Torrengo,* M.C. Paul, A. Halder, S. Das, A. Dhar, J.K. Sahu, **S. Jain**, and A.V. Kir'yanov, and F. d'Acapito, "EXAFS studies of the local structures of Bismuth centers in multicomponent silica glass based optical fiber preforms," Journal of Non-Crystalline Solids, 410, 82-87 (2015)

[4] V. J. F. Rancaño, **S. Jain**, T. C May-Smith, E. Hugues-Salas, S. Yan, G. Zervas, D. Simeonidou, P. Petropoulos and D. J. Richardson "Demonstration of Space-to-Wavelength Conversion in SDM Networks," IEEE Photonics Technology Letters, **27**(8), 828-831, (2015)

[5] S. R. Sandoghchi, G. T. Jasion, N. V. Wheeler, **S. Jain**, Z. Lian, J. P. Wooler, R. P. Boardman, N. Baddela, Y. Chen, J. Hayes, E. Numkam Fokoua, T. Bradley, D. R. Gray, S. M. Mousavi, M. Petrovich, F. Poletti, and D. J. Richardson, "X-ray tomography for structural analysis of microstructured and multimaterial optical fibers and preforms," Opt Express, 22 (21), 26181-26192, (2014)

[6] **S. Jain**, Y. Jung, T. C. May-Smith, S. U. Alam, J. K. Sahu, and D. J. Richardson, "Few-mode multi-element fiber amplifier for mode division multiplexing," Optics Express, 22(23), 29031-29036, (2014)

[7] S. Yan, E. Hugues-Salas, V. J. F. Rancaňo, Y. Shu, G. M. Saridis, B. R. Rofoee, Y. Yan, A. Peters, **S. Jain**, T. May-Smith, P. Petropoulos, D. J. Richardson, G. Zervas, and D. Simeonidou, "Archon: A Function Programmable Optical Interconnect Architecture for Transparent Intra and Inter Data Center SDM/TDM/WDM Networking," Journal of Lightwave Technology, **33**(8), 1586 - 1595, (2015)

[8] N. K. Thipparapu, **S. Jain**, T. C. May-Smith, and J. K. Sahu, "Wideband multi-element Er-doped fiber amplifier," Laser Physics Letters, 11(9), 095104, (2014)

[9] **S. Jain**, J. B. Duchez, Y. Mebrouk, M. M. A. N. Velazquez, F. Mady, B. Dussardier, M. Benabdesselam, and J. K. Sahu, "Thermally-stimulated emission analysis of Bismuth-doped Silica fibers," Optical Materials Express, 4(7), 1361-1366, (2014)

[10] **S. Jain**, V. J. F. Rancaño, T. C. May-Smith, P. Petropoulos, J. K. Sahu, and D. J. Richardson, "Multi-element fiber for space-division multiplexing operations," Optics Express, 22(4), pp.3787-3796, (2014)

[11] **S. Jain**, T. C. May-Smith, A. Dhar, A. S. Webb, M. Belal, D. J. Richardson, J. K. Sahu, and D. N. Payne, "Erbium-doped multi-element fiber amplifier for space-division multiplexing operations," Optics Letters, 38(4), 582-584, (2013)

Conference

[1] N. K. Thipparapu, **S. Jain**, A. A. Umnikov, P. Barua, and J. K. Sahu, "1180nm Bi-doped aluminosilicate fiber amplifier," in European Conf. on Lasers and Electro-Optics (CLEO-Europe), CJ_P_33, (2015)

[2] **S. Jain**, N. K. Thipprapu, P. Barua, and J. K. Sahu, "Multi-element fiber for next generation optical communication," ICP, Kuala lumpur, D2-PM1-R1, (2014) (Invited)

[3] S. Yan, E. Hugues-Salas, V. J. F. Rancano, S. Yi, G. Saridis, B. Rofoee, Y. Yan, A. Peters, **S. Jain**, T. May-Smith, P. Petropoulos, D. J. Richardson, G. Zervas, and D. Simeonidou, "First Demonstration of All-Optical Programmable SDM/TDM Intra Data Centre and WDM Inter-DCN Communication," in ECOC, PD.1.2, (2014)

[4] Y. Feng, J. Nilsson, **S. Jain**, T. C. May-Smith, J. Sahu, F. Jia, D. Wilson, M. Lengden, and W. Johnstone, "LD-seeded thulium-doped fibre amplifier for CO2 measurements at 2 μm," 6th Europhoton Conference (EPS-QEOD) Neuchâtel, Switzerland 24-29 Aug, TuP-T1-P-12, (2014)

[5] Y. Jung, **S. Jain**, T. May-Smith, J. Sahu, S-U. Alam, and D. J. Richardson, "Few-mode multi-element fiber amplifier for mode division multiplexing," European Conference on Optical Communications (ECOC), Cannes 21-25 Sep, Tu.3.4.4, (2014)

[6] N. K. Thipparapu, **S. Jain**, T. C. May-Smith, J. K. Sahu, "Configurable Er-doped core-pumped multi-element fiber amplifier," OECC/ACOFT '14 Melbourne 6-10 Jul, (2014)

[7] V. J. F. Rancaño, **S. Jain**, T. C. May-Smith, J. K. Sahu, P. Petropoulos, and D. J. Richardson, "Multi-Element Fiber Technology for High-Capacity Optical Communication Systems," Advanced Photonics Conference Barcelona, Spain 27-31 Jul, SoW2B.1, (2014)

[8] V. J. F. Rancaño, **S. Jain**, T. C. May-Smith, J. K. Sahu, P. Petropoulos, and D. J. Richardson, "Space Division Multiplexing using Multi-Element Fibers," IEEE Summer Topicals Montréal, Canada 14-16 Jul, (2014)

[9] **S. Jain**, V. J. F. Rancaño, T. C. May-Smith, P. Petropoulos, J. K. Sahu, and D. J. Richardson, "Multi-Element Fiber for Space-Division Multiplexed Optical Communication system," International Conference on Transparent Optical Networks Graz, Austria 6-10 Jul, Th.A2.5, (2014)

[10] J. K. Sahu, **S. Jain**, D. Jain, N. K. Thipparapu, and T. C. May-Smith, "Novel geometry fibres for use in optical communications and high power lasers," Sixth International Conference on Optical, Optoelectronic and Photonic Materials and Applications (ICOOPMA '14) Leeds 27-31 Jul, (2014) (Invited)

[11] J. K. Sahu, D. Jain, **S. Jain**, T. C. May-Smith, and C. Baskiotis, "Novel optical fibers for telecommunications and high-power laser applications," International Conference on Optics and Optoelectronics, IT-LAA-04 Dehradun, India 3-8 Mar, (2014) (Invited)

[12] J. K. Sahu, **S. Jain**, V. J. F. Rancaño, T. C. May-Smith, A. Webb, P. Petropoulos, and D. J. Richardson, "Multi-element fiber for space-division multiplexing," SPIE Photonics West San Francisco 1-6 Feb, 9009, (2014) (Invited)

[13] **S. Jain**, T. C. May-Smith, and J. K .Sahu, "Cladding-pumped Er/Yb-doped Multi-Element Fiber Amplifier for C+L band Operations," Optical Fiber Communications (OFC) San Francisco 9-13 Mar, M2J.3, (2014)

[14] **S. Jain**, T.C.May-Smith, J.K.Sahu, "Cladding-pumped Er/Yb-doped multi-element fiber amplifier," in Workshop on Speciality Optical Fibers and their Applications (WSOF 2013) Sigtuna, Sweden 28-30 Aug, 5.4, (2013)

[15] **S. Jain**, T. C. May-Smith, V. J. F. Rancaño, P. Petropoulos, D. J. Richardson, and J. K. Sahu, "Multi-element fibre for space-division multiplexed transmission, " in European Conference on Optical Communications, London 22-26 Sep, Mo.4.A.2, (2013)

[16] V. J. F. Rancaño, **S. Jain**, T. C. May-Smith, J. K. Sahu, P. Petropoulos, and D. J. Richardson, "First demonstration of an amplified transmission line based on multi-element fibre technology," in European Conference on Optical Communications, London 22-26 Sep, PD1.C.2, (2013) (Postdeadline)

[17] **S. Jain**, T. C. May-Smith, A. Dhar, A. Webb, B. Usmani, and J. K. Sahu, "Gain and noise figure study of Er-doped multi-element fiber amplifier," in Asia Comunications and Photonics Conference (ACP) Guangzhou, China 7-10 November, ATh2A.1, (2012).

Chapter-1

Introduction

1.1. Historical Perspective

Silica fibres have been the best possible means available for long distance communication to-date due to their advantages such as low scattering loss, ease of fabrication and robustness. The development of fibre optical technology experienced a phenomenal growth during the second half of the 20th century. In 1966, Charles Kao and Charles Hockham proposed that optical fibres might become a suitable communication media provided the loss was reduced below 20dB/km [1, 2]. At that time, the best bulk optical glass had a loss of about 1000dB/km. The loss was mainly due to the impurities in the glass. A few years later, an optical fibre with attenuation <20dB/km was developed by Corning glass works [3]. The fact that the advances in fibre fabrication technology were complemented by the development of lasers led to a remarkable growth of fibre-optic communications. Fig 1.1 shows the reduction of losses in silica fibres over the years. Following the development in fibre fabrication, fibre based communication was commercially implemented in 1975. Subsequently, several generations of fibre optical communication systems were deployed, and these

are briefly reviewed in the following.

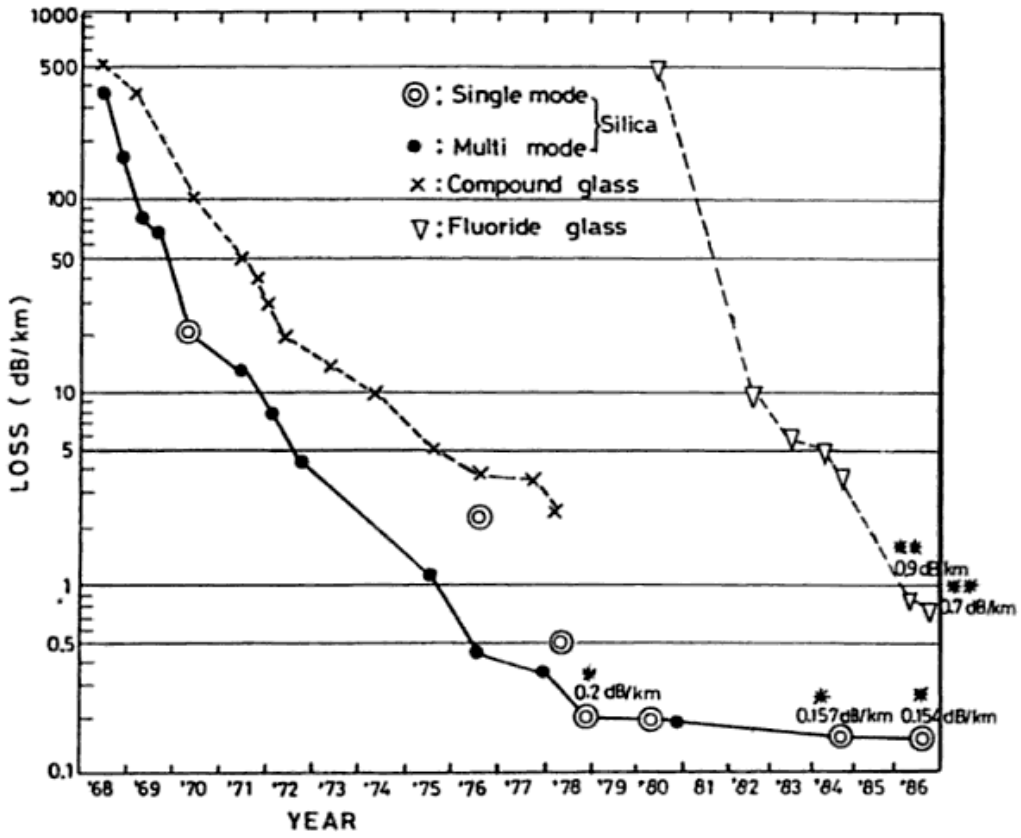

Fig. 1.1 Reduction in the loss of optical fibre during the development years. (losses at 1550nm, ** loss at 2550nm) [4]*

1st Generation Systems

The first generation fibre-optic communications system operated around 850nm due to the availability of compact GaAs semiconductor lasers, which were suitable for long distance transmission [5, 6]. It used multimode fibres. These systems operated at a bit rate of the order of few Mbit/s with a repeater spacing up to 10km. This window was initially used due to the availability of low cost detectors and already optimised emitters, despite the attenuation being about 3dB/km. These systems became commercially available in 1980.

2nd Generation Systems

In the early 1980s, the 2nd generation fibre-optics communication systems were commercially developed. These systems operated around a wavelength of 1300nm, and used InGaAsP semiconductor lasers and detectors. The shift to this window was due to the fact the silica fibre losses at 1300nm were below 1dB/km, which could allow a considerable increase in the repeater spacing. Furthermore, the optical fibre had minimum dispersion in this wavelength region. Despite these advantages, the lack of

an efficient semiconductor laser and detector prevented an early shift to 2nd generation systems. The bit rate was of the order of few 100 Mbit/s which saw another leap when multimode fibres were replaced with single mode fibres to prevent intermodal dispersion. By 1987, systems were commercially available operating at a bit rate of 1.7 Gbit/s and with a repeater spacing up to 50km [7].

3rd Generation Systems

The shift to 3rd generation fibre-communication systems was spurred by the discovery of InGaAs diodes. These lasers operated around a wavelength of 1550nm, where the fibre attenuation was 0.2dB/km, a loss value achieved in 1979. By 1992, commercial systems based on this technology were operating at a bit rate of 2.5Gbit/s with repeater spacing >100km. There was a rather long delay in the shift from 2nd to 3rd generation systems. Firstly, conventional InGaAsP lasers could not be used at 1550nm due to multiple longitudinal wavelength at 1550nm and dispersion-induced pulse broadening of the signal [6]. This was mitigated by using dispersion shifted fibres and the development of InGaAs sources.

4th Generation Systems

The 4th generation fibre-optic system used wavelength division multiplexing (WDM) to further increase the data capacity and high-bandwidth optical amplifiers instead of opto-electrical repeaters. This allowed signal transmission without digital regeneration after every 70-80km. The optical amplifiers, optimised for operation in the 1530nm-1565nm band were developed after 1985. In 1991, an experiment showed data transmission over 21,000 km at a rate of 2.5Gbit/s. This demonstrated the possibility of intercontinental communication through optical amplifiers without the need for expensive optical/electrical/optical signal conversions. In the late 1990s through 2000, the use of internet increased substantially, which led to demand for cables that could handle high data capacities in a cost-effective manner. The copper-wires were replaced then with their inexpensive fibre-optic counterparts, allowing e.g. the cost of phone calls to drop significantly. These two developments, WDM and optical amplifier implementation, revolutionised the fibre-optic communications industry, and resulted in a doubling of the capacity every 6 months from 1992 till 2001 when bit rate reached 10Tbit/s.

1.2. Economics and Rise of Internet

One of the reasons for the astonishing growth of commercial telecom systems in the late 1990s was a drastic rise in internet traffic also referred to as dotcom boom. This led to over investment and spending in the infrastructure intensive telecommunication development. The investors were looking to capture the market due to the speculation of very high demand, which would result in significant revenue generation for them. However, when the dotcom bubble burst it became clear that the predicted explosion in demand would not happen, and the stocks of telecom companies dropped and the investment reduced (see fig.1.2) [8]. The increase in the demand over that period could have easily been accommodated with the existing technologies. Nevertheless, the industry saw monotonous increases in demand and revenue generation [9].

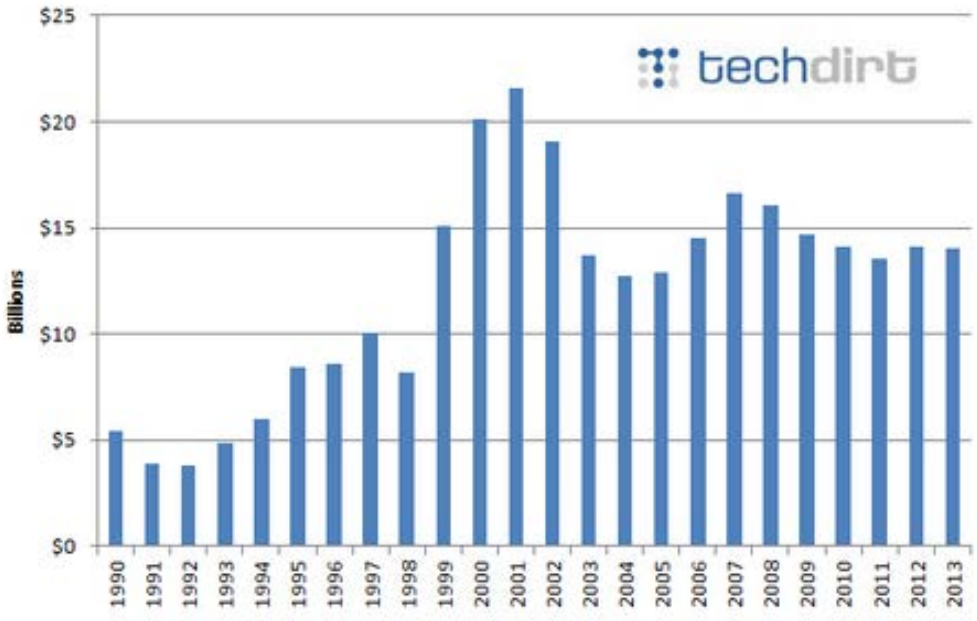

Fig. 1.2 Investment in telecom market development [8]

The demand for communication technology has picked up in speed in recent years as the internet has penetrated into the lives of the common public. This is associated with the advent of social networking, video streaming, cloud storage, and the 'internet of things'. Also, there are numerous internet based user applications ranging from online gaming to e-shopping and e-governance. Today, YouTube has more than 100hrs of video uploaded every minute. These social websites provide a massive platform for entrepreneurs to obtain better customer reach. There has also been drastic increase in

the number of internet users and websites [10].

1.3. Capacity Crunch in Telecommunications

The capacity increase of the optical fibre has increased by a factor of 10 every 4 years (see Fig. 1.3) [11-14].

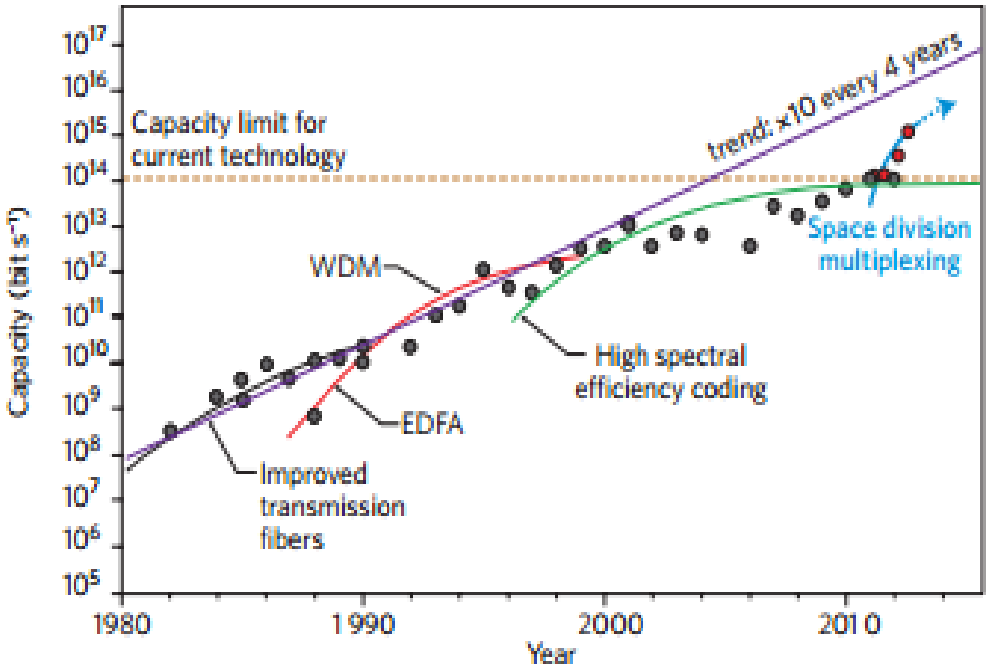

Fig. 1.3 Evolution of the transmission capacity of the optical fibre (the dots represent the highest reported capacity in their time, and red dots correspond to the recent SDM demonstrations). [11]

Figure 1.4 shows the possible physical dimensions in which the information can be multiplexed to maximise the capacity for a given transmission medium and operation bandwidth. Alike every other resource, current single mode optical fibre (SSMF) systems also has its limit to the extent it can serve the communication needs. The physical dimensions; frequency, polarisation, quadrature, and time along with efficient coding, have already been explored nearly to their limit in single mode optical fibre systems. As shown in Fig. 1.3, the capacity limit of current SSMF based systems is about 100Tbit/s The industry is just a factor of 6 behind the single-mode capacity limit whereas research is behind by a factor of 2 [15]. The available bandwidth of existing systems is predicted to be exhausted by 2020 due the rapid increase in internet traffic [15]. Hence, there is an urgent need for new innovations in fibre-optic technology to allow for even higher communication capacities. Space is the only dimension that is left to be exploited in fibre-optics communication systems.

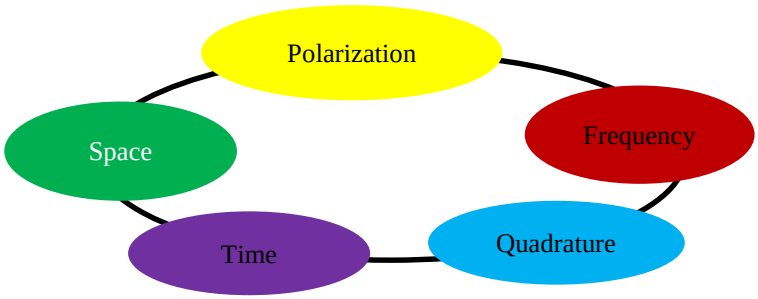

Fig. 1.4 Physical dimensions in optical fibres that are available for multiplexing information.

1.4. Handling the Future Capacity Crunch

Several approaches have been proposed to overcome the potential crisis. There have been mainly two popular approaches, (1) bandwidth expansion and (2) space-division multiplexing (SDM) in optical fibres.

The bandwidth expansion can be achieved by exploring new operating bands. The operation of current optical fibre based telecom systems is mostly limited to the C-band. The C-band covers the wavelength range of 1530-1565nm in the 3rd telecommunication window of silica fibres. However, the Erbium (Er)-doped fibre amplifier is the limiting factor when it comes to the available bandwidth. It serves as an optical amplifier to boost the optical signal, which decays over larger lengths due to intrinsic losses such as Rayleigh scattering. This narrow bandwidth of the C-band amplifiers limits the usable band in SSMF based communication systems. Though, Er has the potential to amplify in the region of 1500-1620nm, covering both the C and L (Long) band [16]. However, it has maximum gain efficiency in the C-band. Amplifiers for the L-band require long gain fibre lengths and have low gain efficiency. There has also been significant efforts to develop amplifiers for other low loss windows in silica fibres [6]. Thulium-doped fibre and Bi-doped fibre for the 1700-2100nm and 1150nm-1500nm wavelength bands, respectively, have been intensively investigated with the aim of developing fibre amplifiers [17-18]. The silica loss increases significantly above 2μm and is not preferred for transmission applications. On the other hand, hollow core fibres, also referred to as holey core fibres, have been investigated for the transmission at a wavelength around 2μm. Holey core fibre has a theoretical loss lower than that of silica at 2μm [17]. Raman amplifiers for amplification in wavelength bands shorter than the C-band have also been studied. However, these unconventional

amplifier still require further research to enable broadband communication.

The other approach, SDM, has received significant research attention. It aims to efficiently use the last available physical dimension, space. Whilst this dimension could in principle be explored by installing more parallel SMF systems, the economy of this approach is not favourable. In parallel SMF systems, the cost per additional bit added will essentially be fixed once optimal spectral-efficiency transmitters and receivers are commercially deployed. Such a scenario is not desirable for network operators, who have experienced a historical trend of both cost-per-bit reductions and capacity increases by upgrading terminal equipment to more efficient and exploit the bandwidth of deployed SMF fibres. On the other hand, SDM [11-13] has emerged as a possible route to significantly increase per-fibre capacity and to reduce the associated cost-per-bit. This would be achieved through the potential for device integration and sharing of expensive components, such as optical amplifiers and reconfigurable optical add drop multiplexers (ROADMs). For example, a cladding-pump SDM amplifier provides an additional advantage of pump sharing. This could potentially result in reduction of the operational cost of the amplifiers. The bulk of research on SDM has so far been focused on either multicore fiber (MCF) or multimode fibre (MMF), resulting in impressive demonstrations of capacity increases [11]. However, both MCF and MMF require that additional components to couple/decouple the spatial channels into these fibres be developed for their implementation in commercial systems. In the current state, lack of availability of these components reduces the advantages of cost optimisation that SDM technology could provide in next generation telecommunication system. Moreover, without the development of these MUX/DEMUX component these technologies are limited to transatlantic transmission networks at best. The deployment of the fibre cables for terrestrial networks is carried out by deploying short lengths (4-5km) and connecting them through established splicing programs. A connector with high crosstalk and/or loss could lead to decrease in the span length. While the main application of SDM is in long haul transmission scenarios, it also attracts significant interest in data centres where it could reduce the network complexity.

1.5. Outline of Thesis

The main objective of the thesis is to develop a novel technology of multi-element fibres (MEFs) for implementing SDM in optical fibres. MEFs consist of multiple individual fibre-elements with reduced cladding diameter that are drawn and coated together in a common polymer coating. The use of this technology has been studied for the development of passive as well active fibres. In the thesis, development of MEFs for both core-pumped and cladding-pump amplifiers has been discussed. These amplifiers have also been characterised for their gain and NF performance. The advantages MEF based system has been demonstrated over their MCF and MMF counterpart throughout the work. The fabrication of passive MEFs for transmission networks have also been discussed in detail. These passive MEFs have also been characterised and tested along with MEF amplifier for their performance in transmission networks. It should be noted that the aim of MEFs is in direct coherence with the commercial industry targets. The commercial fibre optical industry is trying to maximise the use of current infrastructure capabilities by efficiently using the space in optical fibre cable and provide an economically positive outlook towards accommodating the future capacity trends [19]. In that context, today the optical fibres with coated diameter of 200μm are commercially available as compared to the conventional 250μm optical fibre and efforts towards further reduction are in progress [19, 20]. Development of passive MEFs aim towards further miniaturisation of the optical fibre cables in which the polymer coating could be shared between multiple spatial channels. It is shown that with the implementation of MEFs, the flexibility of the SSMF systems is not compromised. In MEFs, unlike in MCF and MMF, the advantage of developing the optical cables with reduced diameter is that it would not incur an additional cost for the development of current networks and training of operators.

Chapter 2 discusses the various methods aimed towards meeting the exponential data capacity demand in an economically viable scenario. A review of MCF and MMF based SDM methods has been performed. Section 2.3 introduces our technique Multi-element Fibre (MEF), an approach used in this thesis for increasing the density of the cables in the network.

Chapter 3 provides introduction of MEF, and the general fibre fabrication procedure.

The MEF fabrication procedure is discussed in section 3.2. Section 3.3 describes the demonstration of Er-doped core-pump 3-MEF and 7-MEF, and sections 3.4 provide the result of MEF amplifier with different element diameter and fabrication conditions. Section 3.5 presents the novel cascading scheme in SDM amplifier to provide the flexibility in terms of gain profiling and bandwidth tuning. The work presented in this chapter has been published in ref. [21-24].

In Chapter 4, Section 4.1 introduces the MEF based cladding-pump Er-Yb doped fibre amplifier. Section 4.2 discusses the fabrication steps and basic measurements on the preform and the fibre. Section 4.4 illustrates the results of the C-band SDM amplifier. The amplifier performance characterisation based on MEF length is also covered. The novel cascading configuration of different elements in MEF to obtain a broadband gain has been demonstrated along with performance variation with different cascading combination. Section 4.5 demonstrates the first cladding-pump few mode multi-element amplifier which incorporates two of the SDM technologies, FMF and MEF, to obtain a spatial multiplicity of 12. The results in this chapter have been published in ref. [25-30].

The details of development of passive MEFs is presented in Chapter 5. In Section 5.2, modifications in MEF fabrication procedure for passive MEF have been described, and the advantages of new process have been explained. Section 5.3 presents the characterisation of background loss, mechanical strength and transmission performance of passive MEFs. Section 5.3.3 describe the performance of passive MEFs and cladding-pumped MEF amplifier in SDM system. The work reported in this chapter led to the publications of refs. [25], [31-34].

Chapter 6 concludes the PhD work, and briefly discusses the direction of the future work.

References:

[1] K. C. Kao and G. A. Hockham, "Dielectric-fibre surface waveguide for optical frequencies," Proc. IEE, **113**(7), 1151-1158, (1966)

[2] C. K. Kao, "Sand from centuries past: Send future voices fast," Rev. Mod. Phys. 82, 2299–2303 (2010)

[3] "Milestones: world's first low-loss optical fiber for telecommunications," IEEE Global history networks, http://www.ieeeghn.org/wiki/index.php/Milestones:World's_First_Low-Loss_Optical_Fiber_for_Telecommunications

[4] H. Murata, in Handbook of optical fibers and cables, 2nd Edition, Marcel Dekker Inc. (1996)

[5] "Fiber optics", IEEE Global history networks, http://www.ieeeghn.org/wiki/index.php/Fiber_Optics

[6] "Optical fibers and Systems," International Telecommunication Union, http://www.itu.int/dms_pub/itu-t/opb/hdb/T-HDB-OUT.10-2009-1-PDF-E.pdf

[7] G. P. Agrawal, in Fiber-optic communication systems, 3rd Edition, John Wiley & Sons Inc. Publication, (2002) ISBN: 0-471-22114-7

[8] "M. Masnick, "Cable Industry's Own Numbers Show General Decline In Investment Over Past Seven Years," Techdirt, May 2014 https://www.techdirt.com/articles/20140514/06500227230/cable-industrys-own-numbers-show-general-decline-investment-over-past-seven-years.shtml

[9] "Beyond the bubble", The Economist, 2003, http://www.economist.com/node/2098913

[10] "Internet live stats," http://www.internetlivestats.com/internet-users/

[11] D. J. Richardson, J. M. Fini, O. E. Nelson, "Space-division multiplexing in optical fibers," Nature Photonics, 7, 354–362 (2013)

[12] P. Winzer, "Modulation and multiplexing in optical communication systems," IEEE LEOS Newsletter 23, 4 (2009).

[13] Guifang Li and Xiang Liu,"Focused Issue: space multiplexed optical transmission", Optics Express 19, 16754-16575(2011)

[14] R. J. Essiambre, G. Kramer, P. J. Winzer, G. J. Foschini, and B. Goebel, "Capacity limits of optical fiber networks," J. Lightwave Technol., 28(4), 662–701, (2010)

[15] R. J. Essiambre, "The capacity limit of single-mode fibers and technologies enabling high capacities in multimode and multicore fibers," in III WCOM, 28th May 2014.

[16] W. J. Miniscalco, "Optical and electronic properties of rare earth ions in glasses," in Rare-earth-doped fiber lasers and amplifiers, ed. M. J. F. Digonnet, Marcel Dekker Inc., 2001

[17] M. N. Petrovich, F. Poletti, J. P. Wooler, A. M. Heidt, N. K. Baddela, Z. Li1, D. R. Gray, R. Slavík, F. Parmigiani, N. V. Wheeler, J. R. Hayes, E. N. Fokoua, L. Grüner-Nielsen, B. Pálsdóttir, R Phelan, B. Kelly, John

O'Carroll, M. Becker, N. MacSuibhne, J. Zhao, F. C. G. Gunning, A. D. Ellis, P. Petropoulos, S. U. Alam, and D. J. Richardson, "Demonstration of amplified data transmission at 2 microns in a low-loss wide bandwidth hollow core photonic bandgap fiber," Opt. Exp., **21**(23), 28559, (2013)

[18] E. M. Dianov, "Bismuth-doped optical fibers: a challenging active medium for near-IR lasers and optical amplifiers," Light Sci. Appl. 1(5), e12 (2012).

[19] V. Diaz, "Miniaturisation and the space races," www.corning.com/WorkArea/downloadasset.aspx?id=64155

[20] K. Nakajima, P. Sillard, D. Richardson, M.-J. Li, R.-J. Essiambre, and S. Matsuo, "Transmission media for an SDM-based optical communication system," IEEE Communication Magazine, **53**(2), 44-51 (2015)

[21] S. Jain, T. C. May-Smith, A. Dhar, A. S. Webb, M. Belal, D. J. Richardson, J. K. Sahu, and D. N. Payne, "Erbium-doped multi-element fiber amplifiers for space-division multiplexing operations," Optics Letters, 38 (4), 582-584 (2013).

[22] S. Jain, T. C. May-Smith, A. Dhar, A. Webb, B. Usmani, and J. K. Sahu, "Gain and noise figure study of Er-doped multi-element fiber amplifier," in Asia Comunications and Photonics Conference (ACP) Guangzhou, China 7-10 November 2012 ATh2A.1

[23] N. K. Thipparapu, S. Jain, T. C. May-Smith, and J. K. Sahu, "Wideband multi-element Er-doped fiber amplifier," Laser Physics Letters, 11(9), 095104, (2014)

[24] N. K. Thipparapu, S. Jain, T. C. May-Smith, and J. K. Sahu, "Configurable Er-doped core-pumped multi-element fiber amplifier," OECC/ACOFT '14 Melbourne 6-10 Jul 2014

[25] S. Jain, V. J. F. Rancaño, T. C. May-Smith, P. Petropoulos, J. K. Sahu, D. J. Richardson, "Multi-element fiber for space-division multiplexing operations," Optics Express, **22**(4), 3787-3796 (2014)

[26] S. Jain, N. K. Thipparapu, P. Barua, and J. K. Sahu, "Cladding-Pumped Er/Yb-Doped Multi-Element Fiber Amplifier for Wideband Applications," IEEE Photonics Technology Letters, 27 (4), 356 - 358 (2015)

[27] S. Jain, T. C. May-Smith, and J. K. Sahu, "Er/Yb-doped cladding-pumped multi-element fiber amplifier," in Workshop on Specialty Optical Fibers and Their Applications, W5.4, (2013).

[28] S. Jain, Y. Jung, T. C. May-Smith, S. U. Alam, J. K. Sahu, and D. J. Richardson, "Few-mode multi-element fiber amplifier for mode division multiplexing," Optics Express, 22(23), 29031-29036, (2014)

[29] Y.Jung, S. Jain, T.May-Smith, J.Sahu, S-U.Alam, D.J.Richardson, "Few-mode multi-element fiber amplifier for mode division multiplexing," European Conference on Optical Communications (ECOC), Cannes 21-25 Sep, Tu.3.4.4, 2014

[30] S. Jain, T.C.May-Smith, J.K.Sahu, "Cladding-pumped Er/Yb-doped Multi-Element Fiber Amplifier for C+L band Operations," in Opt. Fiber Commun. (OFC) San Francisco 9-13 Mar, M2J.3, (2014).

[31] S. Jain, T.C.May-Smith, V.J.F.Rancaño, P.Petropoulos, D.J.Richardson, J.K.Sahu, "Multi-element fibre for space-division multiplexed transmission, " in European Conference on Optical Communications, London 22-26 Sep, Mo.4.A.2, 2013

[32] V. J. F. Rancaño, S. Jain, T. C May-Smith, E. Hugues-Salas, S. Yan, G. Zervas, D. Simeonidou, P. Petropoulos and D. J. Richardson "Demonstration of Space-to-Wavelength Conversion in SDM Networks," IEEE Photonics Technology Letters, (2015) (accepted)

[33] S. Yan, E. H.-Salas, V. J. F. Rancaňo, Y. Shu, G. M. Saridis, B. R. Rofoee, Y. Yan, A. Peters, S. Jain, T. May-Smith, P. P., D. J. Richardson, G. Zervas, D. Simeonidou, "Archon: A Function Programmable Optical Interconnect Architecture for Transparent Intra and Inter Data Center SDM/TDM/WDM Networking," Journal of Lightwave Technology, 33(8), 1586-1595 (2015)

[34] S. Yan, E. Hugues-Salas, V. J. F. Rancano, S. Yi, G. Saridis, B. Rofoee, Y. Yan, A. Peters, S. Jain, T. May-Smith, P. Petropoulos, D. J. Richardson, G. Zervas, and D. Simeonidou, "First Demonstration of All-Optical Programmable SDM/TDM Intra Data Centre and WDM Inter-DCN Communication," in ECOC, PD.1.2, (2014).

Chapter-2

Background of SDM Technologies

2.1. Introduction

This chapter contains an introduction and literature review of SDM approaches, MCF and MMF. The potential impact and challenges of SDM transmission fibre and amplifier for next generation system are discussed in section 2.2.1 and section 2.2.2, respectively. Section 2.2.3 introduces the MEF and its advantages towards the realisation of SDM systems.

2.2. Space-division Multiplexing

The SDM technique in optical fibre communication has been used from wireless communication with a special case of multiple-input-multiple-output (MIMO). In general, SDM could enable a reduction of the number of components in a

communication system. Considering specifically the transmission medium, the integration of N fibre cores into a single transmission fibre could potentially provide huge cost savings. However, with the increase in core density per fibre the complexity of operation also increases which thereby hinders the full exploitation of advantages offered by SDM technology. At the time the work on MEF was started, there were two main approaches for implementing SDM in optical fibres, MCF and MMF. In the following, a review of MCF and MMF is provided.

2.2.1. Multimode Fibre

The passive fibre and amplifier fibre are both integral components of a communication system and they can have different opto-geometrical parameter requirements based on their use.

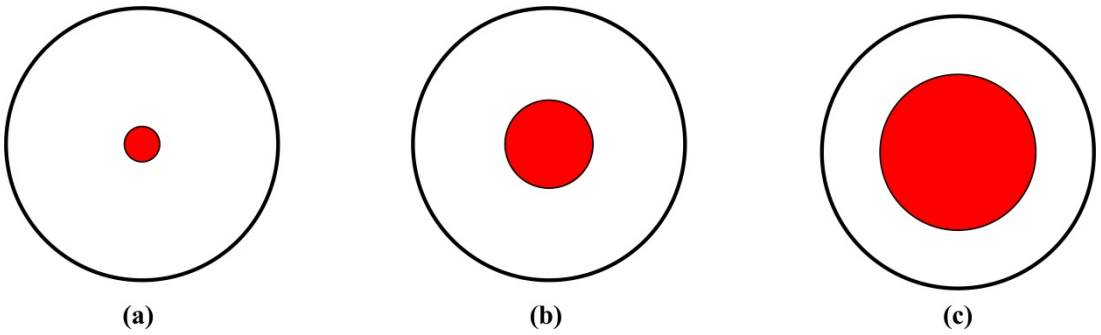

Fig. 2. 1 Schematic of (a) SMF, (b) FMF, and (c) conventional MMF.

The MMFs consists a single multimode core and can support large number of modes. However, Few Mode Fibres (FMFs), supporting a few modes have been of particular interest in SDM to incorporate mode-division multiplexing (MDM). They allow parallel transmission of independent channels defined by the different propagation modes. Figure 2.1 schematically shows the cross-sections of SMF, FMF and conventional MMF in order to provide a perspective of the different core sizes. The MMFs were used in the first generation telecommunication systems due to their advantage of easy splicing of the fibre and power coupling in to the core. However, the intermodal dispersion limited the data rate in MMFs. With the development of technologies such as coherent detection and digital signal processing, it became possible to multiplex the information in orthogonal polarisation and spatial modes, and

double the data rates [4].

Passive Few Mode Fibres

FMFs particularly have been interesting as they can provide very high spatial channel density by using large number of modes. Two approaches of FMF, weakly coupled and strongly coupled FMF, have been demonstrated in the recent years for implementing SDM.

The first approach is the weakly coupled scenario where MIMO signal processing technique can be avoided and the LP modes are separately detected. In this scenario, the set of modes are chosen such that there is minimum spatial overlap between the modes. Further, to prevent inter modal coupling and hence crosstalk, the difference between their effective indices, $\Delta n_{eff,}$ should be as large as possible. The step index profile with higher step index can be used to obtained higher Δn_{eff}. Also, large effective area, A_{eff}, of the modes is desirable to prevent non-linear effects. With the rigid constraints on Δn_{eff} and A_{eff}, it becomes harder to limit the losses of all the modes to lower values [5].

Since, the modes spatially overlap in the core and it becomes difficult to prevent mode coupling for large number of modes. The second category involves strong coupling where the modes are detected simultaneously using the coherent detection and decoupled using MIMO. These types of fibre require that the differential mode group delay (DMGD) or DGD is minimised in order to allow strong coupling between the modes and reduce the complexity and power consumption of the MIMO processing. The step index profile, however, generate high DMGD [5]. Trench-assisted graded-index profile have been shown to provide minimised DMGD [6, 7]. The low DMGD imposes stringent requirements on fibre fabrication and it becomes difficult to achieve ultra-low DMGD for higher number of modes. Another method to achieve the low differential delay is to concatenate alternate fibres with positive and negative DMGD, which can be achieved by varying the graded index profile [8]. There have been experimental demonstrations of FMF with strong coupling incorporating up to 6 modes [8, 10] and transmission reach of up to 1200km in 3-mode fibre [11]. The mode dependent losses (MDLs) in case of strong coupling become higher compared to first approach when the number of modes are increased [12]. Furthermore, FMFs requires that the differential mode gain (DMG) and losses in the link should be compensated [13]. Recently, it has been observed that the fibre non-linearity could

give rise to cross-phase modulation and four-wave mixing interaction in the entire C-band due to phase matching of higher order modes with the fundamental mode at longer wavelength [14, 15].

In the recent years, there have been investigations of mode division multiplexing using orbital angular momentum (OAM) modes [16, 17]. The fact that these are the eigenmodes circular waveguide, they offer higher resistance to modal coupling as compared to the conventional LP modes. The OAM modes are generally unstable in conventional fibres and require vortex fibre to suppress the intermodal coupling. An experimental demonstration of 4-OAM modes over 1.1km of fibre had about -15dB of crosstalk [18]. However, it becomes hard to maintain pure modes over long distances.

Active FMF

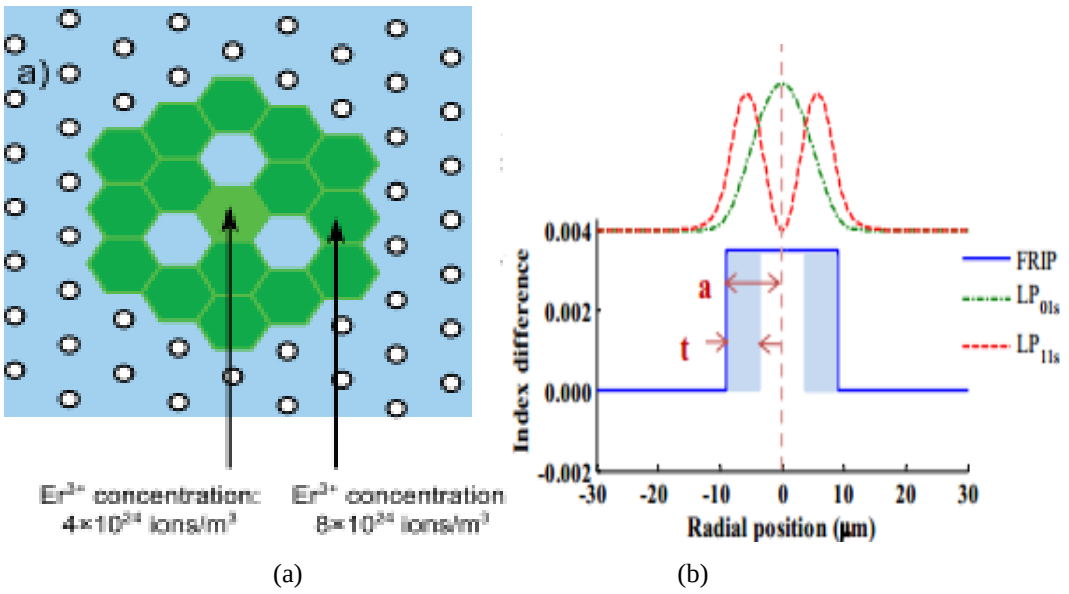

(a) (b)

Fig. 2.2 Schematic of (a) dopant distribution in micro-structured core fibre (green color with Er-ion doping), and (b) refractive index profile with blue color shown as a ring of dopant ions [23, 24]

Multimode amplifiers have been investigated in the 90s and 2000s [19, 20]. In MDM for few-modes, an amplifier is required that could provide flat gain or at least similar gain profiles for the modes over the bandwidth of operation (C-band). There have been various investigations of FMF amplifiers for the minimisation of DMG and compensation of MDLs. The low DMG could be achieved by either controlling the pump modes and/or designing the fibre refractive index profile to control the signal overlap with active ion concentration [21, 22]. However, the latter is preferred where a double clad structure of the fibre could be used due to the ease of operation as compared to pump mode control

[23]. Selective doping of active ions in fibres such as microstructure core fibre, ring core fibre and accurately tailored profile fibre for the reduction of mode dependent gain in FMF amplifiers have been studied [24-27]. Fig. 2.2 (a) and (b) show the schematic image of microstructure core fibre with selective doping of active ions and the refractive index profile of a ring core fibre respectively. A few-mode amplifier supporting 4 mode groups has been experimentally demonstrated with 4dB of DMG [23].

Challenges in FMF

The FMFs derive the advantage of easy and low loss splicing to itself and other fibres from MMFs. However, the accessibility of individual modes has been difficult up to date. Mode MUX and DEMUX are vital components for the realisation of MDM transmission systems. In MDM, the signals from SMFs are converted to the desired modes and coupled in to the FMF. Over the last few years, there have been reports of free-space couplers using phase plate and spatial light modulators and all-fibre coupler using photonic lanterns and long period fibre grating [28 ,32]. The phase plate based couplers are easier to use but simplicity comes with higher losses which often are mode dependent. Furthermore, the MDL in the couplers makes the MIMO equalisation process difficult. Moreover, components such as gain flattening filters need to be investigated that could accommodate for the variation in the amplifier gain profile for different modes. The reported MDM systems have shown impressive initial results and to date provide the highest spatial density among all the available fibre technologies for SDM. However, a thorough investigation of the above issues is required for MDM technology to be compatible with the current systems and hence to be considered for commercial implementation.

2.2.2. Multicore Fibre

MCF comprises multiple cores, which share a common cladding. The spatial channel density in MCF is lower than FMF. Fig. 2.3 shows the schematic cross-section image of MCFs with 3, 7 and 19 cores respectively.

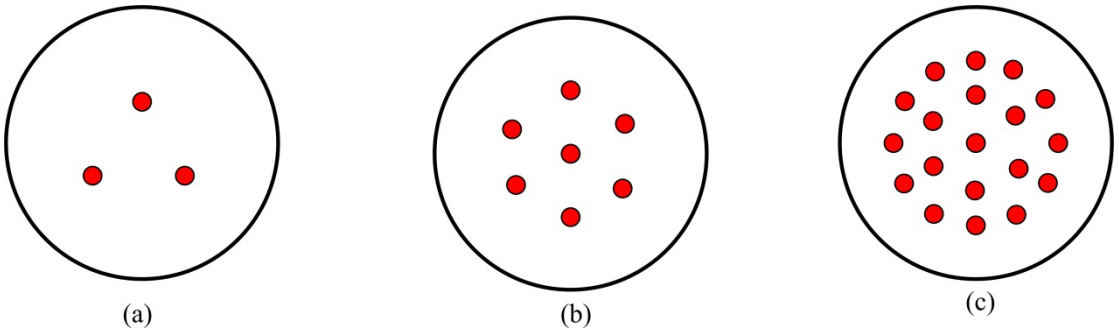

Fig. 2.3 Schematic of MCFs consisting 3, 7 and 19 cores respectively.

Passive MCF

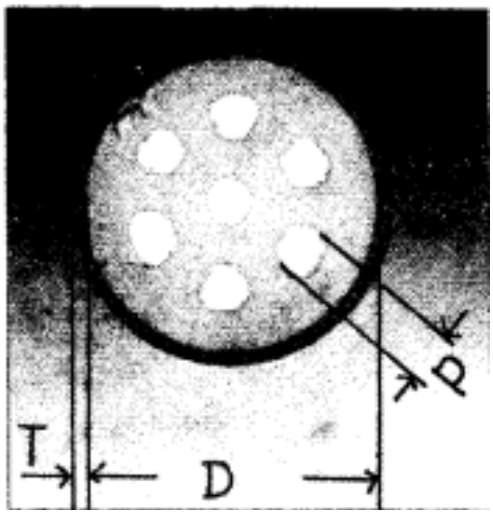

Fig. 2.4 Cross-sectional image of first 7-MCF with D= 150μm [33]

The concept of incorporating multiple cores is not new, and in fact, Inao et al. from Furukawa electric Co. Ltd. experimentally demonstrated a multicore fibre in 1979 [33, 34]. The main aim of developing MCF was to demonstrate a high density cable as opposed to conventional optical fibre cables. The MCF was fabricated through stacking 7-preform rods in a circular jacketing tube under vacuum condition. The resulting fibre consisted of 7-cores in hexagonal geometry as shown in Fig. 2.4. The core loss was measured to be about 3dB/km at a wavelength of 850nm which was similar to single-core fibres. However, it suffered from crosstalk between neighbouring cores. The crosstalk was about -43dB for a 430m MCF. In addition, there was the difficulty of splicing and aligning the cores.

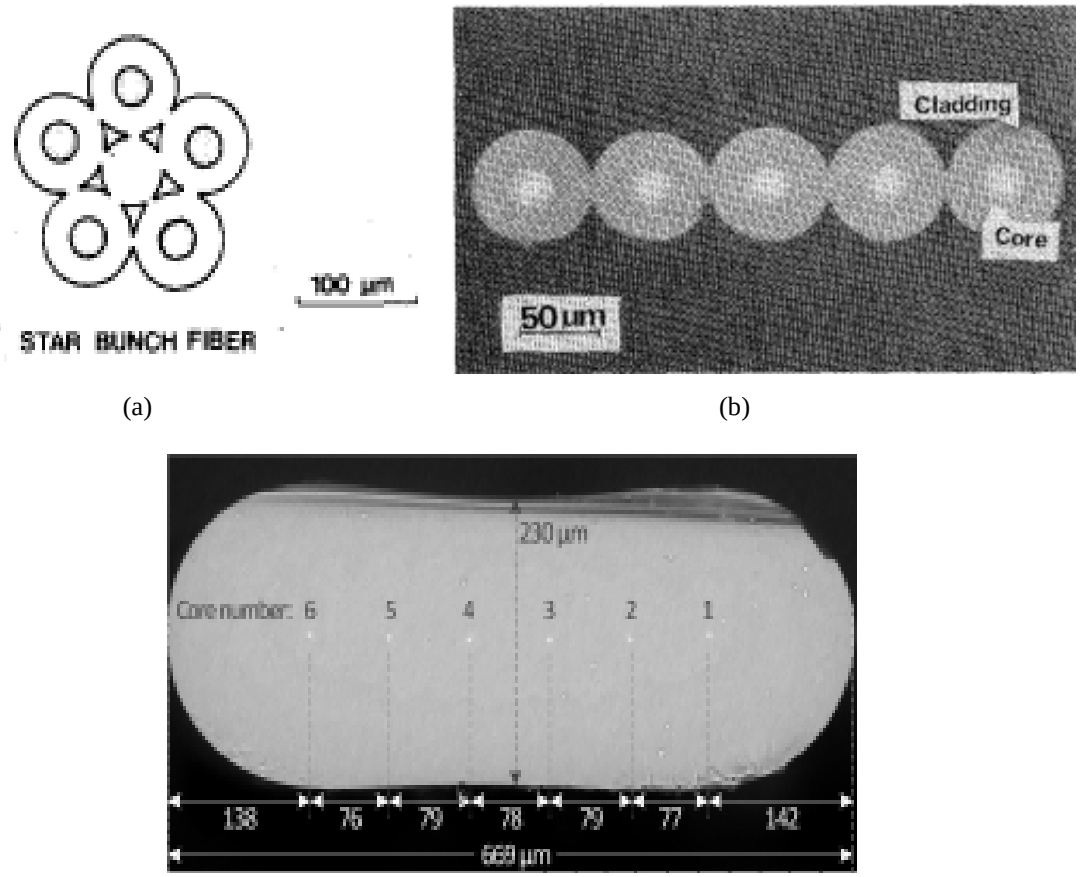

Fig. 2.5 Cross-sectional image of (a) star bunch fibre, (b) flat bunch fibre and (c) multicore flat fibre [35, 36]

As shown in Fig. 2.5 (a) and (b), further advancement saw the variation in the form of non-circular outer cladding to counter the aligning issues [35, 36]. Fig. 2.5 (c) shows the multicore flat fibre which was proposed as an alternative to counter the diameter constraint in MCFs. The development of MCFs was not pursued at that time due to the spectacular growth of SSMF based passive optical networks. In the 2000s, the rapid traffic growth and the saturation of SSMF capacity has led to a renaissance of research in MCFs [37, 38].

Recent demonstration of MCFs for SDM can be also be classified into two categories, depending on the interaction between the spatial channels, coupled core MCF (CC-MCF) and uncoupled core MCF.

In CC-MCF, the spacing between the cores is small which results in higher spatial density than uncoupled MCF. There is strong coupling between the spatial channels such that the signal travelling as a super-mode. The higher core density achieved in

the CC-MEF comes at a cost of using the MIMO digital signal processing required to untangle the strongly coupled output. It is effectively similar to FMF with strong coupling. On the other hand, the CC-MCF has advantage over coupled FMF in terms of lower MIMO complexity. Due to strong coupling, the signal travels same distance in the cores hence resulting in small DMGD. Moreover, MDL is minimal in CC-MCF. Initial investigations of CC-MCF showed promising results with a record transmission distance of 4200km in 3-core microstructure core fibre demonstrated in 2012 [39-41]. The reduced complexity in CC-MCF compared to FMFs is obtained at the cost of decreased spatial channel density.

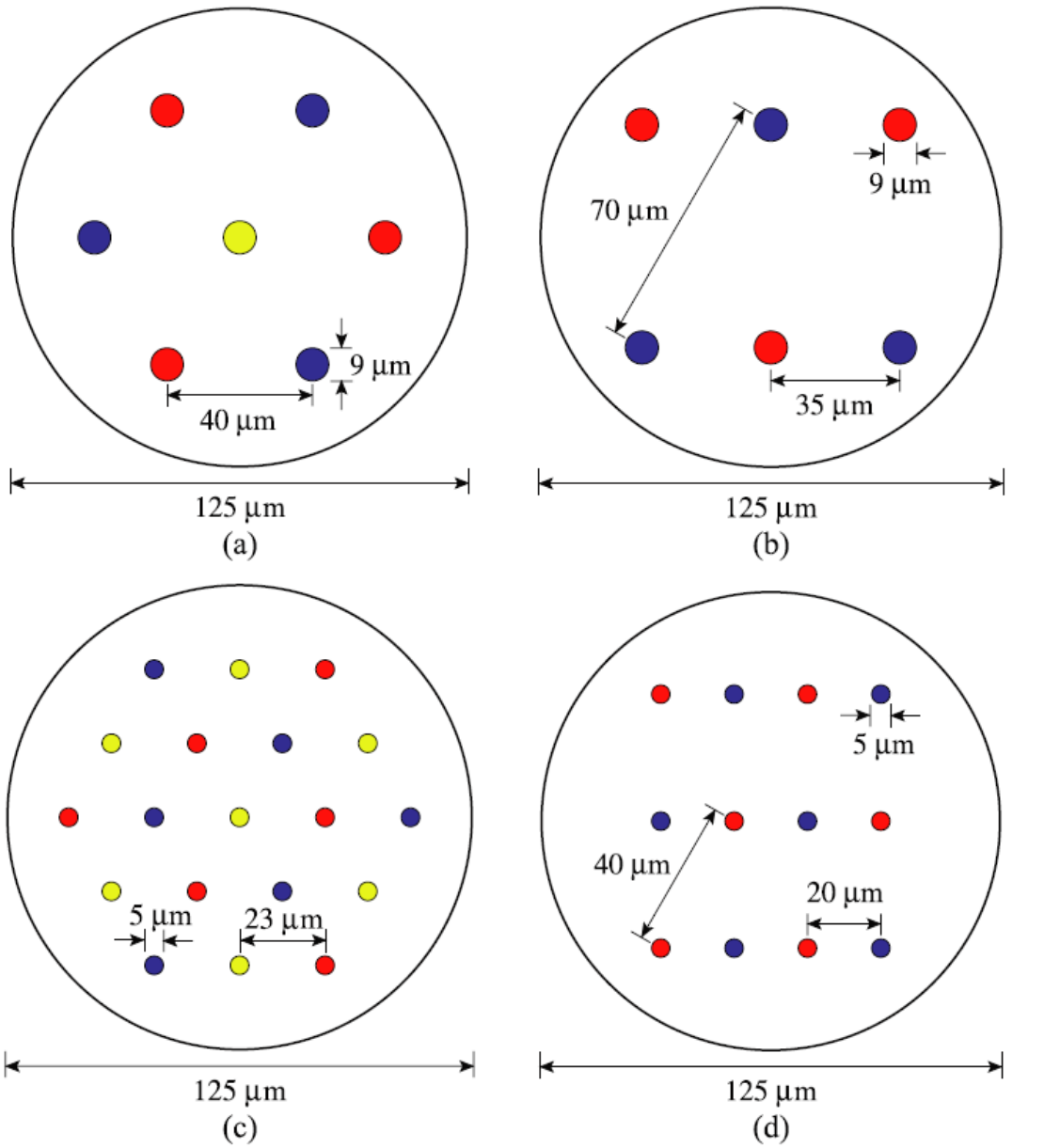

Fig. 2.6 Heterogeneous MCF with (a) 7-cores in a triangular lattice pattern, (b) 6-cores in a rectangular lattice pattern, (c) 19-cores in triangular lattice, and (d) 12-cores in rectangular pattern [42] (different colour represent slightly different cores to prevent coupling)

In uncoupled MCF, the cores are desired to have no interaction between each other. The cores can also be different from each other in terms of size and refractive index. This approach has received most attention among all of the SDM technology due to the possibility of avoiding MIMO processing. In uncoupled MCF, Koshiba et al. performed a theoretical investigation in heterogeneous MCFs by placing the cores in triangular and rectangular lattice pattern as shown in Fig. 2.6 [42]. It was found that a slight difference in effective indices or propagation constants between the adjacent cores could help in mitigation of crosstalk (see Fig. 2.7 (a) for cross-section image). By using the different refractive index values (Δ), the phase matching between the cores could be avoided. The initial heterogeneous MCFs based on different core sizes were found to provide higher than expected crosstalk values. It was observed that fibre bending and twisting caused random phase matching between the adjacent cores thereby increasing the crosstalk [43-45].

Further, to increase the core density and reduce the crosstalk, various modifications around the core of MCFs such as trench-assisted core and hole-assisted profiles were investigated [46-48]. Figure 2.7 (b) and (c) shows the cross-section of these fibres. Also, the study of microbending loss with outer cladding thickness was performed to optimise the overall cladding thickness [49, 50]. The mechanical reliability of the outer diameter was also investigated in order to ensure that the strength of the fibre is not compromised and fibres have long operational life without degradation in their performance [50, 51]. Under this restriction, the cladding-diameter of about 225μm is shown to be the theoretical limit of MCFs [51]. Following the development of 7-MCFs, the number of cores were increased up to 19 in MCF [52, 53]. However, the crosstalk with 19 cores in hexagonal geometry was higher than -30dB even for the effective area of 80μm^2 with 100km fibre length [53]. As shown in Fig. 2.7 (d), the cores were then arranged in circular geometry in order to reduce the crosstalk to about -40dB [54]. The inner circle core were placed at a radius slightly larger than outer circle which resulted in 4-5dB crosstalk reduction as compared to hexagonal geometry. The developmental progress of MCF based SDM system has resulted in 10 times enhancement in the capacity compared to SSMFs with a demonstrated record data rate of 1.01Pb/s [55].

It should be noted that the MCF and FMF concepts have been combined to develop few-mode MCFs, in order to further increase the spatial multiplicity up to 36 [56-58]. The highest capacity reported to-date used 14 cores, 12 single mode and 2 few-mode

cores, resulting in a total transmission rate of 1.05Pb/s [56]. Recent MCF demonstrations with 36 cores, each carrying 3 modes, and with 19 cores, each carrying 6 modes, have shown the highest spatial multiplicity of 108 and 114 respectively [59, 60]. The cladding diameter of these 36 core and 19 core fibres was 304µm and 318µm respectively suggesting a possibility to relax the outer diameter constraint of 225µm. However, no proof test was reported for these fibres.

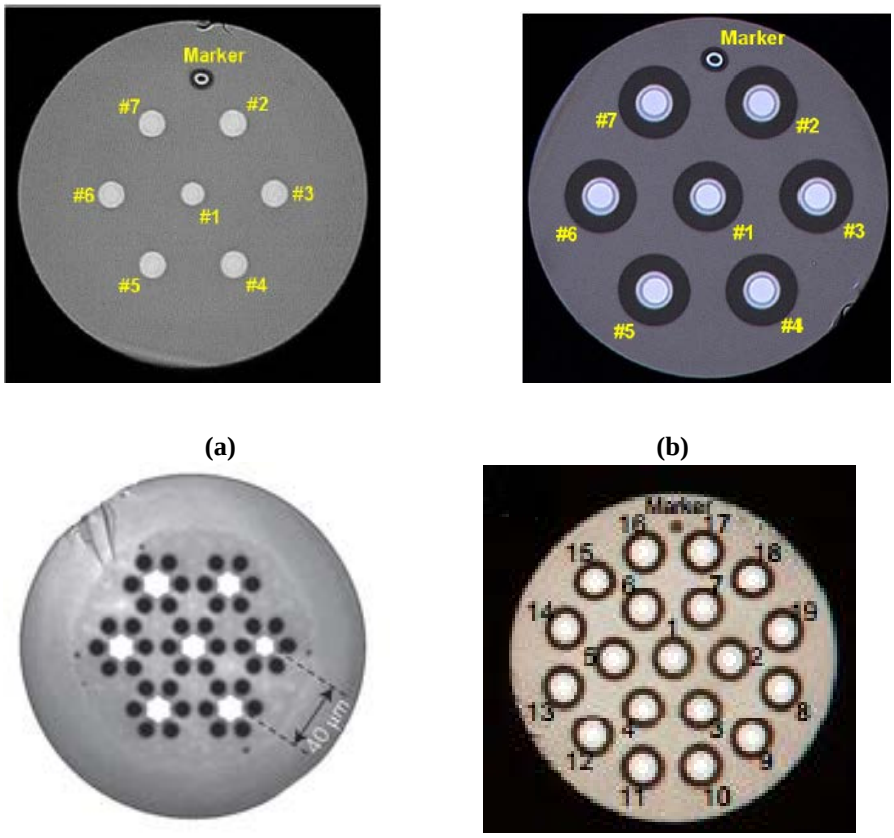

Fig. 2. 7 Cross-section images of 7-MCFs; (a) Conventional, (b) Trench-assisted, (c) Hole-assisted, (d) 19-core with circular core arrangement. [46-48, 54]

Active MCF

Both, transmission fibre and amplifier fibre are vital to the implementation of SDM technology. Core-pumped 7-MCF EDFAs employing uncoupled cores with an outer cladding diameter of 148µm and 180µm have been respectively (see Fig. 2.8 (a) and (b)) [61-64]. Both demonstrations used fan-in/fan-out tapered fibre bundles for multiplexing/de-multiplexing of the spatial channels. The former demonstration showed that the maximum crosstalk level from neighbouring channels were 25dB below the ASE level of the amplifier while the latter had a signal crosstalk of about 40dB. Since then there have continuous push to take the technology forward, and

recently, a 19-core core-pumped MCF amplifier (see Fig. 2.8(d)) has been demonstrated using 10 pump LDs (9 were followed by a 3dB coupler to provide pump power to all 19 cores) [54].

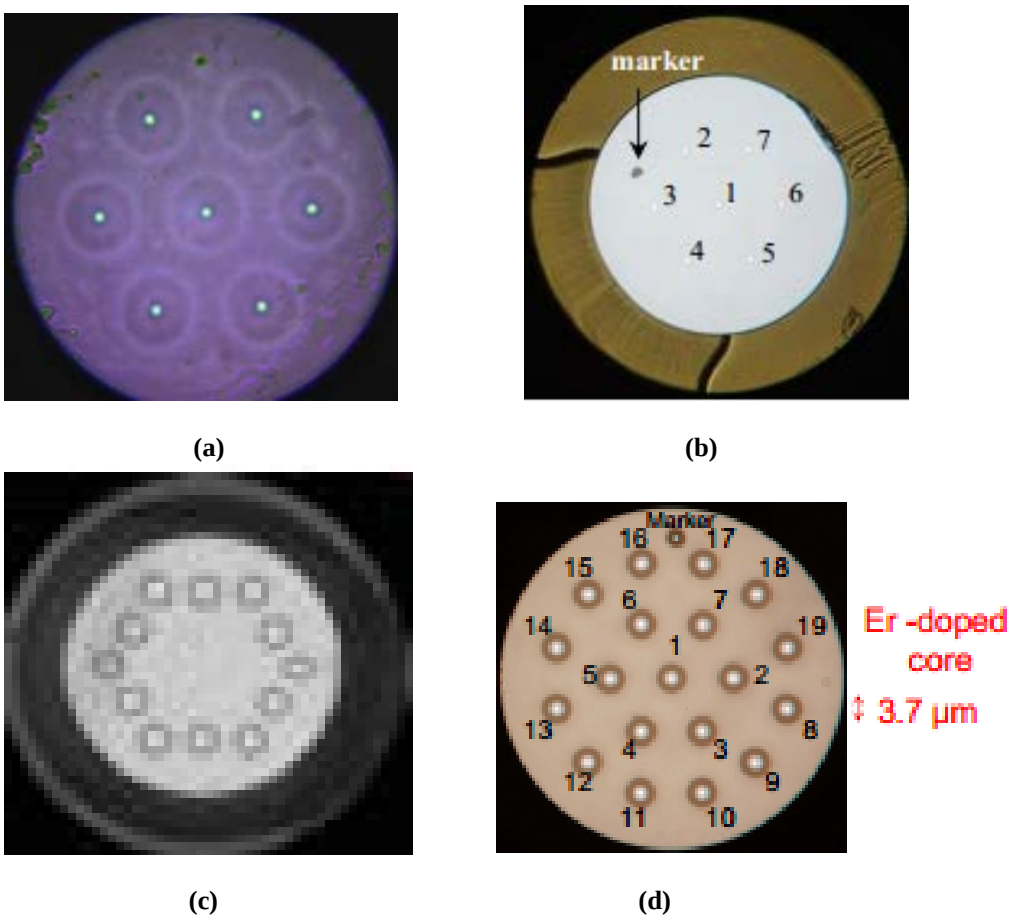

Fig. 2.8 (a)-(b) 7-core Er-doped MCF for core-and cladding pumping , (c) 12-core Er/Yb-doped MCF for cladding-pumping, and (d) 19-core Er-doped MCF for core-pumping [54, 64, 65, 68].

C-band MCF amplifiers in cladding-pump configuration have also been presented using both free-space optics and tapered fibre bundle with central fibre being coreless [64, 68]. The number of cores in the cladding-pump configuration have been increased up to 12 [65]. The cross-section image of 12-core MCF is shown in Fig. 2.8 (c).

Challenges in MCF

Similar to FMF, the use of MCF requires the development of specialized MUX/DEMUX components for accessing the individual cores with low crosstalk [67-70]. Free space, integrated optic and fibre based devices are all now available, but with additional cost, appreciable loss and requiring very precise alignment [70-73]. Figure 2.9 shows some of the MUX/DEMUX components that have been developed over the

years. Compared with bundled fibre couplers, free-space couplers have shown lower crosstalk and coupling loss even for a core pitch down to 35μm [73]. However, free-space couplers might not be favourable for practical deployment due to their relatively high sensitivity to environmental perturbations. Couplers for cladding pump amplification in MCF also face the above challenges for pump and signal coupling. MCF based transmission would be limited to point-to-point network transmission due to its inability to separately access spatial channels. It should be that noted unlike the fibre links for transatlantic connections, the fibre in terrestrial networks are deployed in short lengths which are then connected together. In that case, an optimum coupling program/technique to achieve low loss and low crosstalk such as fusion splicing in SSMF is a necessary requirement.

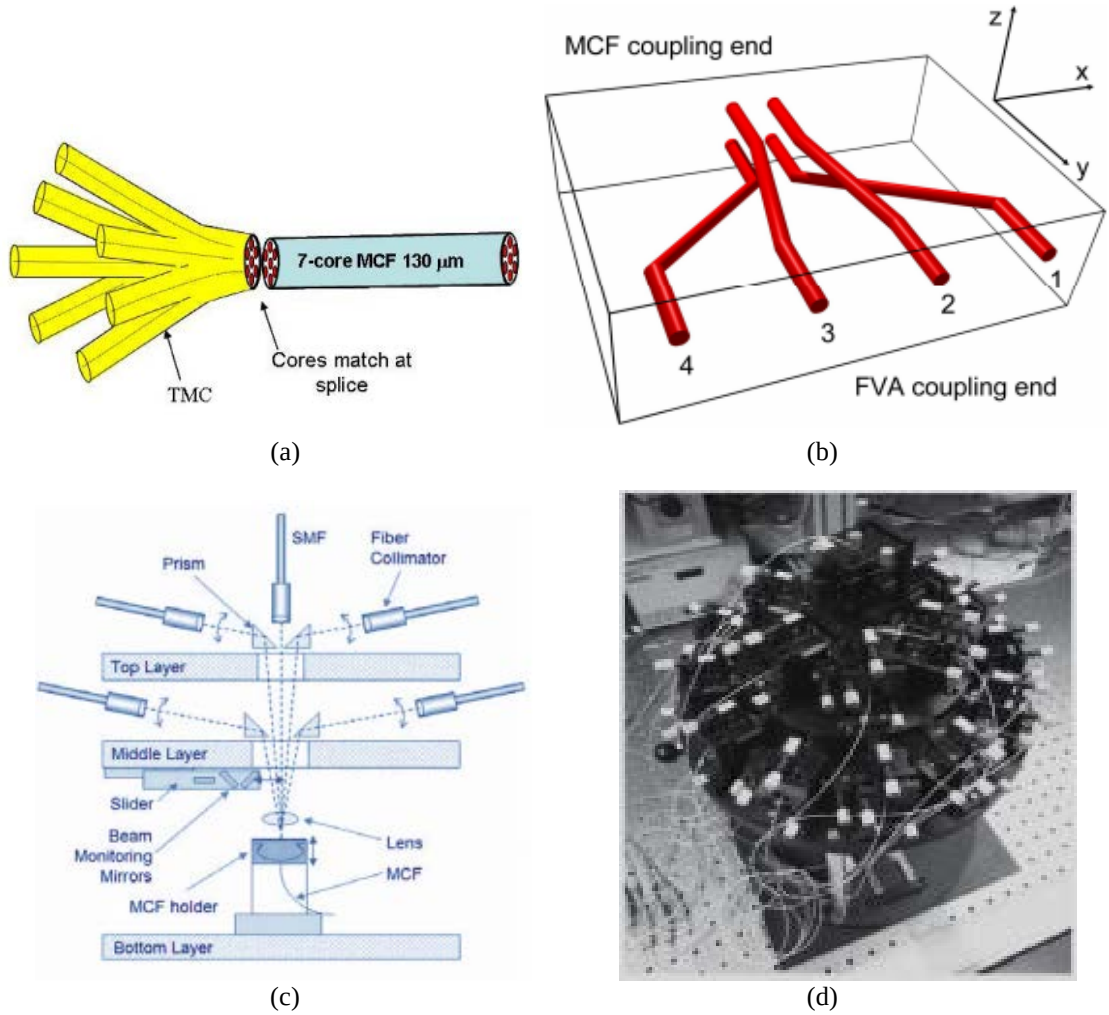

Fig. 2.9 Coupling scheme for MCFs; (a) Tapered multicore connector (TMC), (b) encrypted 3-D fan-in/fan-out device, (c) schematic of free-space coupling in 19-core fibre, and (d) image of free space-coupler for 19-core MCF [70-73]

In addition, the cladding diameter in MCF is restricted to 225μm by mechanical

reliability considerations, although, some experiments have shown the possibility to go to higher diameters [50, 51]. This constraint, along with the minimum pitch required for low crosstalk, restricts the effective core area (Aeff) and the maximum number of cores that can be accommodated in an MCF design. With these constraints the maximum number of cores up to now have restricted to 19. A multicore flat fibre has shown the potential for reduced crosstalk and also better mechanical reliability as it could be bent only on the thin axis [74]. A cross-section image of such a fibre is shown in Fig. 2.5 (c). These issues/impairments reduce the cost-advantage that MCF could offer in a SDM system.

2.2.3. Multi-element Fibre

Multi-element fibre (MEF) is a robust and practical approach to implement SDM. MEFs can help towards avoiding many of the current practical limitation and rigidity associated with MCF and MMF systems. MEFs comprise multiple fibre-elements that are drawn and coated together in a common polymer coating. They could enable high density optical fibre cables as compared to the currently used SSMF cables with conventional fibre of 250μm coated diameter or even fibres with reduced coated diameter of 200μm. They allow for a more compact configuration of fibres as compared to a bundle of SSMFs, allowing increased spatial channel densities and efficient space utilization of the fibre cables. The higher core density in MEF is enabled by the use of common polymer coating. The mechanical stiffness provided by the common cladding potentially allows the use of significantly thinner fibre-elements in MEF. In single fibre, micro-bending loss becomes significant as its diameter is reduced. There is in principle no fundamental upper limit to the overall diameter of a MEF (and associated number of elements) provided that the mechanical robustness of the individual elements is maintained. In addition, the independent nature of fibre-elements in MEF geometry ensures that ultralow crosstalk can be maintained between the individual elements.

Although, the spatial density of MEF is less than MCF and MMF, it maintains the compatibility with current SSMF based systems and could allow for a smooth transition to SDM systems. MEFs provide convenience in fibre handling compared to other SDM technologies since each fibre-element i. e. spatial channel, can be accessed individually by simply stripping-off the polymer coating. These fibre-elements can

then be connected to the SMF components using conventional fusion splicing. The development of fan-in, fan-out multiplexing components is therefore not required. Due to this, the incorporation of MEFs in current systems might help towards maintaining their flexibility.

It is envisaged that the system capacity in future will scale with bandwidth per mode, modes per core, cores per fibre and fibres per cable [75]. It should be noted that MEF technology is compatible with both MCF and MMF i.e. individual fibre-elements could also have multiple core and/or multimode core. MEF can provide a bridging gap between the fibres enabling higher spatial channel density and current network flexibility.

In this work, the MEF technology has been developed to build a bundle of multiple amplifiers. A core-pumped multi-element Er-doped fibre amplifiers (ME-EDFAs), comprising 3 and 7 Er-doped fibre-elements has been demonstrated, which will be discussed in detail in Chapter-3 [76, 77]. More importantly, a cladding-pumped Er/Yb-doped 5-element MEF amplifier (ME-EYDFA) has also been realized [78]. In the cladding-pumped ME-EYDFA, a central fibre-element carries the pump light. The pump light is shared between several surrounding active (signal) fibres, four in the case of the work described here. The cladding-pumping is particularly attractive for SDM systems as it demonstrates component integration through pump sharing. Moreover, it is shown that the ME-EYDFA in novel cascading configuration can allow for the possibility to improve the gain flatness and/or wavelength tuneability [79, 80]. It has also been demonstrated the wavelength tuneability of the ME-EDYFA could be exploited to develop a broadband amplifier in split-band configuration. Such an amplifier could provide an amplification bandwidth of larger than 80nm whilst using a single pump source. Furthermore, in order to demonstrate the possibility to further increase the spatial multiplicity in SDM fibre amplifiers, a first cladding pump amplifier combining MEF and FMF was designed which included 4-fibre-element with each guiding 3 modes (LP_{01} and LP_{11}) thereby enabling a spatial multiplicity of 12 [81]. The cladding-pump amplifiers have been discussed in detail in Chapter-4.

Passive MEFs have also been developed [82-85]. The fabrication technique for implementing the SDM in passive MEFs has been developed. Various passive MEFs with different fibre-element diameters have been fabricated. The loss, proof-test strength characterisation and transmission tests have been performed on the developed

fibres to demonstrate the benefits of this technology. It has been shown that high proof-test strength could be achieved in MEF whilst maintaining low loss, provided the fibre-elements do not touch each other. The details of the passive MEF fabrication and the characterisation of resulting MEFs has been discussed in Chapter-5 and a general MEF fabrication is discussed in Chapter-3.

References:

[1] D. J. Richardson, J. M. Fini, O. E. Nelson, “Space-division multiplexing in optical fibers,” Nature Photonics, 7, 354–362 (2013)

[2] R. J. Essiambre, G. Kramer, P. J. Winzer, G. J. Foschini, and B. Goebel, “Capacity limits of optical fiber networks,” J. Lightwave Technol., 28(4), 662–701, (2010)

[3] W. J. Miniscalco, “Optical and electronic properties of rare earth ions in glasses,” in Rare-earth-doped fiber lasers and amplifiers, ed. M. J. F. Digonnet, Marcel Dekker Inc., 2001

[4] Y. Han and G. Li, "Coherent optical communication using polarization multiple-input-multiple-output," Opt. Express, 13, pp. 7527-7534, (2005).

[5] K. Jespersen, Z. Li, G. Nielson, N. Palsdottir, F. Poletti, and J. Nicholson, “Measuring distributed mode scattering in long, few-moded fibers,” in Opt. Fiber Commun. (OFC), paper OTh3I.4 (2012)

[6] L. Grüner-Nielsen, Y. Sun, J. W. Nicholson, D. Jakobsen, R. Lingle, and B. Pelasdotirr, “Few mode transmission fiber with low DGD, low mode coupling, and low loss,” IEEE J. Lightwave Technol. 30, 3693–3698 (2012).

[7] P. Sillard, and D. Molin, “A review of few-mode fibers for space-division multiplexed transmissions,” in European Conf. on Opt. Commun. (ECOC), Mo.3.A.1 (2013)

[8] R. Ryf, S. Randel, N. K. Fontaine, M. Montoliu, E. Burrows, S. Chandrasekhar, A. H. Gnauck, C. Xie, R.-J. Essiambre, P. Winzer, R. Delbue, P. Pupalaikis, A. Sureka, Y. Sun, L. Gruner-Nielsen, R. V. Jensen, R. Lingle “32-bit/s/Hz spectral efficiency WDM transmission over 177-km few-mode fiber,” in Opt. Fiber Commun. Conf. (OFC), paper PDP5A.1 (2013).

[9] P. Sillard, D. Molin, M. Bigot-Astruc, H. Maerten, D. V. Ras, and F. Achten, “Low-DMGD 6-LP-mode fiber,” Opt. Fiber Commun. Conf. (OFC), paper M3F.2 (2014).

[10] R. Ryf, N. K. Fontaine, M. A. Mestre, S. Randel, X. Palou, C. Bolle, A. H. Gnauck, S. Chandrashekhar, X. Liu, B. Guan, R. J. Essiambre, P. J. Winzer, S. G. Leon-Saval, J. Bland-Hawthorn, R. Delbue, P. Pupalaikis, A. Sureka, Y. Sun, L. Gruner-Neilsen, R. V. Jensen, R. lingle, “12 × 12 MIMO transmission over 130-km few-mode fiber,” in Frontier in Opt. (FIO), FW6C.4 (2014)

[11] S. Randel, R. Ryf, A. H. Gnauck, M. A. Mestre, C. Schmidt, R. J. Essiambre, P. J. Winzer, R. Delbue, P. Pupalaikis, A. Sureka, Y. Sun, X. Jiang, and R. lingle, “Mode-multiplexed 6×20-GBd QPSK transmission over 1200-km DGD-compensated few-mode fiber,”

[12] K. Nakajima, P. Sillard, D. Richardson, M.-J. Li, R.-J. Essiambre, and S. Matsuo, “Transmission media for an SDM-based optical communication system,” IEEE Communication Magazine, **53**(2), 44-51 (2015)

[13] K.-P. Ho and J. M. Kahn, “Frequency diversity in mode-division multiplexing systems,” Journal of Lightwave Technology, 29 (24), 3119 (2011).

[14] R.-J. Essiambre, M. M. Mestre, R. Ryf, A. H. Gnauck, R. W. Tkach, A. R. Charplyvy, Y. Sun, X. Jiang, and R. Lingle, “Experimental observation of inter-modal cross-phase modulation in few-mode fibers,” IEEE Photon.

Technol. Lett., **25** (6), 535-538 (2013)

[15] R.-J. Essiambre, M. M. Mestre, R. Ryf, A. H. Gnauck, R. W. Tkach, A. R. Charplyvy, Y. Sun, X. Jiang, and R. Lingle, "Experimental investigation of inter-modal four-wave mixing in few-mode fibers," IEEE Photon. Technol. Lett., **25** (6), 539-542 (2013)

[16] N. Bozinovic, Y. Yue, Y. Ren, M. Tur, P. Kristensen, A. E. Willner, and S. Ramachandran, "Terabit-scale orbital angular momentum mode division multiplexing in fibers," Science, **340**(6140), 1545-1548, (2013)

[17] S. Ramachandran, and P. Kristensen, "Optical Vortex in fiber," Nanophotonics, **2** (5-6), 455–474, (2013)

[18] N. Bozinovic, Y. Yue, Y. Ren, M. Tur, P. Kristensen, A. E. Willner, and S. Ramachandran, "Orbital angular momentum (OAM) based mode division multiplexing (MDM) over a Km-length fiber," in European Conf. on Opt. Commun. (ECOC 2012), postdeadline paper Th.3.C.6

[19] G. Nykolak, S. A. Kramer, J. R. Simpson, D. J. DiGiovanni, C. R. Giles, and H. M. Presby, "An erbium doped multimode optical fiber amplifier," IEEE Photon. Technol. Lett., 3(12), 1079–1081 (1991)

[20] N. W. Spellmeyer, "Communications performance of a multimode EDFA," IEEE Photon. Technol. Lett., 12(10), 1337–1339, (2000).

[21] N. Bai, E. Ip, T. Wang, and G. Li, "Multimode fiber amplifiers with tunable modal gain using a reconfigurable multimode pump," Opt. Express, **19**(17), 16601–16611, (2011).

[22] E. Ip, "Gain equalization for few-mode fiber amplifiers beyond two propagating mode groups," IEEE Photonics Tech. Lett., **24**(21), 1933-1936 (2012)

[23] E. L. Lim, Y. Jung, Q. Kang, T. C. May-Smith, N. H. L. Wong, R. Standish, F. Poletti, J. K. Sahu, S. U. Alam, and D. J. Richardson, "First demonstration of cladding pumped few-moded EDFA for mode division multiplexed transmission," in Opt. Fiber Commun. (OFC), paper M2J.2, (2014)

[24] Y. Jung, Q. Kang, V. A. J. M. Sleiffer, B. Inan, M. Kuschnerov, V. Veljanovski, B. Corbett, R. Winfield, Z. Li, P. S. Teh, A. Dhar, J. Sahu, F. Poletti, S. -U. Alam, and D. J. Richardson, "Three mode Er3+ ring-doped fiber amplifier for mode-division multiplexed transmission," Optics Express, 21(8), 10383-10392 (2013).

[25] G. L. Cocq, L. Bigot, A. L. Rouge, M. Bigot-Astruc, P. Sillard, C. Koebele, M. Salsi, and Y. Quiquempois, "Modeling and characterization of a few-mode EDFA supporting four mode groups for mode division multiplexing," Opt. Express, **20**(24), 27051-27061 (2012)

[26] G. L. Cocq, Y. Quiquempois, A. L. Rouge, G. Bouwmans, H. E. Hamzaoui, K. Delplace, M. Bouazaoui, and L. Bigot, "Few mode Er3+-doped fiber with micro-structured core for mode division multiplexing in the C-band," Opt. Express, **21** (25), 31646-31659 (2013)

[27] Y. Jung, Q. Kang, V. A. J. M. Sleiffer, B. Inan, M. Kuschnerov, V. Veljanovski, B. Corbett, R. Winfield, Z. Li, P. S. Teh, A. Dhar, J. Sahu, F. Poletti, S. -U. Alam, and D. J. Richardson "Three mode Er3+ ring-doped fiber amplifier for mode-division multiplexed transmission," Opt. Express, **21**(8), 10383-10392 (2013)

[28] R. Ryf, S. Randel, A. H. Gnauck, C. Bolle, R.-J. Essiambre, P. Winzer, et al., "Space-division multiplexing over 10 km of three-mode fiber using coherent 6 × 6 MIMO processing," in Opt. Fiber Commun. Conf. (OFC),

PDPB10, (2011)

[29] W. Q. Thornburg, B. J. Corrado, and X. D. Zhu, “Selective launching of higher-order modes into an optical fiber with an optical phase shifter,” Optics Letters, 19(7), 454-456 (1994).

[30] A. Li, A. Al Amin, X. Chen, and W. Shieh, "Reception of mode and polarization multiplexed 107-Gb/s CO-OFDM signal over a two-mode fiber," in in Opt. Fiber Commun. Conf. (OFC), PDPB8, (2011).

[31] S. Yerolatsitis, and T. Birks, “Tapered mode multiplexers based on standard single fibre,” in European Conf. on Opt. Commun. (ECOC), PD1.C.1 (2013)

[32] S. G. Leon-Saval, A. Argyros, and J. Bland-Hawthorn, “Photonic lanterns: a study of light propagation in multimode to single-mode converters,” Optics Express, 18(8), 8430 (2010).

[33] S. Inao, T. Sato, S. Sentsui, T. Kuroha, and Y. Nishimura, “Multicore optical fiber,” in Opt. Fiber Commun. Conf. (OFC), 1979, paper WB1.

[34] S. Inao, T. Sato, H. Hondo, M. Ogai, S. Sentsui, A. Otake, K. Yoshizaki, K. Ishihara, and N. Uchida, “High density multicore-fiber cable,” in Int. Wire Cable Symp. (IWCS), 1979, pp. 370–384.

[35] N. Kashima, E. Maekawa, and F. Nihei, “New type of multicore fiber,” in Opt. Fiber Commun. Conf. (OFC), 1982, paper ThAA5.

[36] S. Sumida, E. Maekawa, and H. Murata, “Fundamental studies on flat bunched optical fibers,” J. Lightwave Technol., vol. 3, no. 1, pp. 159–164, Feb. 1985.

[37] P. Winzer, "Modulation and multiplexing in optical communication systems," LEOS Newsletter (2009).

[38] Guifang Li and Xiang Liu,”Focused Issue: space multiplexed optical transmission”, Optics Express 19, 16754-16575(2011)

[39] Y. Kokubun and M. Koshiba, “Novel multi-core fibers for mode division multiplexing: proposal and design principle,” IEICE Electron. Express, vol. 6, no. 8, pp. 522–528, Apr. 2009.

[40] C. Xia, N. Bai, I. Ozdur, X. Zhou, and G. Li, “Supermodes for optical transmission,” Opt. Express, vol. 19, no. 17, pp. 16 653–16 664, Aug. 2011.

[41] R. Ryf, R. J. Essiambre, A. H. Gnauck, S. Randel, M. A. Mestre, C. Schmidt, P. J. Winzer, R. Delbue, P. Pupalaikis, A. Sureka, T. Hayashi, T. Taru, and T. Sasaki “Space-division multiplexed transmission over 4200-km 3-core microstructured fiber,” in Opt. Fiber Commun. Conf. (OFC), PDP5C.2 (2012)

[42] M. Koshiba, K. Saitoh, and Y. Kokubun, “Heterogeneous multi-core fibers: proposal and design principle,” IEICE Electron. Express, vol. 6, no. 2, pp. 98–103, Jan. 2009.

[43] Tetsuya Hayashi, Takuji Nagashima, Osamu Shimakawa, Takashi Sasaki, Eisuke Sasaoka, “Crosstalk Variation of multi-core fibre due to fibre Bend,” in European Conf. on Opt. Commun. (ECOC), 2010, paper We.8.F.6

[44] J. M. Fini, B. Zhu, T. F. Taunay, and M. F. Yan “Statistics of crosstalk in bent multicore fibers,” Opt. Express, **18**(14), 15122 (2010)

[45] S. Matsuo, K. Takenaga, Y. Arakawa, Y. Sasaki, S. Tanigawa, K. Saitoh, and M. koshiba, “Crosstalk behaviour of multi-core fiber under Bent condition,” IEICE Electronics Express, **8**(6), 385-390 (2011)

[46] T. Hayashi, T. Taru, O. Shimakawa, T. Sasaki, and E. Sasaoka, “Design and fabrication of ultra-low crosstalk and low-loss multi-core fiber,” Optics Express, vol. 19, no. 17, pp. 16576–16592, 2011.

[47] K. Saitoh, T. Matsui, T. Sakamoto, M. Koshiba, and S. Tomita, "Multi-core hole-assisted fibers for high core density space division multiplexing," in OptoElectron. Commun. Conf. (OECC), Sapporo, Japan, Jul. 2010, paper 7C2-1.

[48] T. Hayashi, T. Taru, O. Shimakawa, T. Sasaki, and E. Sasaoka, "Low-crosstalk and low-loss multi-core fiber utilizing fiber bend," in Optical Fiber Communication Conference (OFC), 2011, paper OWJ3.

[49] K. Takenaga, Y. Arakawa, Y. Sasaki, S. Tanigawa, S. Matsuo, K. Saitoh, and M. Koshiba, "A large effective are multi-core fiber with an optimized cladding thickness," Opt. Express, **19**(26), B543 (2011)

[50] K. Imamura, I. Shimotakahara, K. Mukasa, N. Oyama, and R. Sugizaki, "A study on reliability for large diameter multi-core fibers," in Int. Wire Cable Symp. (IWCS), 2011, paper P-2, pp. 284–288.

[51] S. Matsuo, K. Takenaga, Y. Arakawa, Y. Sasaki, S. Tanigawa, K. Saitoh, and M. Koshiba, "Large-effective are ten-core fiber with cladding-diameter of about 200μm," Opt. Lett., **36**(23), 4626-4628, (2011)

[52] J. Sakaguchi, B. Puttnam, W. Klaus, Y. Awaji, N.Wada, A. Kanno, T. Kawanishi, K. Imamura. H. Inaba, K. Musaka, R. Sugizaki, T. Kobayashi, and M.Watanabe, "19-core fiber transmission of 19x100x172-Gb/s SDM-WDM-PDM-QPSK signals at 305Tb/s," in Opt. Fiber Conf, (OFC/NFOEC 2012), paper PDP.5C.1

[53] S. Matsuo, Y. Sasaki, I. Ishida, K. Takenaga, K. Saitoh, and M. Koshiba, "Recent progress on multi-core fiber and few-mode fiber," in Opt. Fiber Conf. (OFC/NFOEC 2013) OM3I.3

[54] J. Sakaguchi, W. Klaus, B. J. Puttnam, J. M. D. Mendinueta, Y. Awaji, N. Wadam Y, Tsuchida, K. Maeda, M. Tadakuma, K. Imamura, R. Sugizaki, T. Kobayashi, Y. Tottori, M. Wantabe, and R. V. Jensen, "19-core MCF transmission system using EDFA with shared core pumping coupled via free-space optics," Opt. Express, **22** (1), 90, (2014)

[55] H. Takara, A. Sano, T. Kobayashi, H. Kubota, H. Kawakami, A. Matsuura, Y. Miyamoto, Y. Abe, H. Ono, K. Shikama, Y. Goto, K. Tsujikawa, Y. Sasaki, I. Ishida, K. Takenaga, S. Matsuo, K. Saitoh, M. Koshiba, and T. Morioka, "1.01-Pb/s (12 SDM/222 WDM/456 Gb/s) crosstalk-managed transmission with 91.4-b/s/hz aggregate spectral efficiency," in European Conf. on Opt. Commun. (ECOC), 2012, paper Th.3.C.1

[56] D. Qian, E. Ip, M.-F. Huang, M.-J. Li, A. Dogariu, S. Zhang, Y. Shao, Y.-K. Huang, Y. Zhang, X. Cheng, Y. Tian, P. Ji, A. Collier, Y. Geng, J. Linares, C. Montero, V. Moreno, X. Prieto, and T. Wang, "1.05Pb/s transmission with 109b/s/Hz spectral efficiency using hybrid single- and few-mode cores," Frontiers in Optics (FIO2012), PDP FW6C.3 (2012).

[57] R. G. H. van Uden, R. Amezcua Correa, E. Antonio Lopez, F. M. Huijskens, C. Xia, G. Li, A. Schülzgen, H. de Waardt, A. M. J. Koonen, and C. M. Okonkwo "Ultra-high-density spatial division multiplexing with a few-mode multicore fibre," Nature Photonics 8(11), pp. 865-870, (2014)

[58] Y. Sasaki, Y. Amma, K. Takenaga, S. Matsuo, K. Saitoh, and M. Koshiba, "Few-mode multicore fiber with 36 spatial modes (three modes (LP01, LP11a, LP11b) × 12 cores)," Journ. of Lightwave Tech., **33**(5), 964-970 (2015)

[59] J. Sakaguchi, W. Klaus, J.-M. D. Mendinueta, B. J. Puttnam, R.S. Luis, Y. Awaji, N. Wada, T. Hayashi, T. Nakanishi, T. Watanabe, Y. Kokubun, T.

Takahata, and T. Kobayashi, "Realizing a 36-core, 3-mode fiber with 108 spatial channels," in Optical Fiber Comm. (OFC), Th5C.2 (2015)

[60] K. Igarashi, D. Souma, Y. Wakayama, K. Takeshima, Y. Kawaguchi, T. Tsuritani, I. Morita, and M. Suzuki1, "114 Space-dvision-multiplexed transmission over 9.8-km weakly-coupled-6-mode uncoupled-19-core fibers," in Optical Fiber Comm. (OFC), Th5C.2 (2015)

[61] K. S. Abedin, T. F. Taunay, M. Fishteyn, M. F. Yan, B. Zhu, J. M. Fini, E. M. Monberg, F. V. Dimarcello, and P. W. Wisk, "Amplification and noise properties of an erbium-doped multicore fiber amplifier," Opt. Express, **19** (17), 16715, (2011)

[62] Y. Tsuchida, K. Maeda, K. Watanabe, T. Saito, S. Matsumoto, K. Aiso, Y. Mimura, and R. Sugizaki, "Simultaneous 7-core pumped amplification in multicore EDF through fibre based fan-in/out," in European Conf. on Opt. Commun. (ECOC 2012), paper Tu.4.F.2

[63] Y. Tsuchida, K. Maeda, K. Wantabe, T. Ito, K. Fukuchi, M. Yoshida, Y. Mimura, R. Sugizaki, and M. Nakazawa, "Multicore EDFA for DWDM transmission in full C-band," in Opt. Fiber Conf. (OFC/NFOEC 2013), paper JW2A.I6

[64] Y. Tsuchida, and R. Sugizaki, "Multicore erbium doped fiber amplifier for space division multiplexing," in IEEE Photonics Summer Topical Meeting 2013, paper TuC3.1

[65] H. Ono, K. Takenaga, K. Ichii, S. Matsuo, T. Takahashi, H. Masuda, and M. Yamada, "12-core double-clad Er/Yb-doped fiber amplifier employing free-space coupling pump/signal combiner module," in European Conf. on Opt. Commun. (ECOC), We.4.A.4 (2013)

[66] Y. Mimura, Y. Tsuchida, K. Maeda, R. Miyabe, K. Aiso, H. Matsuura, and R. Sugizaki, "Batch multicore amplification with cladding-pumped multicore EDF," in European Conf. on Opt. Commun. (ECOC 2012), paper Tu.4.F.1

[67] K. S. Abedin, T. F. Taunay, M. Fishteyn, D. J. DiGiovanni, V. R. Supradeepa, J. M. Fini, M. F. Yan, B. Zhu, E. M. Monberg, and F. V. Dimarcello, "Cladding-pumped erbium-doped multicore fiber amplifier" Opt. Express, **20** (18), 20191, (2012)

[68] S. Takasaka, H. Matsuura, W. Kumagai, M. Tadakuma, Y. Mimura, Y. Tsuchida, K. Maeda, R. Miyabe, K. Aiso, K. Doi, and R. Sugizaki, "Cladding-pumped 7-core EDFA using a multimode pump light coupler," in European Conf. on Opt. Commun. (ECOC 2013), paper We.4.A.5

[69] B. Zhu, T. F. Taunay, M. Fishteyn, X. Liu, S. Chandrasekhar, M. F. Yan, J. M. Fini, E. M. Monberg, and F. V. Dimarcello, "112-Tb/s Space-division multiplexed DWDM transmission with 14-b/s/Hz aggregate spectral efficiency over a 76.8-km seven-core fiber," Optics Express, 19 (17), 16665-16671 (2011).

[70] W. Klaus, J. Sakaguchi, B. J. Puttnam, Y. Awaji, N. Wada, T. Kobayashi, and M. Watanabe, "Free-space coupling optics for multicore fibers," IEEE Photonics Technology Letters, **24**(21), 1902, (2012).

[71] R. R. Thomson, H. T. Bookey, N. D. Psaila, A. Fender, S. Campbell, W. N. MacPherson, J. S. Barton, D. T. Reid, and A. K. Kar, "Ultrafast-laser inscription of a three dimensional fan-out device for multicore fiber coupling applications," Optics Express 15(18), 11691-11697 (2007).

[72] B. Zhu, T. F. Taunay, M. F. Yan, J. M. Fini, M. Fishteyn, E. M. Monberg,

and F. V. Dimarcello, "Seven-core multicore fiber transmissions for passive optical network," Opt. Express, **18**(11), 11117-11122 (2010)

[73] N. Wada, J. Sakaguchi, W. Klaus, B. J. Puttnam, R. Luis, J. M. D. Mendinueta, and Y. Awaji, "Space division multiplexing (SDM) transmission and related technologies," in Telecommunications Network Strategy and Planning Symposium (Networks), 1-6 (2014)

[74] G. A. Mahdiraji, F. Amirkhan, D. M. Chow, Z. Kakaie, P. S. Yong, K. D. Dambul, and F. R. M. Adikan, "Multicore flat fiber: a new fabrication technique," IEEE Photonics Tech. Lett., **26**(19), 1972-1974 (2014)

[75] N. S. Bergano, "Undersea fiber optic cables –Enabling a connecting world," in Opt. Fiber Commun. Conf. (OFC) Planery session, (2015).

[76] S. Jain, T. C. May-Smith, A. Dhar, A. S. Webb, M. Belal, D. J. Richardson, J. K. Sahu, and D. N. Payne, "Erbium-doped multi-element fiber amplifiers for space-division multiplexing operations," Optics Letters, 38 (4), 582-584 (2013).

[77] S. Jain, T. C. May-Smith, A. Dhar, A. Webb, B. Usmani, J. K. Sahu, "Gain and noise figure study of Er-doped multi-element fiber amplifier," in Asia Communications and Photonics Conference (ACP) Guangzhou, China 7-10 November, ATh2A.1, 2012

[78] S. Jain, T. C. May-Smith, and J. K. Sahu, "Er/Yb-doped cladding-pumped multi-element fiber amplifier," in Workshop on Specialty Optical Fibers and Their Applications, W5.4, (2013)

[79] S. Jain, N. K. Thipparapu, P. Barua, and J. K. Sahu, "Cladding-Pumped Er/Yb-Doped Multi-Element Fiber Amplifier for Wideband Applications," IEEE Photonics Technology Letters, 27 (4), 356 - 358 (2015)

[80] S. Jain, T. C. May-Smith, J. K. Sahu, "Cladding-pumped Er/Yb-doped Multi-Element Fiber Amplifier for C+L band Operations," Optical Fiber Communications (OFC) San Francisco 9-13 Mar, M2J.3, 2014

[81] S. Jain, Y. Jung, T. C. May-Smith, S. U. Alam, J. K. Sahu, D. J. Richardson, "Few-mode multi-element fiber amplifier for mode division multiplexing," Optics Express, 22(23), 29031-29036, (2014)

[82] S. Jain, V. J. F. Rancaño, T. C. May-Smith, P. Petropoulos, J. K. Sahu, D. J. Richardson, "Multi-element fiber for space-division multiplexing operations," Optics Express, **22**(4), 3787-3796 (2014)

[83] S. Jain, T. C. May-Smith, V. J. F. Rancaño, P. Petropoulos, D. J. Richardson, J. K. Sahu, "Multi-element fibre for space-division multiplexed transmission, " in European Conference on Optical Communications, London 22-26 Sep, Mo.4.A.2, 2013

[84] V. J. F. Rancaño, S. Jain, T. C. May-Smith, J. K. Sahu, P. Petropoulos, D. J. Richardson, "First demonstration of an amplfied transmission line based on multi-element fibre technology," in European Conference on Optical Communications, London 22-26 Sep, PD1.C.2, 2013 (Postdeadline)

[85] S. Yan, E. Hugues-Salas, V. J. F. Rancano, S. Yi, G. Saridis, B. Rofoee, Y. Yan, A. Peters, S. Jain, T. May-Smith, P. Petropoulos, D. J. Richardson, G. Zervas, and D. Simeonidou, "First Demonstration of All-Optical Programmable SDM/TDM Intra Data Centre and WDM Inter-DCN Communication," in ECOC, PD.1.2, (2014).

Chapter-3

Core-Pumped Er-doped Multi-element Fibre Amplifier

3.1. Introduction

Development of a SDM amplifier is critical to realisation of the SDM transmission system and further helps towards the integration of other components of the system. In particular, core-pumped SDM amplifiers have been given significant attention by the scientific community. Core-pump amplifier can help reduce the complexity of the network which increases with the increase in the number of components. Up to 19-core and 7-core MCF amplifiers with core-pumping have been demonstrated using free space coupling and tapered fibre coupler respectively [1-3]. The use of coupler results in higher losses and crosstalk when compared with free-space coupling.

In this chapter, Core-pumped MEF amplifiers (MEFA) have been proposed and

demonstrated for SDM amplifiers. A general fabrication procedure of MEF has been discussed. Core-pumped MEFAs with 3-MEF and 7-MEF comprising 3 and 7 Er-doped fibre-elements respectively has been demonstrated. The gain and noise figure (NF) performance of MEFAs have been measured in section 3.3.2. The ability of MEFA to tune the gain profile of amplifier has been demonstrated in section 3.3.2.4. Fig. 3.1 shows the cross-sectional image of an Er-doped 7-MEF with OD of 460μm.

Fig. 3.1 Microscope image of a Er-doped 7-MEF showing the arrangement of 7 fibre-elements in the high index coating

3.2. MEF Fabrication

Starting from conventional preform, MEF fabrication is divided into two steps. The first step involves making MEF preform assembly and 2nd step involves drawing of preform assembly into MEF. However, a method of stacking the preforms on tower can be developed which would eliminate the first step of MEF preform assembly (see section 5.3.1).

3.2.1. MEF Preform Assembly

Figure 3.2 shows the schematic of steps involved in the MEF preform assembly for a general X-MEF, where, X is the number of fibre-elements. Here, 3-MEF preform assembly is considered. At first, MEF preform assembly requires stretching of the fabricated preform to obtain the desired preform-element diameter. This can be performed on standard glass working lathe (GWL) machine, which consists of a burner, headstock, tailstock, and temperature controller. Burner and tailstock can be moved relative to each other to stretch the preform to the desired diameter. The tailstock speed, V_t, for a given initial preform diameter, D_i, final diameter, D_f, and burner speed, V_b, can be obtained using the equation 3.1.

$$V_t = V_b\left(1-\left\{\frac{D_f}{D_i}\right\}^2\right) \tag{3.1}$$

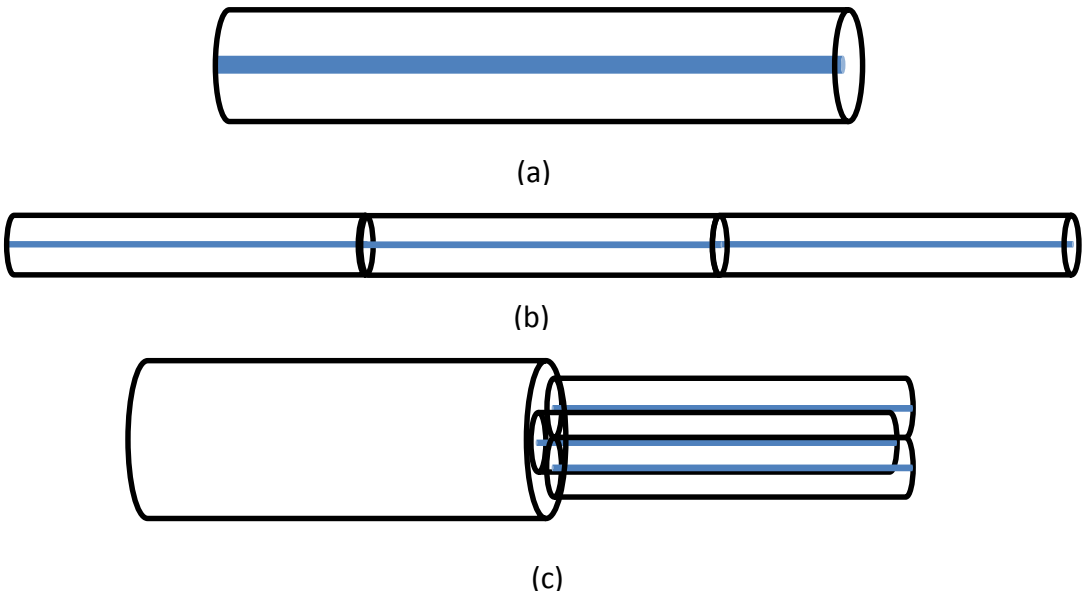

Fig. 3.2 Schematic of 3-MEF preform assembly with processing steps starting with the a) fabricated preform, b) stretching and cutting of preform, and c) stacking in the desired MEF assembly

The stretching operation is carried out in multiple steps to gradually reduce the diameter. As the diameter of the preform decreases it becomes difficult to stretch the preforms because at low diameter the preforms start to flex due to its own weight. This, in-turn changes its position in the flame during stretching. This introduces the diameter fluctuation in the stretched preform and limits the stretchable length. For this reason, the preform stretching was performed at temperatures as low as 1400^{o}C to minimize the fluctuation in the diameter during the process.

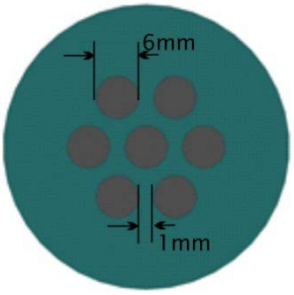

Fig. 3.3 Top view of the jig used for holding the 6mm preforms and fabricate the MEF assembly

After stretching the preforms to a desired diameter, it is cut into desired pieces of equal length. These preforms are then stacked to obtain the MEF assembly. For this purpose, plastic jigs were fabricated to hold the preforms in a desired structure as shown in the Fig. 3.3.

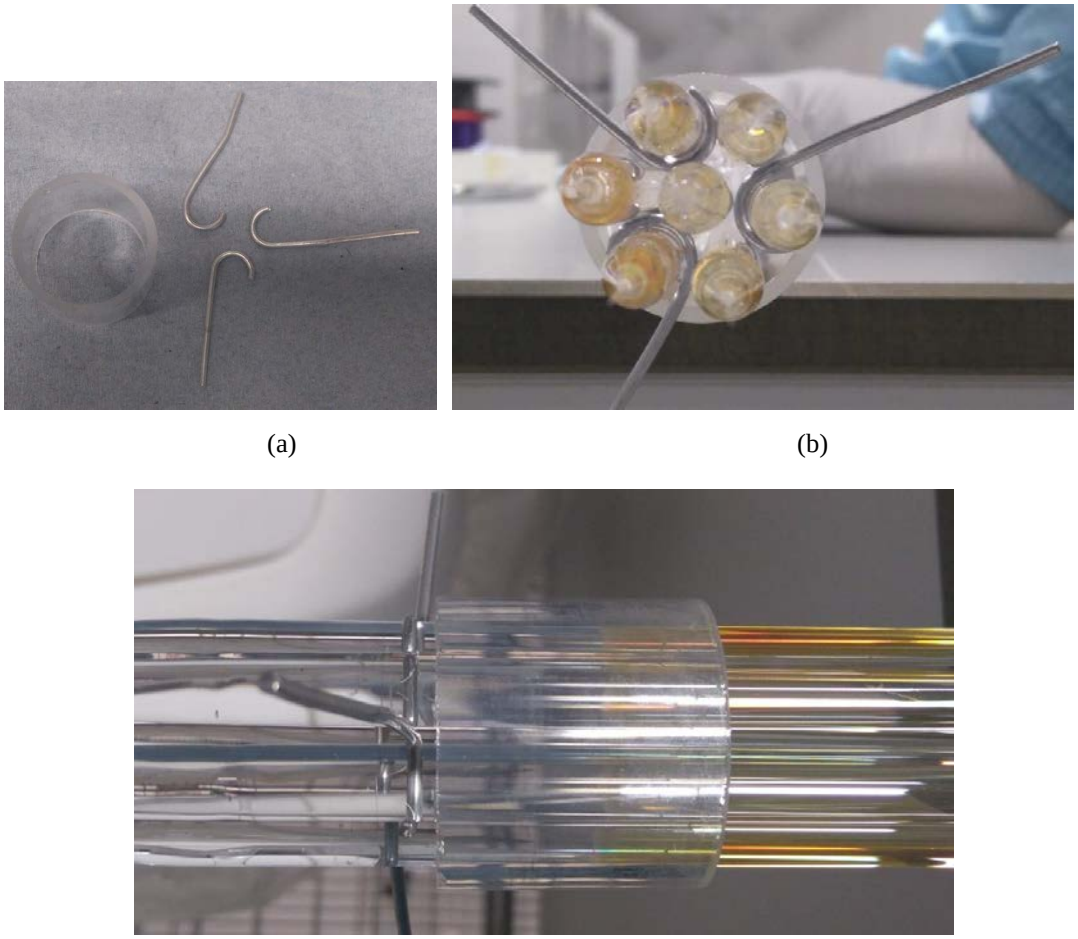

(a) (b)

(c)

Fig. 3.4 (a) Metal hooks and glass tube used to maintain the separation while assembling the preform, (b) front and (c) side view of metal hooks and glass tube placed on the assembly at the handle end

The jig holds the preform on one side and the assembly is joined to the handle on other side using metal hooks and glass tube to maintain the geometry. The J-shaped metal hooks of 0.8 mm diameter were used to keep the separation between the preform-elements in the assembly, whereas, glass tube was used to keep the preform-elements from diverging out. Fig. 3.4 shows the metal hooks used and their placement on the MEF preform assembly. This prevented any stress build up in assembly. The stress can result in the expansion or contraction of assembly in the furnace during fibre fabrication. Separation between the preform-elements in the assembly is required to prevent the assembly from collapsing during the MEF drawing. Although, the separation between the preform-elements can be kept larger but given the size of our furnace it was kept around 1mm (see section 3.2.2). The metal hooks and glass tube could be easily removed from same side. Finally, the jig is removed and a drop is joined on other side of the preform.

3.2.2. MEF Drawing

To draw MEF from preform assembly into fibre, a conventional fibre drawing tower was used. A brief description of the conventional fibre drawing procedure has been mentioned below [4].

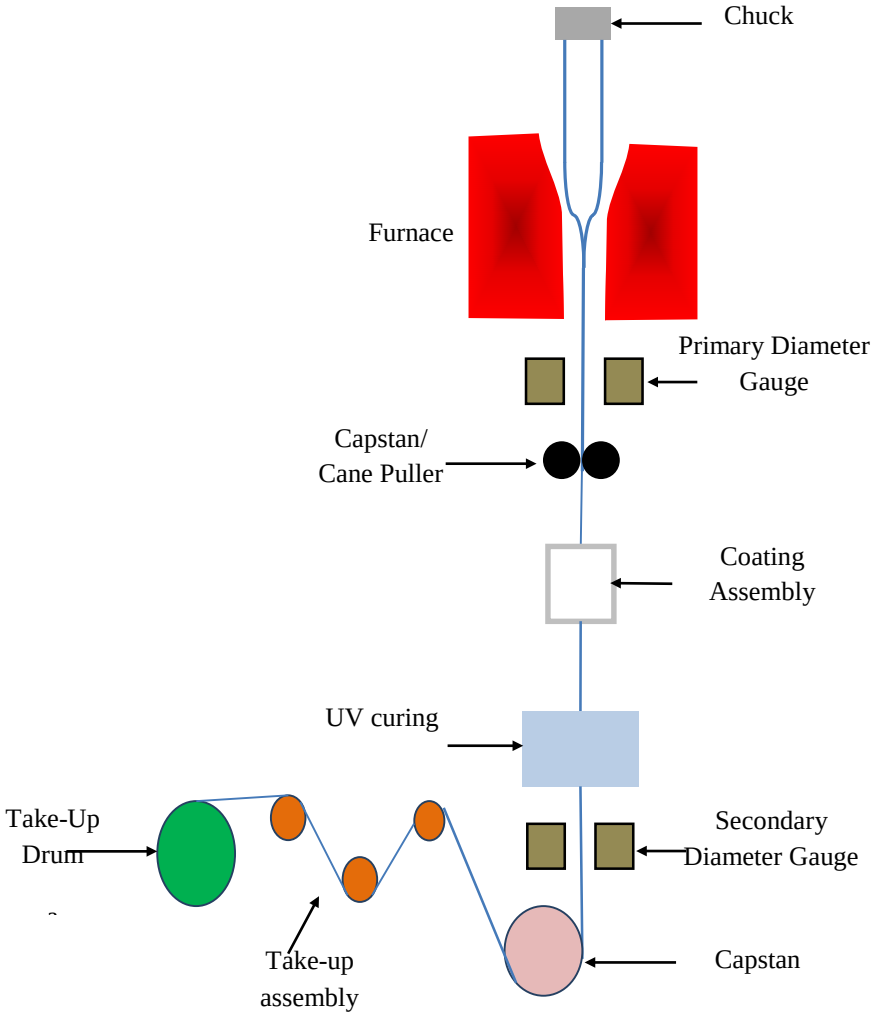

Fig. 3.5 Schematic of conventional fibre drawing tower

Preform goes into the pre-processing stage before executing the drawing process. A handle and a drop are attached to the preform. Drop is used as a weight to initiate the necking in the preform. Figure 3.5 shows the schematic diagram of fibre fabrication tower. At first, the fibre drawing furnace is purged using the inert Argon gas to prevent contamination during drawing process and reduce any turbulent flow of gasses inside the furnace. The turbulent flow in the furnace could lead to fragility of fibre and significant diameter fluctuation during the fibre drawing [4]. The preform is fitted into

the chuck with handle on top and drop on the bottom, and is fed into the furnace. Then, the furnace is ramped to the drop temperature. In silica, this temperature is typically in the range of 1900-2200^{o}C depending on the size of the drop.

The drop temperature is set above the glass softening temperature at which the drop starts falling due to gravity resulting in the formation of neck in the preform. After this, the drop is cut from the preform. Resulting thin cane from the neck is then fed into the tractor/cane puller. The cane puller further reduces the diameter of the glass rod being pulled. The diameter of the fibre being pulled from the glass can be obtained using conservation of mass, and is given by equation 3.2.

$$D_f = D_p * \left(\frac{V_i}{V_f} \right)^{1/2} \tag{3.2}$$

Where, D_f is diameter of the fibre, D_p is the diameter of the preform, V_f is fibre drawing speed, and V_i is the feed speed of the preform. The primary diameter gauge before the cane puller is used to monitor the bare fibre diameter, and allow feedback for diameter control in case there are diameter fluctuations in the preforms. After this, the bare fibre is coated using the acrylate polymer. Two types of polymer coating are used; low-index coating and hi-index coating, depending on the required application, and dual-coating is applied in commercial telecomm fibres. The fibre is fed into the coating assembly consisting of an entry and an exit die. Here, only pressurized coating assembly with single coating was used for the fabrication of all the amplifier fibres in discussion. Apart from the entry and exit die diameters, the thickness of the coating also depends on the fibre diameter, temperature of the coating material and the coating pressure inside the coating die assembly. After this, the fibre is passed through an UV curing chamber to cure the wet coating. Then, it is fed into the capstan through secondary diameter gauge, which then applies the force to pull the fibre, and the cane puller is released. Finally, it is sent to the take-up assembly for collection. The secondary diameter gauge records the coated diameter of the fibre, which gives the information about the coating thickness. The coating thickness can then be controlled by varying the temperature and pressure of the coating assembly system.

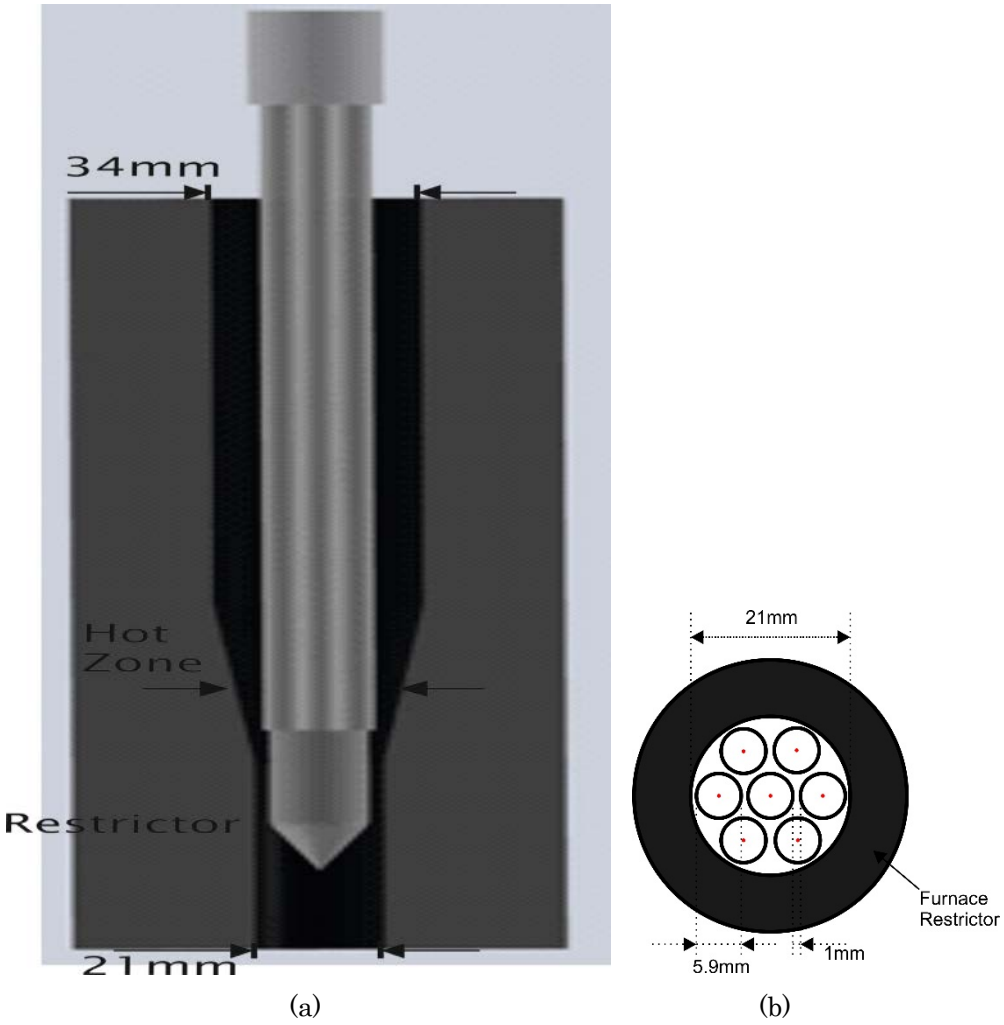

Fig. 3.6 (a) Placement of MEF assembly in the furnace with furnace dimensions, (b) bottom view of the restrictor with 7-MEF preform assembly inside

Fig. 3.6 (a) shows the schematic of a loaded 7-MEF preform assembly inside the furnace. The diameter of the preform-elements is limited by the dimensions of restrictor tube, in the lower part of the furnace. With a 21mm restrictor tube diameter and including the separation between the furnace and preform assembly, the maximum allowed diameter of preforms in 3-MEF and 7-MEF assembly is 8.8mm and 5.9mm (see Fig. 3.6 (b)) respectively. It should be noted that the assembly also requires that the gap should be maintained between the preform-elements to prevent them from collapsing with each other. In MEF fabrication, cladding diameter of one of the fibre-element is observed from primary diameter gauge. Currently, there is no way to control the cladding diameter of the fibre-elements individually. However, the cladding diameter variation from element-to-element in MEF is expected to be negligible as the diameter of all the preform-elements in the assembly is same, and all the fibre-elements

are expected to have same diameter because of conservation of mass.

In a single high-index coating (Desotech DSM 314-1) system, the preform was conventionally drawn (without any spin) as well as spun slowly. The spinning of preform assembly allowed the fibre-elements to coil together providing compactness to the MEF. It was observed that this provided better coating uniformity due to the fact that fibre-elements were not moving in the coating applicator during fabrication. In case of drawing without any spinning, fibre-elements were not stable in the coating applicator i. e. they were changing their position in the coating cup. This resulted in the non-uniform coating of the MEF. It should be noted that in case of passive MEF fabrication the preform assembly is not spun but uniformity is attained by applying the dual coating and optimising the fabrication conditions (see Chapter-5).

3.3. Core-pumped MEFA

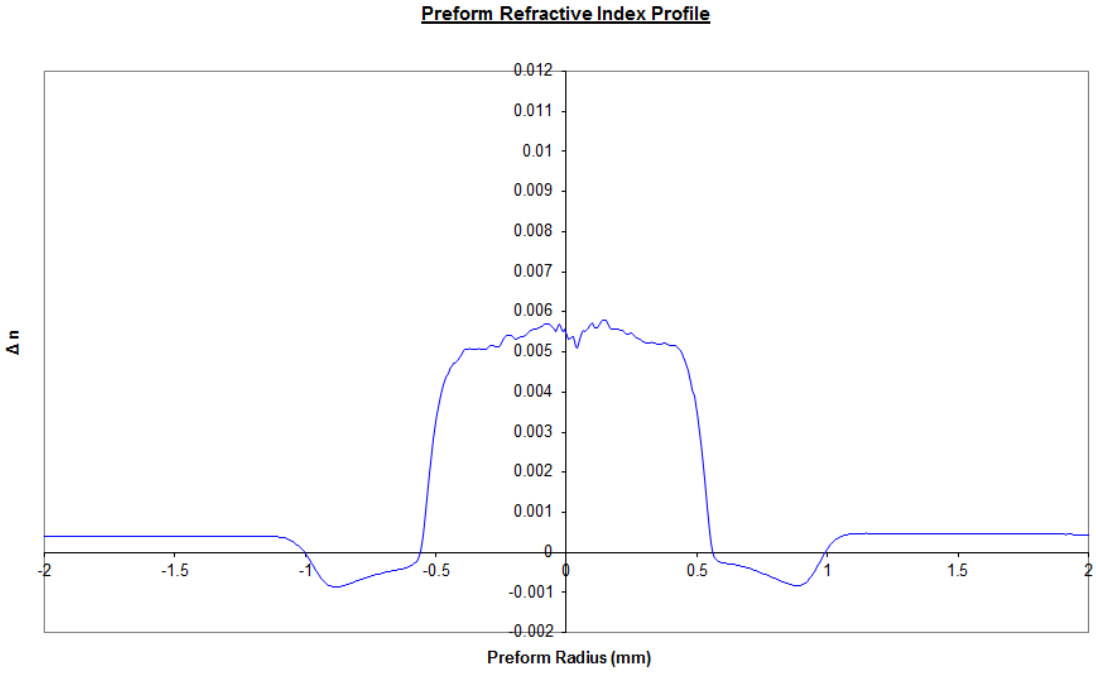

Fig. 3.7 Refractive Index profile of L10057

Er-doped 3-element MEF (3-MEF) and 7-MEF were assembled from two preforms, L10057 and L10058 respectively, which were fabricated by Dr. Anirban Dhar using, modified chemical vapour deposition (MCVD)-solution doping technique. The preform cores were doped with aluminium (Al) and Er ions, producing a measured refractive index step (Δn) of 0.0055. The refractive index profile (RIP) of L10057

preform is shown in Fig. 3.7., and L10058 had similar RIP.

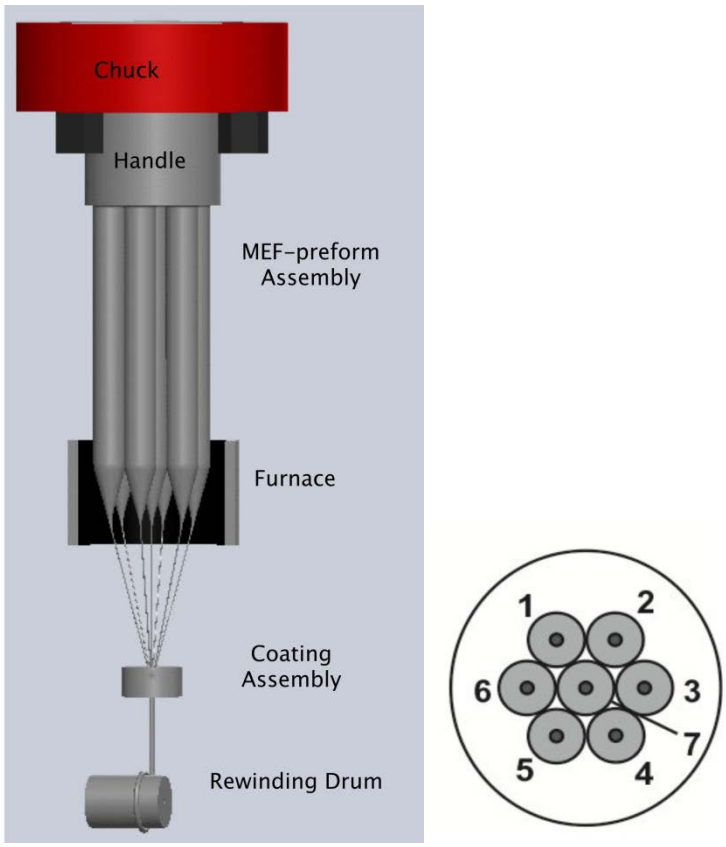

(a) (b)

Fig. 3.8 (a) Schematics of a 7-MEF draw, and (b) Indexing of fibre-elements in 7-MEF

The preforms were stretched and cut into sections of equal length to allow their stacking in the required 3-MEF and 7-MEF configurations. A support handle was joined to the stacks to allow simultaneous drawing of the fibre-elements as shown in Fig. 3.8 (a). The fibres were coated together in single coating with a high-index polymer (Desotech DSM-314). 3-MEFs and 7-MEFs were drawn at different rotation speed of the preform and with different fibre-element diameter. Table 3.1 lists the different fibres drawn by varying diameter of the fibre-element and rotation pitch in the MEF. Initially, Er-doped 3-MEF and 7-MEF in core-pump configuration, and fibre rotation pitch of about 7cm and 16cm respectively, were characterised. The cladding diameter of fibre-elements of both MEFs was 125µm, resulting in a core diameter of 11µm and overall coated diameter of 310µm and 460µm for 3-MEF and 7-MEF respectively. Note that, as opposed to MCF, the core-pumped MEF approach is highly tolerant to any imperfection in fibre geometry due to the independent nature of the individual elements and the means of interconnection.

Table 3.1 List of Core-pump fabricated MEFs

Fibre Type	Fibre No.	Draw Temp. (°C)	Diameter (μm)	Draw Speed (m/min)	Rotation Speed (rpm)	Rotation Pitch (cm)
3-MEF	A0172	2060	125	1	0	Straight
				1	14	7
			100	5	0	Straight
				5	48	5
				5	70	7
7-MEF	A0184	2065	125	4.8	0	Straight
				4.8	30	16
			100	4.8	0	Straight
				4.8	30	16

To enable indexing of the different fibre-elements in the MEFs, the elements were identified by observing one end under a microscope while launching light in the different fibre-elements from the other end. A schematic of the cross-section of the 7-MEF with the relative positions of the fibres and their identifying numbers is shown in Fig. 3.8 (b), and the microscopic image of 7-MEF is shown in Fig. 3.1. Hereafter, when referring to a fibre-element, following nomenclature would be used: X-F_n, where X denotes the number of elements in the MEF and n is the identifier for the elements within that MEF; for example, 7-F_3 denotes fibre number 3 of the 7-MEF.

3.3.1. Experimental Setup for Core-pumped MEFA

The gain, NF and crosstalk was measured using the experimental setup as shown in Fig. 3.9. It was assumed that the excess noise arising in the amplifier is only dominated by the ASE noise which is the case in high gain optical amplifiers [5]. The standard equations as shown below was used for the characterisation of amplifier performance [6].

$$Gain(dB) = 10 \times \log_{10} \frac{P_{out}}{P_{in}} \tag{3.3}$$

$$NF(dB) = \frac{N_{out} - GN_{in}}{h\nu GB_w} + \frac{1}{G} \tag{3.4}$$

Where, P_{out}, P_{in}, N_{out}, and N_{in} are the signal power and noise power for output and input signals respectively. B_w is the noise resolution bandwidth of the optical spectrum analyser (OSA) expressed in Hertz. The noise bandwidth was set to 0.5nm in the OSA

[7]. The spectra in the OSA were calibrated to match the output power values measured with Exfo FoT-90A power meter. To obtain output power measured by OSA, a spectrum with -10dBm signal power at 1550nm was used and the total power was calculated through the area under curve of spectral power density spectrum.

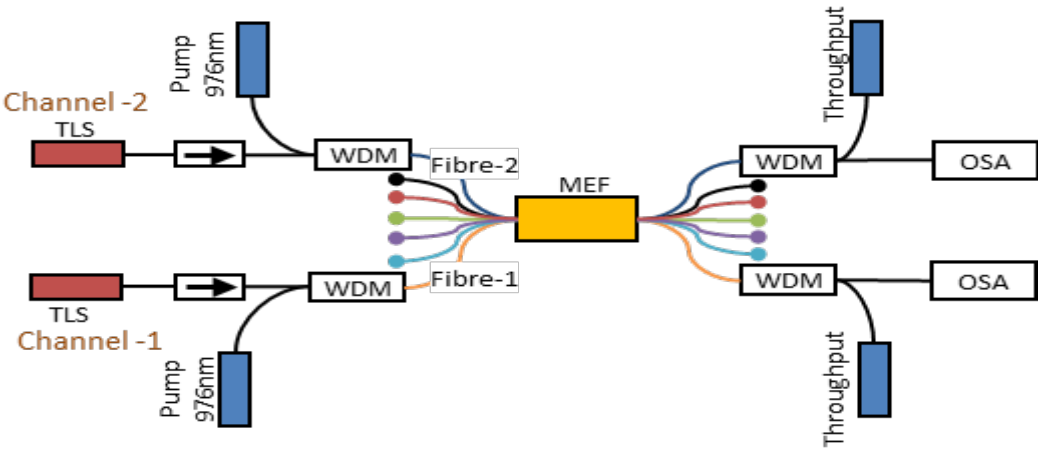

Fig. 3.9 Experimental setup for measuring gain, noise figure and crosstalk containing channel-1 (ch-1) and channel-2 (ch-2)

The setup comprised an Agilent-8164B tuneable laser source (TLS) for input signals in the C-band; a JDS Uniphase laser-diode (LD) as a pump source at a wavelength of 976nm; isolators at a wavelength of 1550nm as a protection for the TLS, and 980/1550nm wavelength division multiplexers (WDM) at the input/output to combine/separate the signal and the pump. The input and output signals for different wavelengths were measured by the OSA. The spectra obtained were then used to calculate the gain and NF of each fibre-element of the MEF under test. Performance for all the fibre-elements of 3-MEF and 7-MEF were calculated using ch-1, as shown in Fig. 3.9, for input signals of -10dBm, -15dBm, -20dBm and -23dBm at wavelengths of 1530nm, 1540nm, 1545nm and 1550nm.

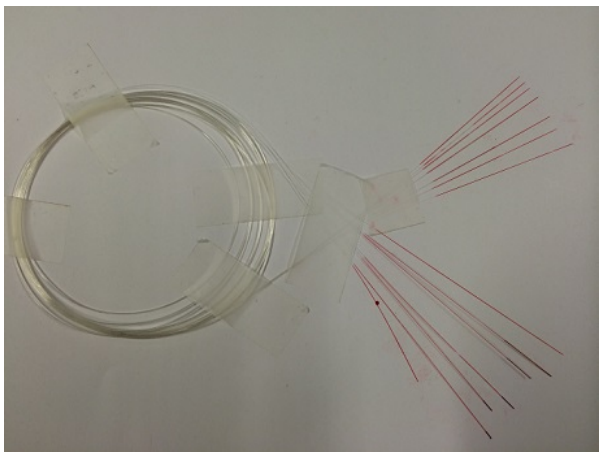

Fig. 3.10 7-MEF sample with fibre-elements fanning out after its coating is removed.

At first, the coating from each end of MEFs were stripped-off. In MEFs, the fibre-elements fan-out after their coating is removed. Figure 3.10 shows one such example of a MEF with fibre-elements fanning out of a 7-MEF sample. SMF pigtails were then spliced to each fibre-element on both sides using fusion splicing.

3.3.2. Result and Analysis

The gain and NF performance of both 3-MEF and 7-MEF core-pumped amplifiers have been characterised in this section [8, 9]. The crosstalk has also been measured in both MEFs.

3.3.2.1. 3-MEF Amplifier

The amplifier was developed with a 3m of MEF length. A maximum available pump power of 172mW (45mW throughput) was used. 3m Er-doped fibre was used because it provided an amplified spontaneous emission (ASE) spectrum corresponding to C-band amplification with peak around 1531nm and flat region around 1550nm. ASE spectra of one of the fibre-element is shown in the inset of Fig. 3.10. The ASE has a maximum around 1530nm and a flat region around 1545nm. This spectrum was typical of all the fibre-elements contained within each MEF with their Er absorption at 980nm being approximately 10dB/m.

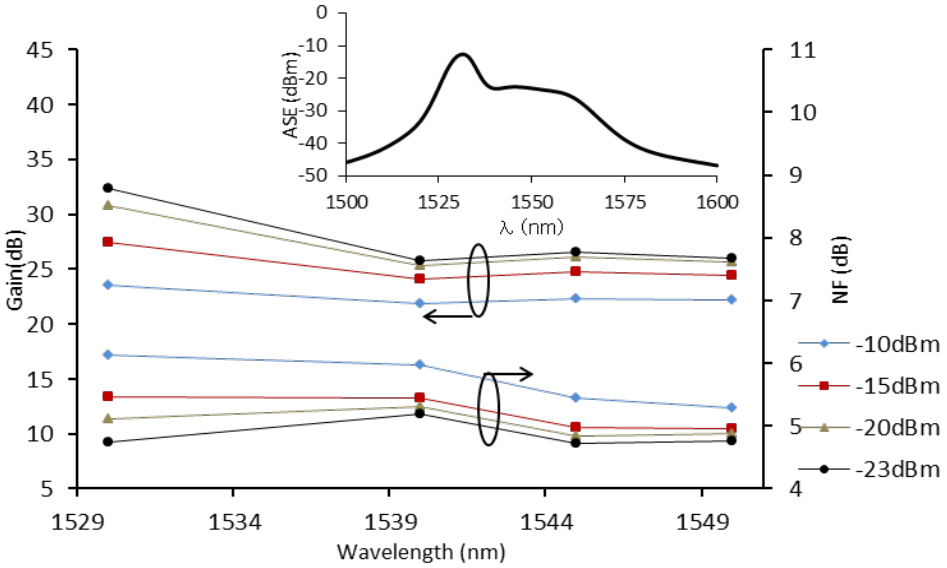

Fig. 3.11 Performance of 3-F_2 at different input signal levels with a pump power of 172mW. The inset shows the corresponding ASE spectrum for the same pump power.

Table 3.2 shows the gain and NF characterisation of 3-MEF (spun, element diameter of 125μm) for an input signal of -23dBm. The performance characteristics of all the fibre-elements in the 3-MEF were similar with gain and NF in the range of 32.2-32.8dB and 4.2-4.8dB respectively, for an input signal of -23dBm at 1530nm. Fig. 3.11 shows the gain and NF variation for 3-F_2.

Table 3. 2 Gain and NF for 3-MEF measured at different wavelengths for an input signal level of -23dBm

Wavelength (nm)	Gain(dB)			NF(dB)		
	3-F_1	3-F_2	3-F_3	3-F_1	3-F_2	3-F_3
1530	32.2	32.3	32.8	4.8	4.7	4.2
1540	25.3	25.7	26.5	5.4	5.2	4.7
1545	25.7	26.5	27.1	5.4	4.7	4.5
1550	25.4	26.0	26.9	5.3	4.8	4.4

The crosstalk was measured for the 3-MEF using both ch-1 and ch-2 as shown in Fig. 3.9. Agilent and Photonetic Tunic-BT TLSs were used as input signal sources in ch-1 and ch-2 respectively. The maximum pump power launched in ch-2 was 244mW and -7dBm of input signal was used to measure crosstalk. The two sources were initially compared using ch-1. Gain and NF for -7dBm of input signal at a wavelength of 1530nm was 21.1dB and 5.8dB respectively for the Agilent TLS, compared with 21.8dB and 6.3dB respectively for the Photonetic TLS. As shown in table 3.3, various permutations of pump and signal states (on/off) were considered in order to measure the crosstalk between two channels operating at wavelengths of 1530nm (ch-1) and 1531nm (ch-2). For crosstalk in 3-MEF, all the possible fibre-pairs (3-F_1↔3-F_2, 3-F_1↔3-F_3 and 3-F_2↔3-F_3) were considered. First ch-1 was monitored, followed by ch-2 to confirm there was no influence on the measurements due to the choice of channel being monitored.

Table 3.3 Pump and signal permutation in ch-1 and ch-2 for crosstalk measurement in 3-MEF for the case of ch-1 being monitored (Subscript 1 and 2 for pump (P) and signal (S) correspond to ch-1 and ch-2 respectively)

Case	P_1	P_2	S_1	S_2	Output (Ch-1)
1	ON	OFF	ON	OFF	Amplified Signal in ch-1
2	ON	OFF	ON	ON	No Change
3	ON	ON	ON	ON	No Change
4	ON	ON	OFF	ON	Only ASE of Ch-1
5	OFF	ON	OFF	ON	OSA noise in Ch-1

Taking the example of ch-1 being monitored, starting with case-1, the pump and signal in ch-1 was switched on to record the amplified signal. Then, in case 2, the signal in ch-2 was switched on at -7dBm to record any changes observed in the amplification in ch-1; <0.05dB change in the amplified signal was observed, which is well within error range. After this, P_2 was switched on but no change was observed. Following this, the signal and pump in ch-1 were shut-off one after another as shown in case 4 and 5. In fact, there was only ASE observed when pump in both channels at their respective maximum power and signal in ch-2 were switched-on. No ASE or signal leakage observed between the fibres of 3-MEF.

3.3.2.2. 7-MEF Amplifier

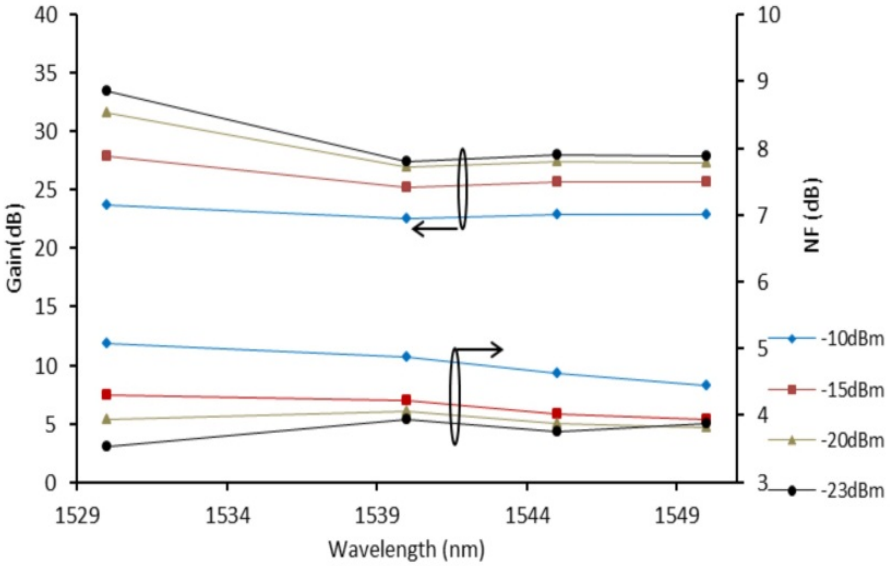

Fig. 3.12 Gain and NF variation for 7-F4 with wavelength, at different input signal levels using a pump power of 172mW

Likewise, Gain and NF measurements were made for all 7 fibre-elements of the 7-MEF (spun, element diameter= 125μm) using a similar pump power (172mW) as used in the case of 3-MEF experiments, and 3m of 7-MEF. Fig. 3.12 shows the gain and NF variation for 7-F_4. Table 3.4 shows the results obtained for all fibre-elements of 7-MEF for -23dBm input signal. The gain and NF for all the fibres were found to be in the range of 32.5-33.5dB and 3.3-4.0dB respectively, for an input signal level of -23dBm at a wavelength of 1530nm. The gain and NF variation of all the fibre-elements of 7-MEF was slightly better than the 3-MEF mainly due to the different preforms used for their fabrication.

Table 3.4 Gain and NF for 7- MEF for -23dBm input signal at different wavelengths

Wavelength	Gain (dB)						
(nm)	7-F_1	7-F_2	7-F_3	7-F_4	7-F_5	7-F_6	7-F_7
1530	33.0	32.5	33.5	33.4	32.5	33.0	33.0
1540	26.9	26.5	28.0	27.4	26.3	27.6	27.0
1545	27.5	27.0	27.0	27.0	26.9	28.2	27.6
1550	27.2	26.8	26.8	26.8	26.7	28.1	27.4
Wavelength	NF (dB)						
(nm)	7-F_1	7-F_2	7-F_3	7-F_4	7-F_5	7-F_6	7-F_7
1530	3.3	3.7	3.7	3.5	3.4	4.0	3.7
1540	3.6	4.0	4.0	4.0	3.9	4.4	4.0
1545	3.4	3.9	3.8	3.8	3.7	4.2	3.8
1550	3.6	4.0	4.0	3.9	3.8	4.3	3.9

To measure the crosstalk in 7-MEF, a similar procedure of taking different pump and signal permutations was followed as in the case of 3-MEF. First, three fibre-pairs comprising randomly chosen fibre-element, 7-F_7, and any one of 7-F_1, 7-F_2 and 7-F_6 were considered. 7-F_1 was observed to have relatively higher bend sensitivity, as observed during gain and NF measurements and all the possible fibre-pair combinations with 7-F_1 were then considered. There was no signal or ASE crosstalk between the fibre pairs in 7-MEF, which is expected from the fibre geometry of MEFs.

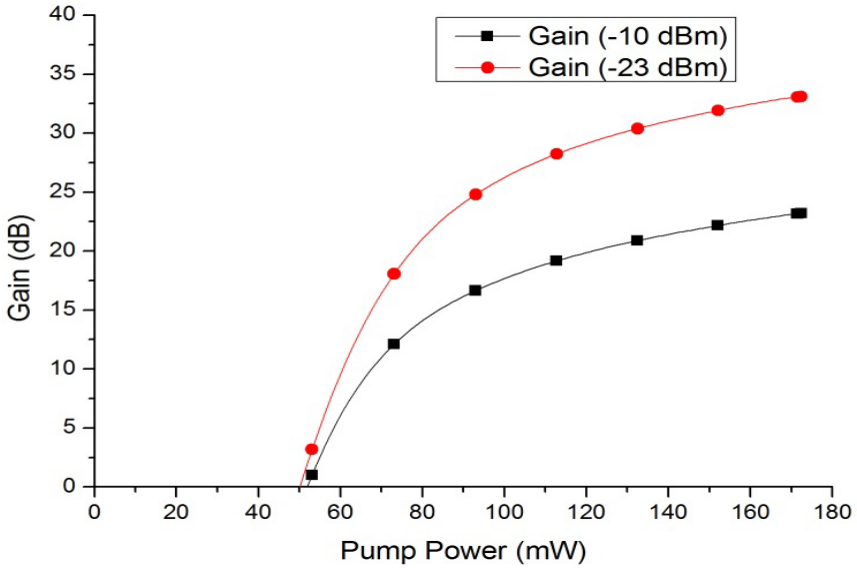

Fig. 3.13 Pump power vs gain measured for -10dBm and -23dBm input signal at 1530nm

The graph of pump power vs gain was also plotted in Fig. 3.13 using two different input signals -10dBm and -23dBm at a wavelength of 1530nm for 7-F_6. From this graph, it can be commented that the gain is limited by available pump power, and increase in the pump power may provide improvement in gain of the amplifiers.

3.3.2.3. Straight vs. Spun

Table 3.5 Gain for spun and straight 3-MEFs with -23dBm of input signal

Wavelength (nm)	Gain(dB) Input (-23 dBm)	
	Spun	Straight
1530	31.7-32.6	32.4-32.9
1540	25.6-26.9	26.7-27.1
1545	25.8-27.1	26.9-27.4
1550	25.4-26.7	26.0 -26.5

The gain performance was compared for 3-MEFs with 100μm fibre-element diameter for straight and spun (7cm pitch) respectively with 172mW of pump power in a 3m MEF. Table 3.5 shows the gain in both cases. The range corresponds to the element-to-element variation in the MEFA. There was no significant variation of gain characteristics in spun fibre as compared to straight fibre. The variation was <1dB which is within the error limits of the measurement. It could be concluded from this that spinning did not induce any detrimental effects on the amplifier performance. The performance of core-pumped MEF is highly tolerant to geometrical imperfections. The results of the 7-MEF were not measured. However, they are also expected to be similar for spun and straight MEF scenario.

3.3.2.4. Gain profiling in core-pumped MEFA

Besides enabling the integration of multiple amplifiers for SDM applications, core-pumped MEFA also enables flexibility of changing the length of the fibre in the amplifier. This in turn allows for the gain profiling of the amplifier. The fibre elements were cascaded in series by connecting the output of one element to the input of the next, and the variation in the gain profile was observed [10, 11]. The schematic of cascaded MEFA for 2-element cascade is shown in Fig. 3.14. SMFs were spliced to each fibre-element on both sides. The output of element-1 was spliced to input of element-2. The cascaded amplifier was pumped bi-directionally.

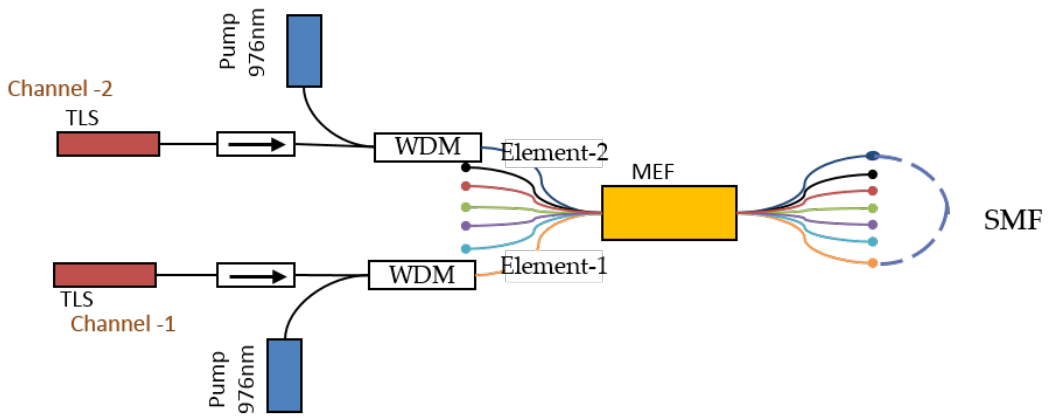

Fig. 3.14 Schematic of 2-element cascade using bi-directional pumping showing the fibre-elements connected by splicing using SMFs

The gain profile and NF of the amplifier using 2-elment cascade with a total pump power of 208mW and 250mW have been shown in Fig. 3.15. For an input signal power of −23 dBm, the average gain in the C-band was 30 dB with a gain variation of ±1.5dB. Moreover, the NF was less than 4.5 dB for the entire C-band. As expected, the gain in the 2-element cascade shifted towards longer wavelength compared to the single element, while reducing the gain at 1530 nm [10].

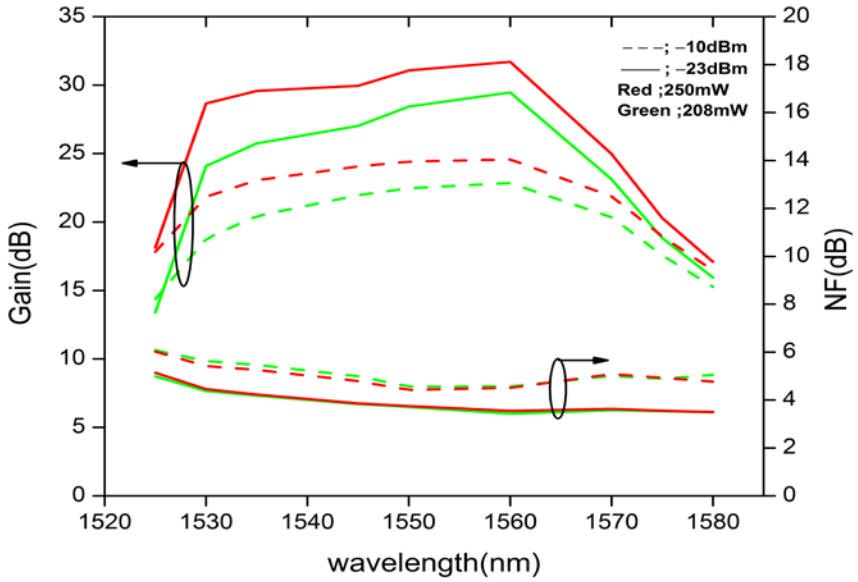

Fig. 3.15 Gain and NF characteristics of the 2-element cascade at pump powers of 208 mW and 250 mW.

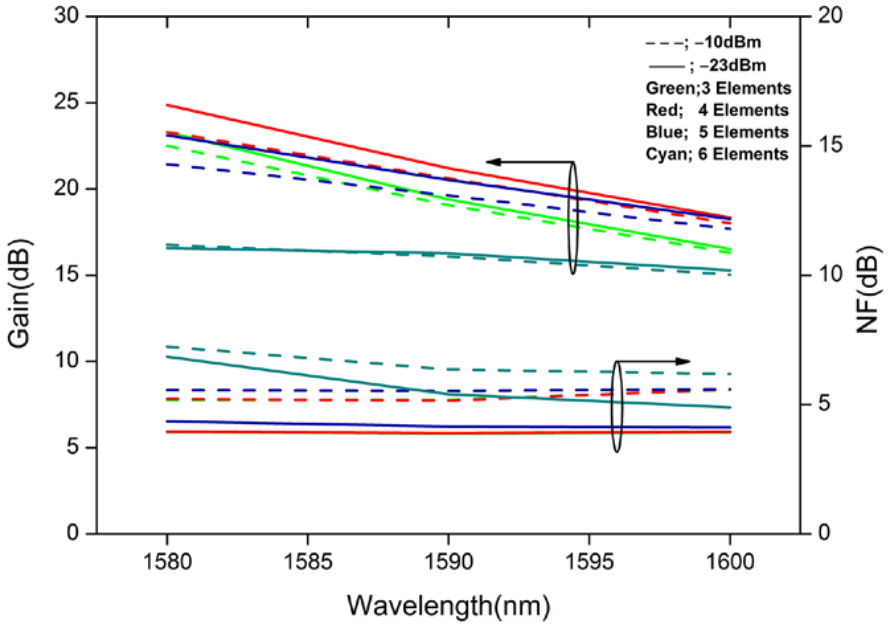

Fig. 3.16 Gain in L-band for different cascades for 320mW of pump power

Similarly, the gain in the L-band was enhanced by cascading more number of fibre-elements. Figure 3.16 shows the gain of different cascades in L-band for total pump power of 320mW. It was observed that the available pump power was not sufficient to provide efficient gain for a cascade containing more than 4 fibre elements. The 4-element cascade in 7-MEF provided the maximum gain in the L-band using bi-directional pumping with a total pump power of 320 mW (forward pump power: 170 mW, backward pump power: 150 mW). A minimum gain of 20 dB and NF less than 4 dB were observed from 1580 to 1595 nm with the input signal power of -23 dBm. Further increase in either forward or backward pump power did not improve the performance of the 4-element cascade amplifier. This tuning characteristic could be used to develop a split broadband amplifier. 3 lines of different amplifier employing single element, 2-element cascade and 4-element cascade could be used to amplify signals in 1520-1530nm, 1530-1560nm and 1560-1595nm wavelength bands respectively. Such an amplifier could provide >20dB gain and <4.5dB NF in wavelength band of 1520-1595nm.

3.4. Conclusions

Core-pumped Er-doped 3-MEF and 7-MEF have been fabricated and characterized in terms of their amplification properties. It has been shown that there is no measurable crosstalk between the signals down the OSA noise level (-90dBm) in different fibre-elements of core-pumped MEFA, i.e. all fibre-elements behave as single fibres in

isolation. The approach of combining multiple fibre-elements in a common coating can be scaled to fabricate long fibre lengths. The MEF geometry can also be scaled to a larger number of fibre-elements. All the fibre-elements in the 3-MEF and 7-MEF had similar amplification characteristics, providing an average gain of 33dB and a NF <5dB for an input signal of -23dBm at a wavelength of 1530nm, typical of EDFAs. The gain variation in spun and straight fibre draw condition was within 1dB. It was shown that the added flexibility of MEF geometry could be further exploited to change the length of amplifier fibre. This could help tune the gain profile of the amplifier. It was shown that the gain in L-band could be enhanced by using 4-element cascade. Using this, the split-band amplifier was proposed which would employ three amplifier consisting of single element, 2-element cascade and 4-element cascade respectively. Such an amplifier was proposed to demonstrate a broad amplification of 20dB in wideband covering wavelength region of 1520nm-1595nm.

References

[1] J. Sakaguchi, W. Klaus, B. J. Puttnam, J. M. D. Mendinueta, Y. Awaji, N. Wadam Y, Tsuchida, K. Maeda, M. Tadakuma, K. Imamura, R. Sugizaki, T. Kobayashi, Y. Tottori, M. Wantabe, and R. V. Jensen, "19-core MCF transmission system using EDFA with shared core pumping coupled via free-space optics," Opt. Express, 22 (1), 90, (2014)

[2] K. S. Abedin, T. F. Taunay, M. Fishteyn, M. F. Yan, B. Zhu, J. M. Fini, E. M. Monberg, F. V. Dimarcello, and P. W. Wisk, "Amplification and noise properties of an erbium-doped multicore fiber amplifier," Opt. Express, 19 (17), 16715, (2011)D. M. Baney, P. Gallion, and R. S. Tucker, "Theory and measurement techniques for the noise figure of optical amplifiers," Optical Fiber Technology **6** (2), 122-154 (2000)

[3] Y. Tsuchida, K. Maeda, K. Watanabe, T. Saito, S. Matsumoto, K. Aiso, Y. Mimura, and R. Sugizaki, "Simultaneous 7-core pumped amplification in multicore EDF through fibre based fan-in/out," in European Conf. on Opt. Commun. (ECOC 2012), paper Tu.4.F.2

[4] S.R. Schmid, and A, F. Toussaint, "Optical fiber Coatings," in Specialty Optical Fibers Handbook, ed. A. Mendez and T. F. Morse, Elsevier Inc., (2007).

[5] D. M. Baney, P. Gallion, and R. S. Tucker, "Theory and measurement techniques for the noise figure of optical amplifiers," Optical Fiber Technology **6** (2), 122-154 (2000)

[6] J. R. Simpson. P. C. Becker and N. A. Olsson, "Amplifier Characteristics and Design Issues," in Erbium-Doped Fibre Amplifiers: Fundamentals and Technology (Academic Press, 1999), pp. 251-262.

[7] "EDFA testing with interpolation technique," in Agilent Product Note 71452-1, notes-application.abcelectronique.com/018/18-27242.pdf

[8] S. Jain, T. C. May-Smith, A. Dhar, A. Webb, B. Usmani, and J. K. Sahu, "Gain and noise figure study of Er-doped multi-element fiber amplifier," in Asia Comunications and Photonics Conference (ACP) Guangzhou, China 7-10 November 2012 ATh2A.1

[9] S. Jain, T. C. May-Smith, A. Dhar, A. S. Webb, M. Belal, D. J. Richardson, J. K. Sahu, and D. N. Payne, "Erbium-doped multi-element fiber amplifier for space-division multiplexing operations," Optics Letters, **38**(4), 582-584, (2013)

[10] N.K.Thipparapu, S.Jain, T.C.May-Smith, J.K.Sahu, "Wideband multi-element Er-doped fiber amplifier," Laser Physics Letters, 11(9), 095104, (2014)

[11] N.K.Thipparapu, S.Jain, T.C.May-Smith, J.K.Sahu, "Configurable Er-doped core-pumped multi-element fiber amplifier," OECC/ACOFT '14 Melbourne 6-10 Jul 2014

Chapter-4

Cladding-Pumped Er/Yb-doped Multi-Element Fibre Amplifier

4.1. Introduction

The cladding-pumped SDM amplifiers have great potential for component sharing and device integration. It can be regarded as one of the drivers for reducing both cost and energy expenditure of the network systems. In cladding pumped SDM amplifiers, a less expensive, low brightness, high-power multimode pump laser diode is used as a pump laser source and multiple spatial channels can be amplified simultaneously However, note that compared to core-pumped MEFAs, the cladding pumped SDM amplifiers require high pump power due to small overlap between pump and signal intensities. There have been various demonstrations of cladding pumped MCF amplifiers [1-6] and a 12-core MCF amplifier is the highest core count cladding

pumped MCF amplifier reported up to date [3]. However, these MCF amplifiers require delicate fan in/out devices to access the individual cores and optical crosstalk between the adjacent cores is an important issue.

In this work, we have developed a cladding pumped MEF amplifier, where a central pump delivery fibre is in physical contacted with the four surrounding signal fibres which allows efficient pump light coupling into the neighbour signal fibres. The combination of pump fibres with a single active fibre has been demonstrated previously for high power fibre laser applications and L-band amplifiers, known as GTWave fibre [7, 8]. Here, the use of cladding-pumped multi-port amplifier concept has been used to amplify multiple signal fibre-elements [9, 10]. The number of fibre-elements have been increased up to 5 (4 signal and 1 pump) in cladding-pump amplifier as compared to GTWave fibre (only one signal fibre-element and multimode pump fibre-elements was used) and a single pump laser diode is used to amplify multiple signal-fibre elements. Also, drawing multiple fibre elements with a common polymer coating offers the advantages of easy access to individual fibre elements by stripping the protective polymer coating and easy side pumping by optically contacting adjacent signal fibre elements. Therefore, this type of MEF configuration can reduce the amount of optical devices such as pump-signal combiners (i.e. WDM couplers) and fan in/out devices.

Significant attention has also been paid to develop broadband optical amplifiers covering C and L bands. Erbium has the potential for broadband amplification with $^4I_{13/2} \rightarrow {}^4I_{15/2}$ transition covering ~1.5 to 1.62μm [11] and a parallel configuration of C (1530-1565nm) and L (1565-1625nm) band EDFAs has been considered to cover the C+L bands. This approach however increases the system cost as the number of components are doubled. On the other hand, Raman amplifiers have shown the potential to achieve broad-gain amplification [12-14] using multiple pump laser diodes but special tailored pump control is required to obtain flat broadband gain. In this chapter, using MEF structure, we also introduce a broadband EDFA covering both C and L-band using a single pump. A novel scheme of combining the signal fibre-elements to make a loop-back cascade in MEFA has been introduced, revealing the ability to increase and/or tune the bandwidth of the device. The MEF based wideband optical amplifier can be developed either by using signal fibre-elements with different Er/Yb-doping concentrations or by cascading the signal fibre-elements.

Similar to core-pumped amplifier, the cascading in cladding-pumped MEFA provides flexibility of length variation by cascading the signal fibre-elements [15, 16]. The MEFA provides advantage over conventional C+L split band EDFA as it uses same pump laser diode for amplification of both bands thereby reducing the overall cost of the amplifier. A detailed study on the gain and NF characteristics of MEFA for different fibre lengths, pump powers and cascading configurations has been presented.

In order to achieve further higher spatial multiplicity in SDM transmission, the integration of MCF and FMF technologies have been demonstrated [17-19] in a passive transmission fibre but, until this work, SDM amplifiers supporting few-mode MCFs had not been demonstrated. However, these hybrid SDM amplifiers are essential to realize a SDM transmission system with higher spatial multiplicity. To fulfil these requirement, we have been experimentally demonstrated the first hybrid SDM amplifier, "few-mode MEFA", in section 4.5. Few-mode MEFA consists 5 fibre-elements (4 signal fibre-elements and 1 pump fibre-element), and each fibre element can amplify three spatial modes (LP_{01}, LP_{11a}, and LP_{11b}), yielding an overall multiplicity of 12 (3 modes x 4 signal fibre-elements) [20, 21]. An average signal gain of 18.3dB and differential modal gain in the range of ~1-6dB were achieved in the wavelength range 1542-1560nm at an input signal power of -12.5dBm per channel. The detailed WDM performance for various pump powers and input signal powers has also been investigated. The experiment of few-mode cladding pumped MEFA was performed with the help of Dr. Yongmin Jung.

4.2. Fibre Fabrication and Characterisation

Cladding-pumped 5-MEFs were fabricated from a commercial preform with outer diameter of 12.55mm and core diameter of 1.13mm. The fibre preform was doped with Er and Yb ions in phospho-silicate host with their concentrations corresponding to the average core absorption of 50dB/m at 1536nm, and 400dB/m at 915nm respectively, as specified by the manufacturer. The RIP at various positions along the length of the preform is shown in Fig. 4.1. The refractive index varied between 0.010-0.015 resulting in numerical aperture variation from 0.17 to 0.20.

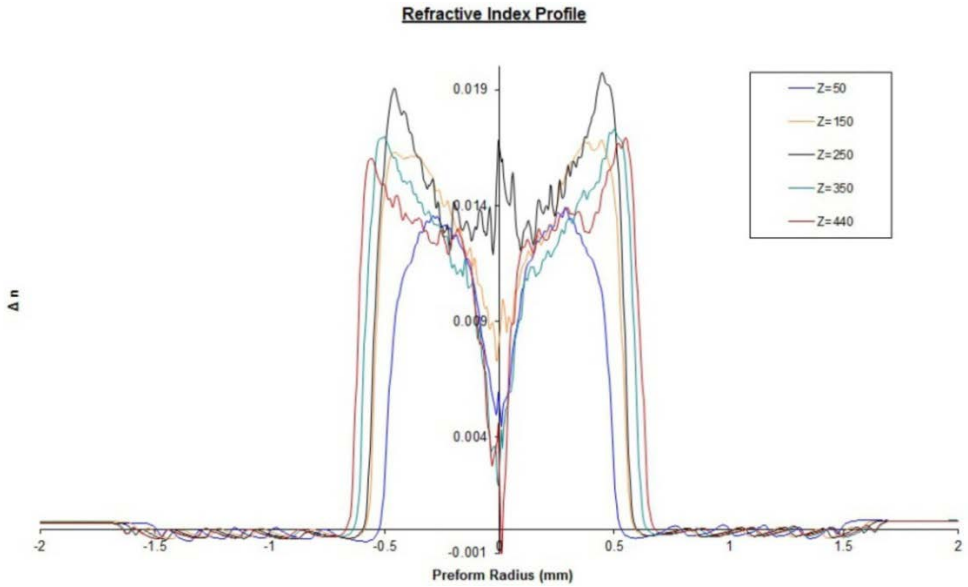

Fig. 4.1 Refractive index profile of the preform along the length

The Er/Yb-doped preform was stretched and cut into four equal lengths and stacked together with a pure silica rod (Suprasil F-300) at the centre to obtain a 5-element MEF (5-MEF) preform assembly as shown Fig. 4.2 (a) [10]. A 7-MEF jig, same as that used for making assembly for core-pumped ME-EDFA (see Fig. 3.3), was used for making the preform assembly by leaving the two opposite holes empty. A drop weight was attached to other side of the assembly. The preform assembly was then drawn into MEF at a temperature of 2040^{o}C and a drawing speed of 10m/min, keeping the elements separate in the process until they were combined in a common polymer coating. The fibres were coated with a low-index acrylate polymer coating (Luvantix PC-373 AP) to form double-clad fibre structure. The resulting 5-MEF comprise of one pure silica rod fibre (i.e. core-less fibre) as a pump delivery fibre at the centre and four surrounding Er/Yb-doped signal fibre-elements as gain medium. Two 5-MEFs were fabricated with two different cladding diameter of fibre-elements; 80µm (overall coated diameter = 305µm), and 55µm (coated diameter = 275µm), resulting in core diameter of about 7.5µm and 5µm respectively. The preform assembly was spun during fibre fabrication to ensure that the signal fibre-elements maintain continuous optical contact with the pump fibre-element. The rotation rate of about 80rpm was chosen so as to maintain the fibre-element bunching point above the coating die. It was also verified by inspecting the cross-section of the fibres at multiple points in a 4m long MEF that signal fibre-elements maintained physical contact with the pump fibre-element. The MEF with fibre-element diameter of 55µm fabricated to obtain single mode cores in C-band. However, all the measurements

were performed on 5-MEF with fibre-element diameter of 80µm due to ease of handling the fibre with thicker diameters. The cores in the fibre-elements of this MEF was two-moded. The cross-section microscope image of 5-MEF is shown in Fig. 4.2 (b).

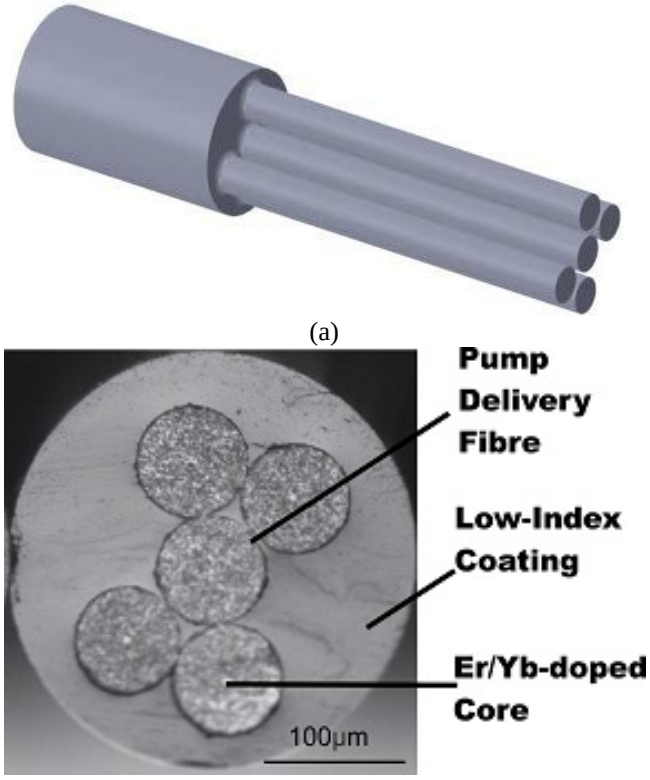

Fig. 4.2 (a) Schematic of preform assembly, (b) microscope image of cross-section of 5-MEF

The pump delivery fibre in 5-MEF was identified by observing the cross-section of all the fibre-elements at input end under the microscope as the pump fibre-element had no core. The signal fibre-elements were arbitrarily coded as S1, S2, S3 and S4 respectively, and the pump fibre-element was coded as P. The core and cladding absorption of the signal fibre-elements were measured using a white light source and an OSA.

Table 4.1 Cladding and Core absorption measured at 975nm and 1536nm respectively

Fibre No.	Core abs. @1536nm	Cladding abs. @975nm
S1	47	3.7
S2	36	2.2
S3	61	4.3
S4	44	3.1

Table 4.1 shows the cladding and core absorption measured at 975nm and 1536nm respectively. For cladding absorption, the measurement was performed on 5-MEF (80µm) with 1.8m fibre length by coupling white light into the pump fibre at input

end and measuring the transmission spectra from the signal fibres at output end using OSA. The cladding absorption at a wavelength of 975nm was found to be varying between 2.2-4.3dB/m between signal fibres. The core absorption at wavelengths of 1536nm was measured by launching the white light into core of each fibre-element in 10cm length by splicing SMF on its both ends, and taking the respective output spectra, and was found to have the element-to-element variation between 36-61dB/m as shown in Fig. 4.3 (output normalised around 1600nm). The lowest and higher absorption was in S2 and S3 fibre-elements respectively. The variation in absorption is due to variation in RIP of the preform along its length resulting in different the Er and Yb doping concentration in the fibre-elements of 5-MEF.

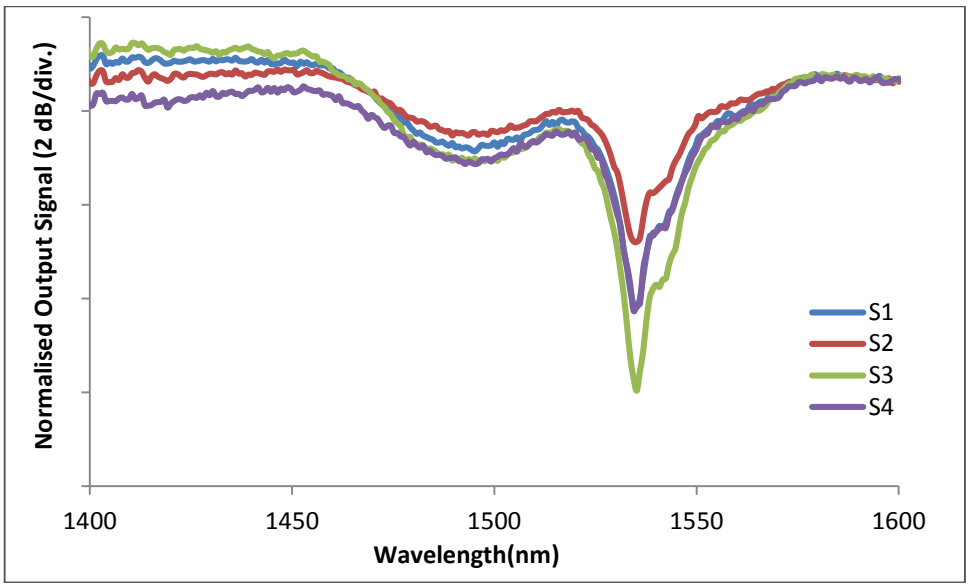

Fig. 4.3 Core absorption spectra of signal fibre elements of 80µm 5-MEF for 10cm of fibre length at 1536 nm.

4.3. Experimental Setup of ME-EYDFA

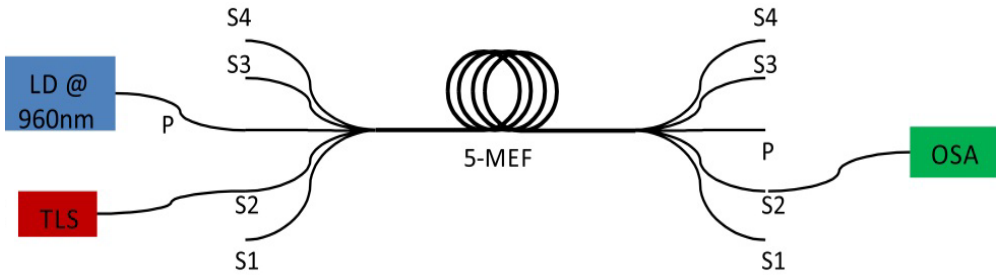

Fig. 4.4 Schematic of experimental setup for gain and NF measurement.

The setup for the gain and NF measurements of the signal fibre-elements is shown in Fig. 4.4. The setup comprised of a pump LD operating at a wavelength of 960nm, a TLS as a signal source and an OSA to record the input and amplified output signals. A 960nm pump chosen to such that flat region of the absorption band is used and effect of pump wavelength shift is not significant. It should be noted that in case of

cladding-pump ME-EYDFA, WDM couplers for combining pump and signal are not required. The signal fibre-elements, in which cores are doped with Er/Yb ions, can be easily separated at the input and output ends by simply removing the polymer coating of the fibre and standard single mode fibres can be spliced at both ends of the signal fibre-elements for efficient launch/extraction of signal light. Also, a pump delivery fibre (105μm core and 125μm cladding) was tapered to 80μm via adiabatic tapering and spliced to the pump fibre-element for efficient launching of the pump light from the laser diode into the pump delivery fibre-element (outer diameter=80μm).

4.4. Results and Discussions

C-band cladding-pump MEFA

A 4m length of 5-MEF was taken and SMF patch cords were spliced to each end of the signal fibre-elements for gain/ NF characterization with the experimental setup as shown in Fig. 4.4. This length was chosen after cutting back and measuring ASE at different length to obtain ASE in the C-band, and prevent the reabsorption of the signal. Fig. 4.5 (a) shows the gain and NF performance of the individual signal fibres using 6.4W of launched pump power in a pump delivery fibre-element (*P*). A minimum NF of 4.7 dB with a maximum gain of 35±2.5 dB was observed per signal fibre element for an input signal of -23dBm. The maximum gain increased to 37±2dB when the launched pump power was increased to 10W. The element-to-element performance variation was a resultant of different doping concentration. Note that the signal fibre-elements were actually two-moded, which is likely to have contributed to the relatively higher noise figures as shown in Fig. 4.5 (a). However, the fibre was coiled tightly to about 5cm diameter and SMF pigtails were carefully spliced to these to ensure effectively SM operation in practice, and the amplifier operated in a stable fashion with no fluctuation in its output power over time. There is no intrinsic reason that the fibre cores should be two-moded, and this issue can be eliminated in the future work with expected improvements in amplifier performance. Another possible cause of increase in NF could be the initial section of MEF where the coating is stripped-off to splice the SMFs to each fibre-elements. The initial section remains un-pumped which contributes to the increase in the NF via increased loss.

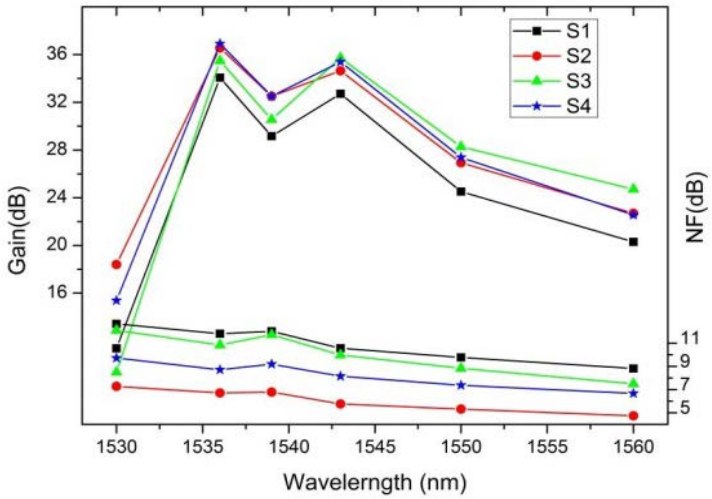

(a)

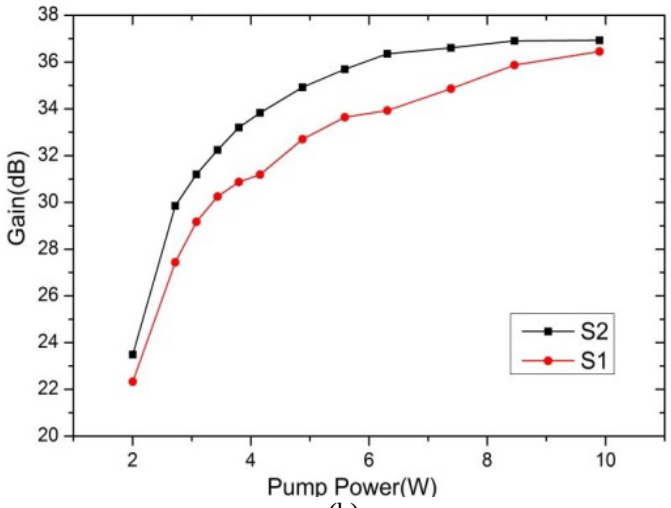

(b)

Fig. 4.5 (a) Gain and noise figure spectra variation of MEF signal fibres with a pump power of 6.4W and input signal of -23dBm, and (b) pump power vs. gain for -23dBm input signal at a wavelength of 1543nm for signal fibres S1 and S2 respectively.

The pump power vs. gain curve is plotted in Fig. 4.5 (b) for signal fibre-elements S1 and S2 respectively, showing the gain saturation beyond about 8W of launched pump power. As similar to the case of the core-pumped ME-EDFA, no signal crosstalk was observed between the signal fibre-elements in a cladding-pumped ME-EYDFA or simply MEFA due to the unique MEF structure. It was difficult to measure the crosstalk in active fibre due to the high absorption in the unpumped cores at the signal wavelengths but ultra-low crosstalk of the MEFA was verified in SDM system demonstration including passive MEF and C-band cladding-pumped MEFA, which is mentioned in section 5.3.3. Furthermore, the signal fibre-elements were connected together serially one by one to form a cascaded amplifier and the change in the ASE spectrum and gain was compared as each signal fibre-element was added. The gain was measured with two different launched pump power of

2.5W and 4.5W for the following configurations: a) S4, b) S4-S1, c) S4-S1-S2, as shown in Fig. 6(a). Note that, pump power requirement is reduced in cascading configuration due to the fact that pump gets replenished in each fibre-element. This works similar to Bi-directional pumping, in which pump power requirement is reduced to better inversion. The fibre-elements were randomly chosen for cascading. An input signal of -23dBm was used to measure the gain at four different wavelengths that are shown in Fig. 6 (b). It was observed that the gain at longer wavelengths was increased significantly as more signal fibre-elements were combined. Also, the amplifier gain spectra became flatter for cascaded amplifier as more signal fibre-elements were added to the device. For a three-elements cascaded (S4-S1-S2) amplifier, a gain of 36dB was observed over a bandwidth of >20nm with a gain flatness of ±1dB. Also, there was a small variation in the gain profile of the amplifier depending on the cascading combination.

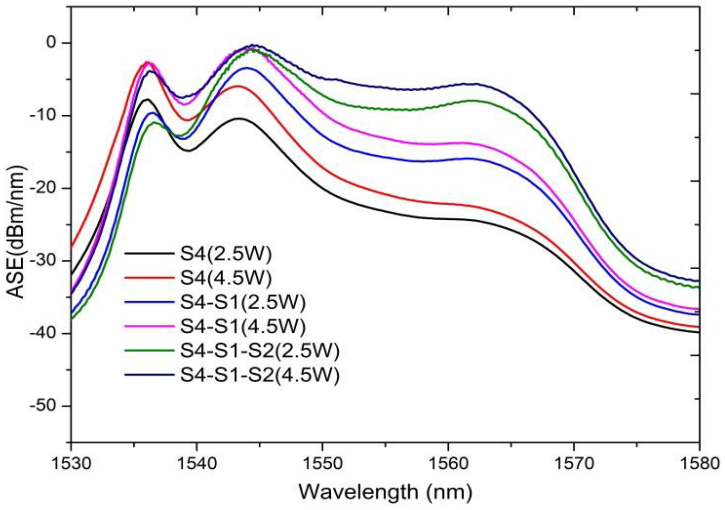

(a)

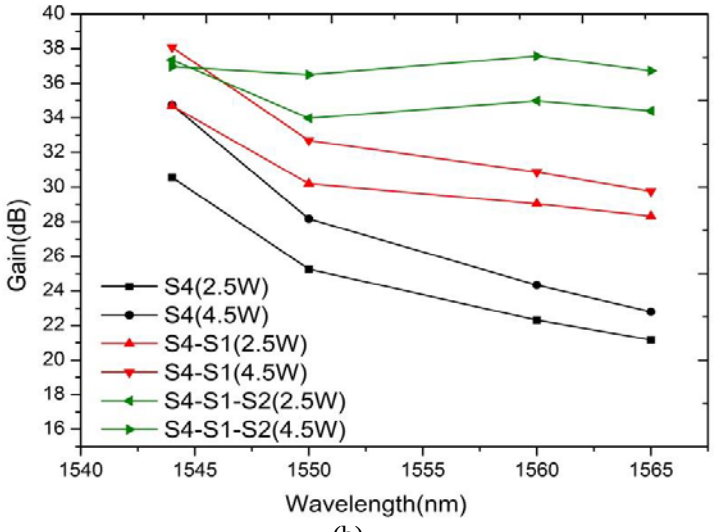

(b)

Fig. 4.6 Variation of (a) ASE, and (b) gain spectra for different loop-back cascade amplifier configurations.

Amplifier Gain variation in different 2-element Cascade

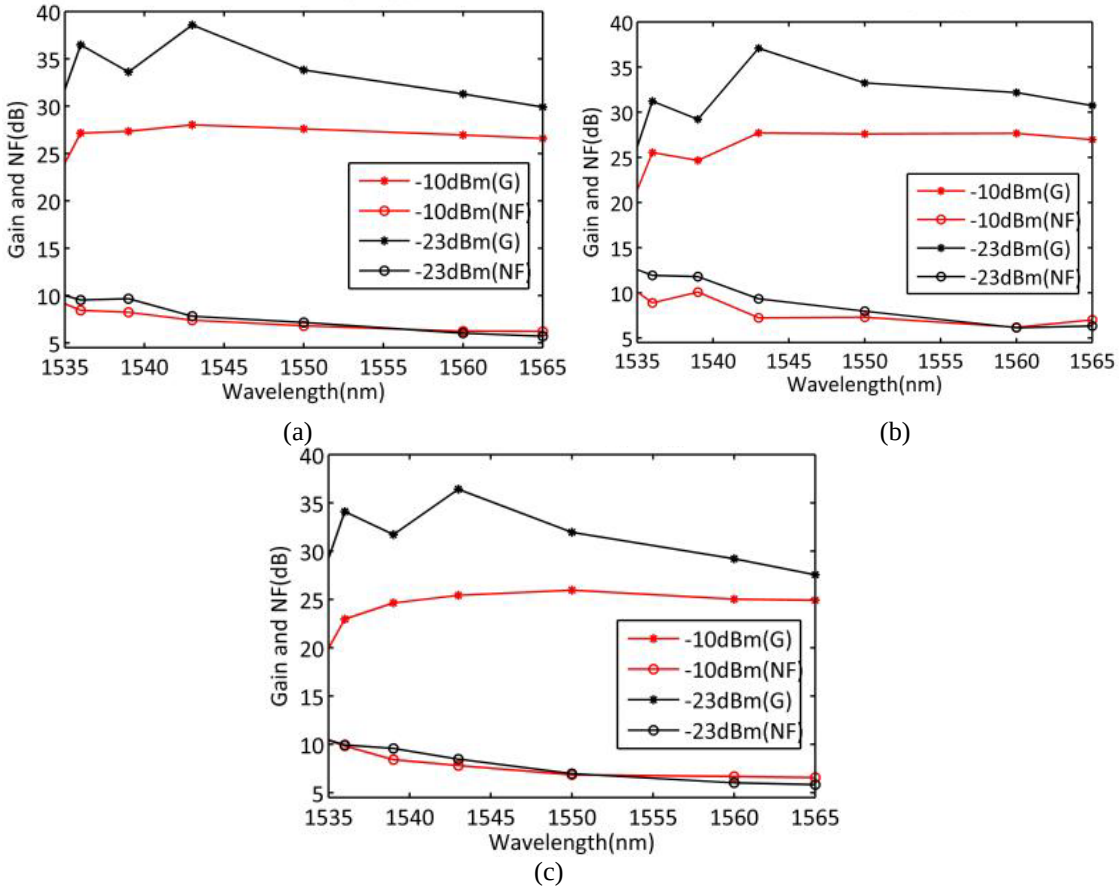

Fig. 4.7 Gain profile with different cascading combinations of 2 fibre-elements; (a) S2-S4, (b) S2-S3, and (c) S2-S1 for pump power of 4.5W.

Figure 4.7 shows the gain spectra over the C-band for different combination of 2-signal fibre-elements in a cascaded configuration at the pump power of 4.5W. S2 fibre-element was used at the start in order to minimise the NF as S2 had best NF performance. It can be seen that the variation in profile for different cascade combination was due to variation in the dopant concentration along the length of the preform. This feature could be used to tune the profile of the amplifier. With the S3 fibre-element (highest absorption) in the cascade, maximum shift of the gain profile towards the longer wavelength was observed. It can be seen that S2-S1 and S2-S4 had similar performance as the absorption in S1 and S4 were close to each other.

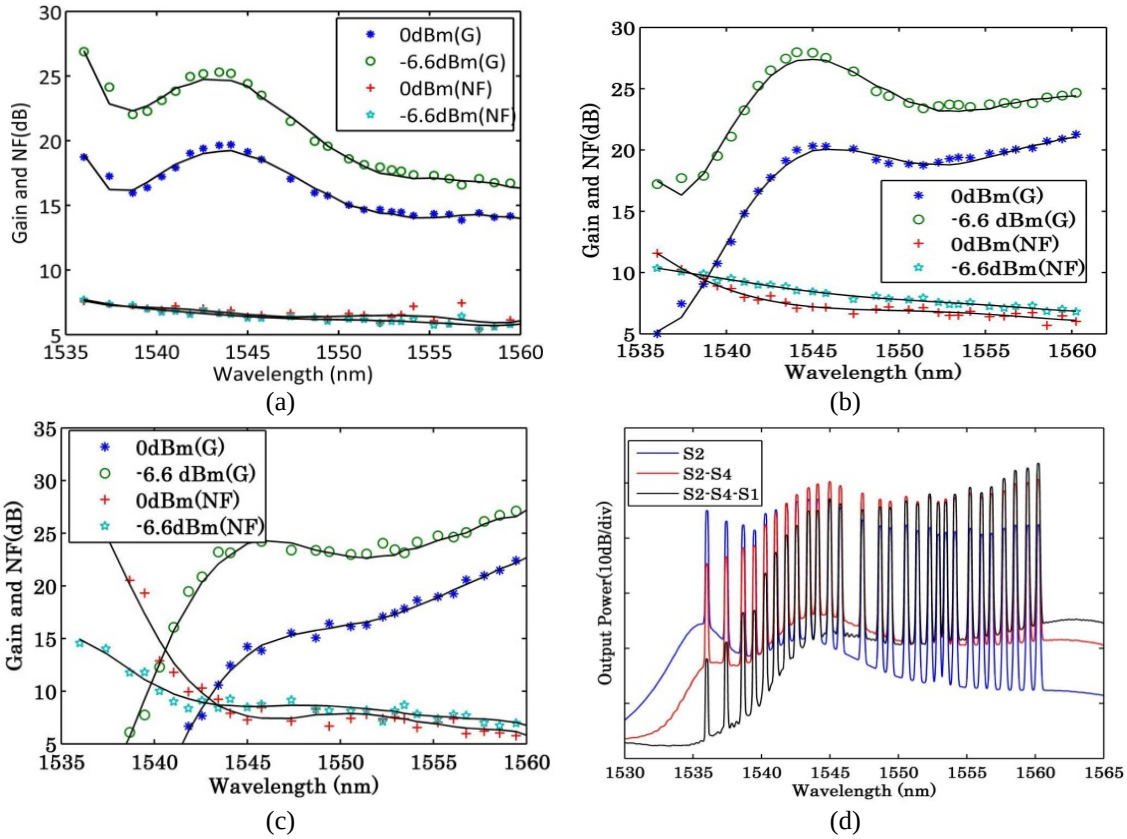

Fig. 4.8 Gain and NF performance of cascade combinations; (a) S2, (b) S2-S4, (c) S2-S4-S1, and (d) output spectra corresponding to three cascading cases. (Note the dots represent the experimental data and solid lines are simply trend lines to help guide the eye)

To test the operation in a WDM environment, a source comprising 28 intensity modulated channels in the range of 1535-1562nm was used in place of the TLS in Fig. 4.4. The amplifier characteristics were measured, both for a single fibre-element and for different cascade configurations, for input signal powers of -6.6dBm and 0dBm, and a launched pump power of 6.4W. Figure 4.8 (a), (b), and (c) show the gain and NF plots for S2, S2-S4, and S2-S4-S1 cases, respectively. The gain increment at longer wavelengths was observed in the multi-channel cases, and can be clearly seen shifting from Fig. 4.8 (a) to (c). Figure 4.8 (d) shows the output amplified signal spectra for S2, S2-S4 and S2-S4-S1 for 6.4W of launched pump power. The results indicate that further improvements in the amplifier characteristics can be obtained by optimizing the amplifier length. Further optimization of the uniformity of the amplifier fibre-element performance is also anticipated with the improvements of preform fabrication process.

Amplifier Characterisation with Length

To characterise the MEFA with respect to length, at first, 12m of MEF was taken for measurement which was then cut to 9m and 6m respectively for further characterisation.

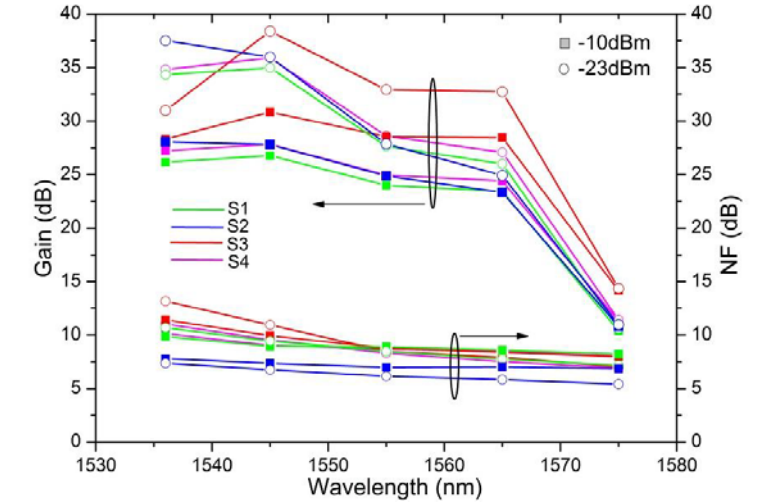

(a)

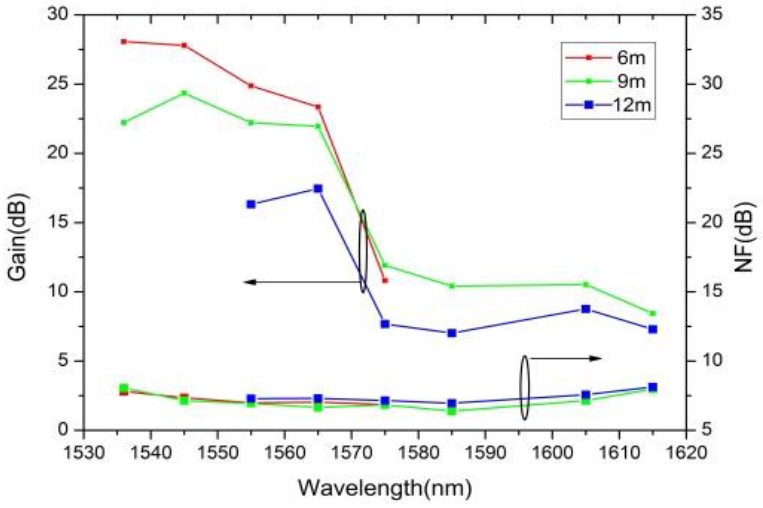

(b)

Fig. 4.9 Gain and noise figure variation for a) signal fibre-elements using a 6m of MEF and -10dBm and -23dBm input signals and b) S2 at different lengths for a pump power of 6.4W and -10dBm of input signal.

Figure 4.9 (a) shows the gain and NF performance of all four signal fibre-elements of MEFA using 6.4W of launched pump power with -10dBm and -23dBm of input signals and 6m long MEF. A maximum gain of about 37 dB and corresponding NF of 7.3dB was obtained for S2 signal fibre-element (with lowest pump absorption) in the C-band (1536nm) for -23dBm of input signal. Figure 4.9 (b) shows the gain variation of S2 for different fibre lengths with the launched pump power of 6.4W and -10dBm of input signal. Gain in only the C-band was measured for 6m fibre length due to significant reduction of gain in L-band. For 9m fibre, the gain in the C-

band decreased whereas the gain in L-band reached >10 dB across the wavelength band 1575–1605 nm. However, for 12m long fibre, the pump power of 6.4W was not enough, and the gain reduced in both C and L bands as compared to 9m fibre. The reduction of gain in C-band was higher compared to the L-band. The gain dependence of launched pump power for 12m MEF with -10dBm input signal is shown in Fig. 4.10 (a) for S2, which had lowest NF. The maximum gain reached to 22.5dB at a wavelength of 1565nm on increasing the pump power to 10W. Moreover, the gain of 26.5dB and NF <6 dB was observed in the L-band (1565–1615nm) for an input signal of -23dBm and 10W of pump power.

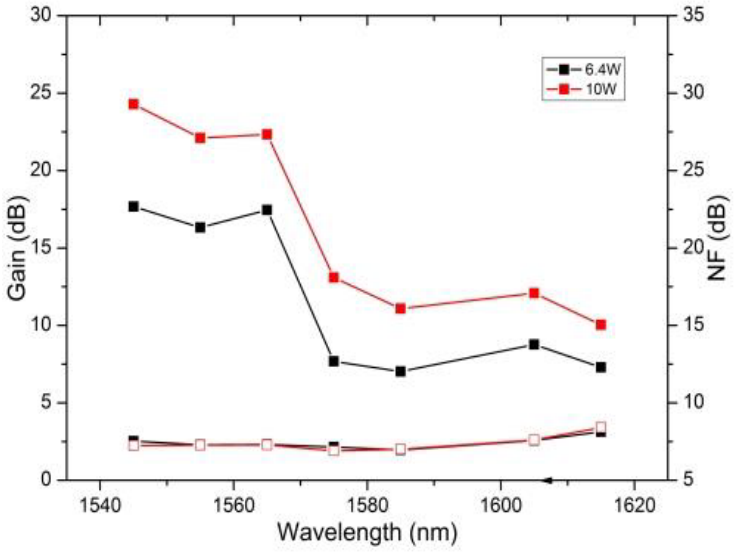

(a)

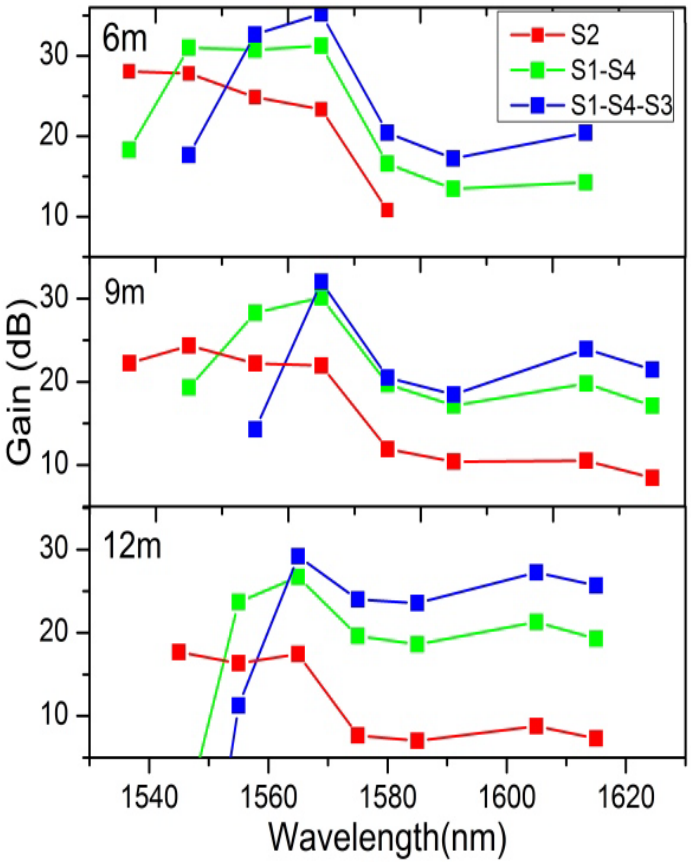

(b)

Fig. 4.10 Gain variation of the MEFA with -10dBm of input signal for (a) 12m of MEF at two different pump powers, and (b) cascading of signal fibre-elements for different MEF lengths at pump power of 6.4W.

The signal fibre-elements were cascaded one by one by connecting the output of one fibre-element to the input of next fibre-element, without using any isolator in-between, and the change in the gain was measured. The gain was measured with a 6.4W of launched pump power for 6m, 9m and 12m MEF lengths as shown in fig. 4.10 (b). An input signal of -10dBm was used. It can be observed from Fig. 4.10 (b) that for 12m of MEF, the gain was <10 dB in the L-band. However, after cascading the fibre-elements (S1-S4-S3) the maximum gain increased to about 29dB at a wavelength of 1605nm with >23.5 dB of gain in entire L-band region from 1565–1615nm. However, 3-element cascade also had higher NF. Relatively flat gain of 18.5±1.2dB was observed for 2-cascade (S1-S4) configuration in the wavelength band of 1575-1615nm. Whereas, for 6m MEF the gain is primarily dominated in the C-band. The MEFA using short fibre lengths can thus provide amplification in the C-band. For 9m of fibre length, single fibre-element provided a maximum gain of 24dB in C-band and 2-cascade provided the gain of >17dB in the L-band. The gain in L-band could be further increased using 3-element cascade, however, it would

have higher NF difference in the C and L-band.

A split-band cladding pumped MEFA can be configured covering both C and L band in which one of the fibre-elements operates in the C-band and other elements are cascaded to provide sufficient gain in the L-band. The expected performance of such amplifiers is shown in Fig 4.11, in which the gain and NF of S2, which provides maximum gain in the C-band, has been put together with the gain and NF of 2-element cascade (S1-S4).

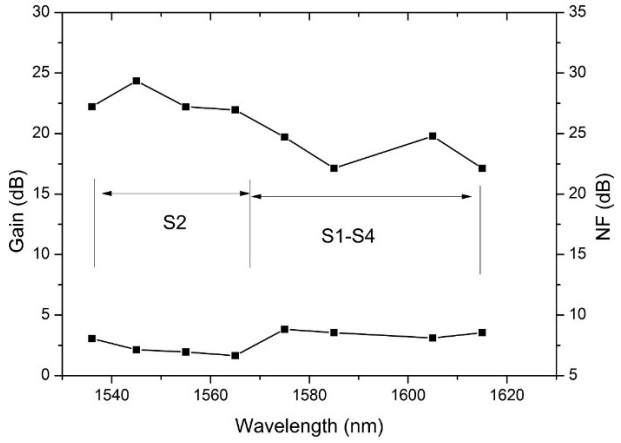

(a)

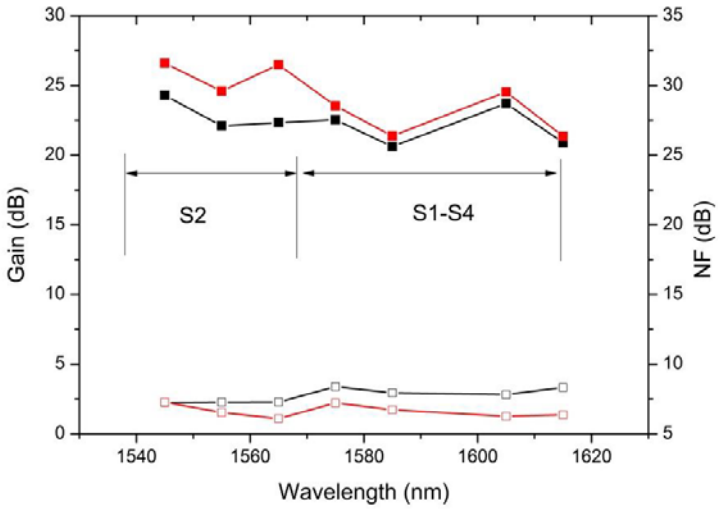

(b)

Fig. 4.11 Performance of a split band MEFA with (a) gain >17dB (1536 – 1615nm) using 9m MEF at 6.4W of pump power and -10dBm input signal, and (b) gain >20dB (1545-1615) using 12m MEF at 10W of pump power for -10dBm (black) and -23dBm (red) of input signal power respectively.

Fig. 4.11 (a) and 4.11 (b) show the performance of a broadband amplifier using 9m and 12m of MEF lengths respectively. For 9m length and -10dBm of input signal, >17dB gain in 80nm bandwidth (1536-1615nm) was achieved for pump power of 6.4W. Whereas, in 12m MEF with pump power of 10W and for an input signal of -23dBm the amplifier provided more than 21dB gain both in C and L

bands (1545-1615nm). Furthermore, relatively flat gain of (22±1.5dB) was achieved for -10dBm of input signal in 12m MEF. The cascading configuration shown in cladding-pumped MEFAs can be exploited to extend the operating window further to C and L-band.

4.5. Cladding-pumped Few-mode MEFA

Experiment setup of 3M-MEFA

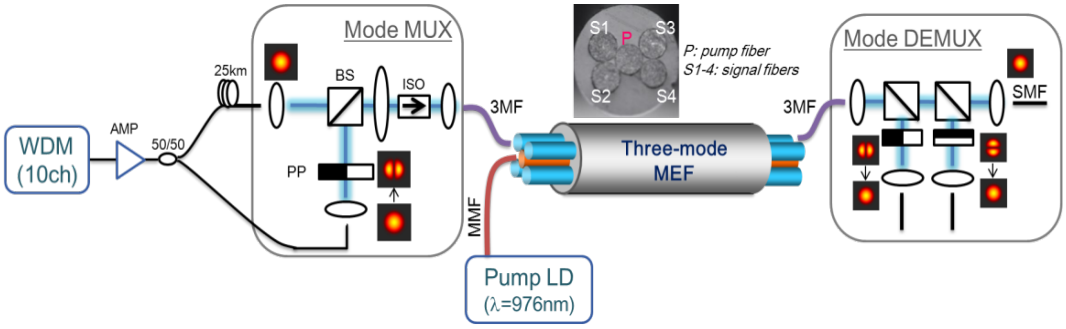

Fig. 4.12 Schematic diagram of 3-moded cladding pumped multi-element fibre amplifier (3M-MEFA) comprising 4 Er/Yb co-doped signal fibres and 1 multimode pump fibre. (BS: Beam splitter, PP: Phase plate, ISO: isolator, AMP: amplifier, 3MF: 3-moded passive fibre)

Figure 4.12 shows the schematic of the setup used for the characterization of the cladding pumped 3-moded MEF amplifier (3M-MEFA). As discussed in section 4.4, the Er/Yb-doped MEF with 80µm element diameter was two-moded which can guide up to three spatial modes (LP_{01}, LP_{11a}, and LP_{11b}). The MEF was loosely coiled to allow 2nd mode to propagate. A multimode laser diode as a pump laser operating at a wavelength of 976nm was used, available at that time in the laboratory, instead of 960nm. The signal source used in the setup consisted of 10 wavelengths multiplexed external cavity lasers spread over the range 1536-1560 nm. The WDM channels were pre-amplified, split into two and fed into the mode multiplexer to allow the gain performance of the individual amplifier elements to be measured. A 25km single mode fibre span was inserted along the LP_{01} path to minimize modal beating due to the high degree of coherence between the seed lasers. A phase-plate based mode multiplexer was used to selectively excite the pure LP_{01} and LP_{11} signal modes in a 10m long passive 3-moded fibre (3MF). The commercial passive fibre (a graded index fibre with 16µm core diameter and an NA of 0.14) was then spliced directly to one of the Er/Yb-doped elements of the 3M-MEF. The amplified output was fed into the mode demultiplexer to analyse the mode dependent gain quantitatively. The large mode field diameter mismatch between the passive and

active fibres resulted in a mode dependent splice loss (~1.1dB for the LP_{01} and ~2.5dB for the LP_{11} mode).

To confirm clean mode amplification of the input signals, mode images were taken using a charge coupled device (CCD) camera before and after amplification at 1550nm. The top row of Fig. 4.13 (a) and (b) shows that two clean spatial modes (LP_{01} and LP_{11}) were excited in the passive 3MF and that the mode quality was well preserved during amplification. The bottom row of Fig. 4.13 (a) and (b) shows the optical spectra of the WDM signals (LP_{01}) before and after the 3M-MEFA demonstrating more than 35 dB optical signal to noise ratio (OSNR) after amplification. The length of the amplifier was chosen to be 3.25m in order to maximize the signal gain whilst maintaining near full C-band operation. The gain peak of the amplifier was located at 1545 nm.

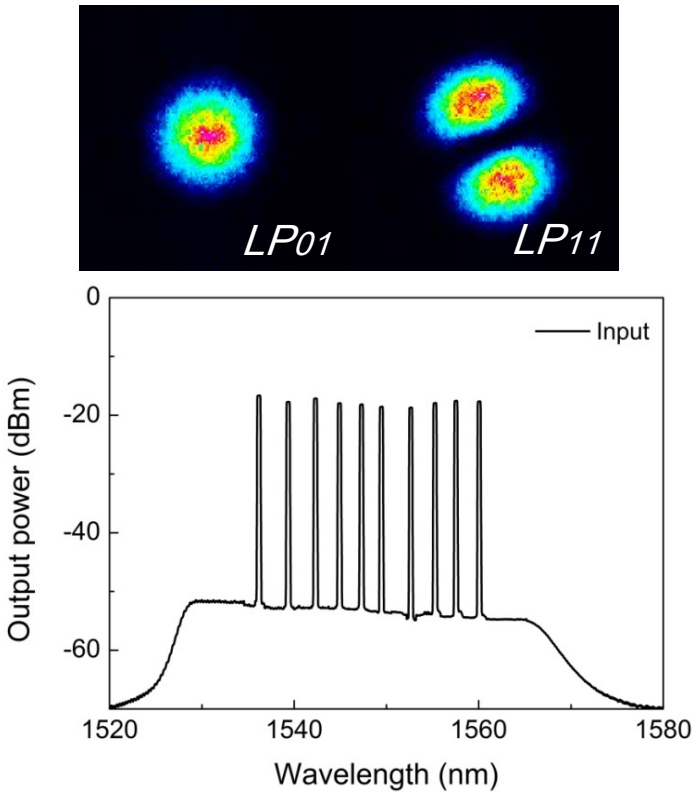

(a)

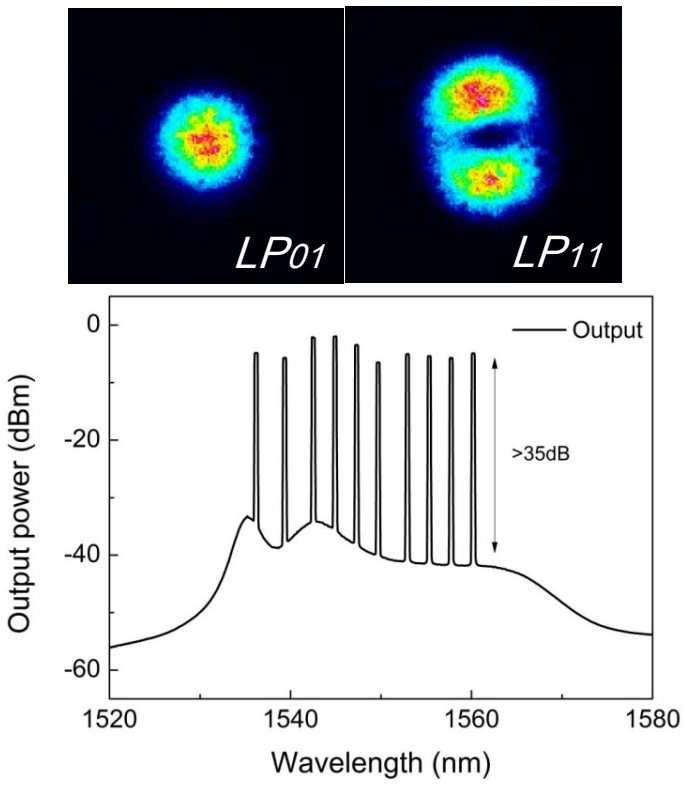

(b)

Fig. 4.13 Measured mode images and optical spectra (LP01) before (a) and after (b) amplification.

Gain performance of 3M-MEFA

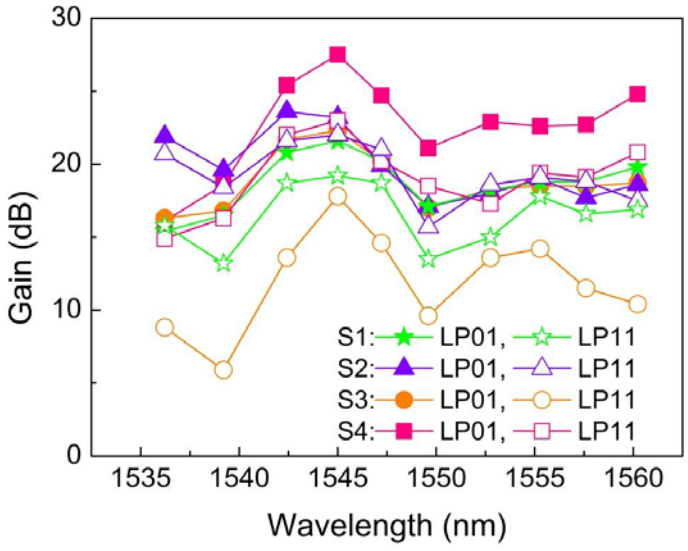

(a)

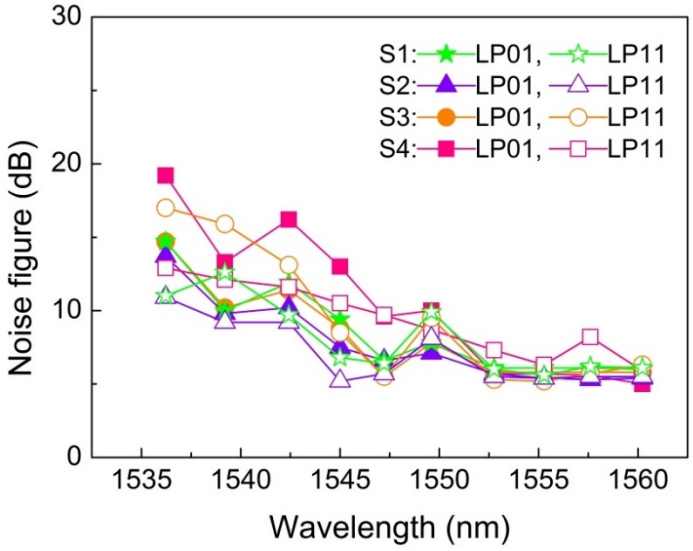

(b)

Fig. 4.14 (a) Gain and (b) noise figure spectra for 4 different signal fibre elements of the 3M-MEFA for an input signal power of -2.5dBm/mode (or -12.5dBm/mode/ch) and pump power of ~7.6W.

Figure 4.14 (a) and 4.14(b) shows the WDM gain and NF spectra for all 4 different signal fibre elements of the 3M-MEFA, referred as S1 to S4, measured consecutively over all active fibre elements. A maximum pump power of 7.6W and an input signal power of -2.5dBm per mode (total signal input power of 0.5dBm) were used. An average WDM signal gain of 18.3dB was measured in the spectral range of 1542-1560nm. The NF was found to increase sharply for wavelengths shorter than 1542nm while it tends to decrease at longer wavelengths. The high NF at shorter wavelengths is mainly due to insufficient population inversion within the active medium and which is clearly evident from the sharp drop in signal gain.

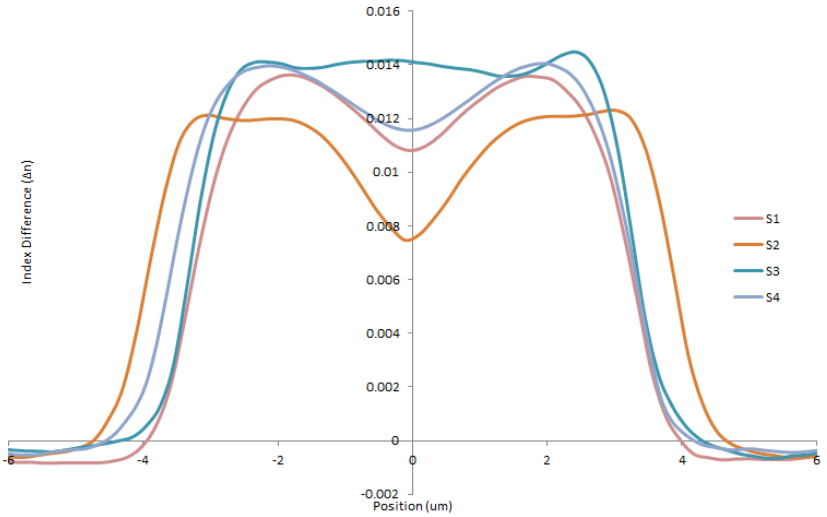

Fig. 4.15 Refractive index profile (RIP) of signal fibre-elements showing fibre-to-fibre index variation

We observed large gain variation amongst the different elements, which is mainly due to the variation in core refractive index profiles and rare-earth doping

concentrations of the non-identical preform elements used. As it can be clearly seen from Fig. 4.15 that, the RIP of S2 fibre-element had dip in the centre emulating a ring core profile which resulted in lower DMG whereas S3 had highest DMG corresponding to its RIP. However, this could certainly be improved through further optimization of the preform fabrication process. The LP_{01} signal mode experienced higher gain than the LP_{11} mode and the DMG between the two guided modes varied by 1-6dB over all 4 active fibre elements. Note that we used a simple step-index core design in the current fibres so this level of DMG is not unexpected, however careful tailoring of the doping profile within the individual elements (as illustrated in [22]) could certainly help in reducing the DMG in few-mode cladding-pumped MEFAs. As shown in Fig. 4.14 , fibre element-2 (S2) showed the best performance in terms of differential modal gain (average DMG ~1.1dB, maximum DMG ~3dB) and spectral gain flatness across the C-band, and the detailed gain profiles for various pump power and input signal power levels were investigated for this fibre-element.

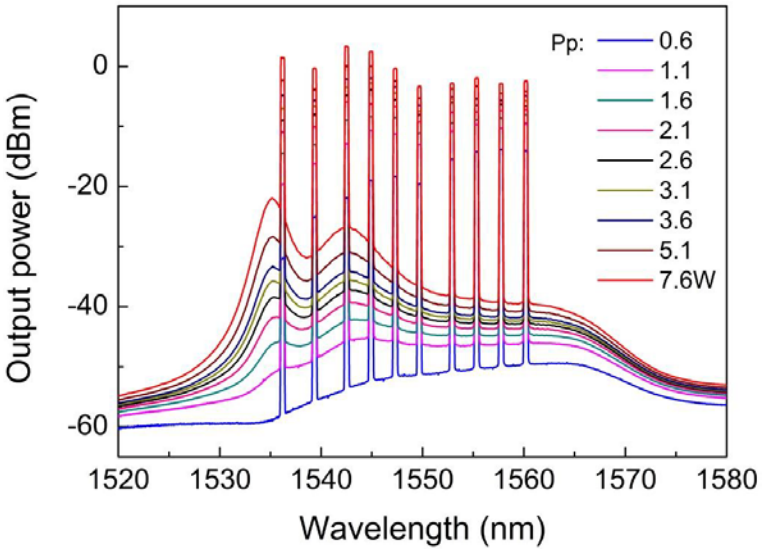

(a)

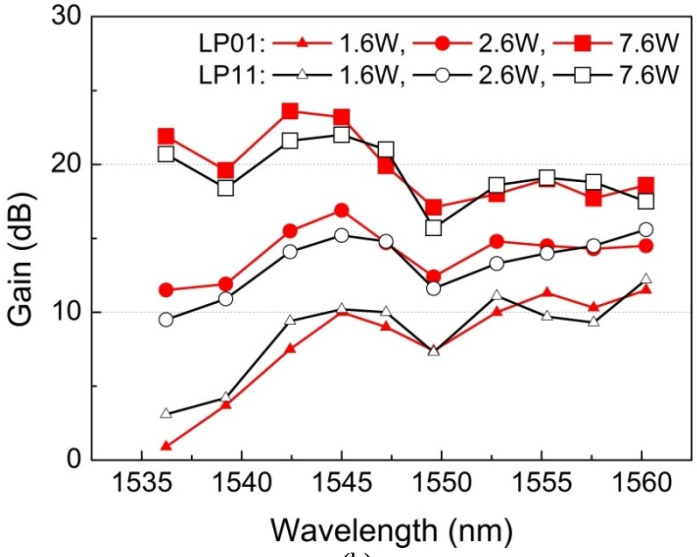

(b)

Fig. 4.16 (a) Output spectra of the LP01 mode after the mode demultiplexer and (b) mode-dependent gain for different pump powers with an input signal power of -2.5dBm/mode (or -12.5dBm/mode/ch).

Figure 4.16 (a) and (b) shows the output spectra and the mode dependent gain as a function of pump power at a fixed input signal power of -2.5 dBm/mode. As shown in Fig. 4.16 (a), for low pump power (~0.6 W) the ASE peak is located at ~1565 nm and it shifts towards the shorter wavelength side with increasing pump power. A similar trend can be observed in the measured modal gain of the amplifier shown in Fig. 4.16 (b). At low pump power the gain at the short wavelength edge was measured to be very low due to an insufficient inversion level. As the pump power, Pp, was increased from 0.6 W to 7.6 W, the gain of each of the guided modes increased due to the increased level of population inversion. It should be noted that the gain increment at the shorter wavelengths is higher compared to longer wavelengths resulting in a shift of gain peak from 1560 nm to 1545 nm.

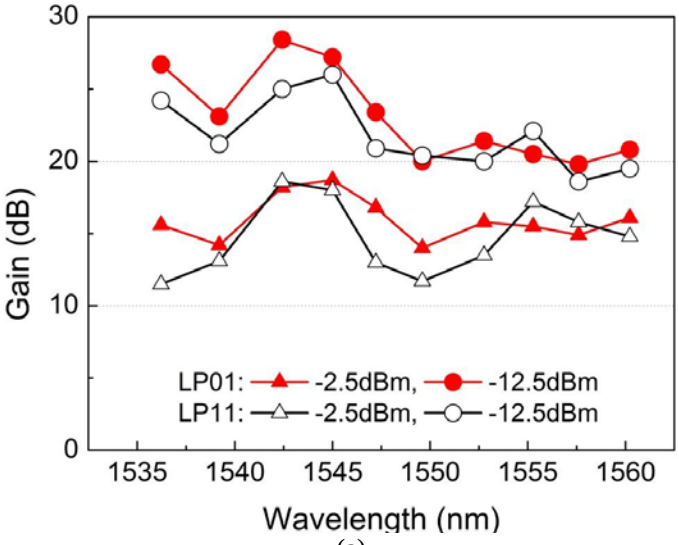

(a)

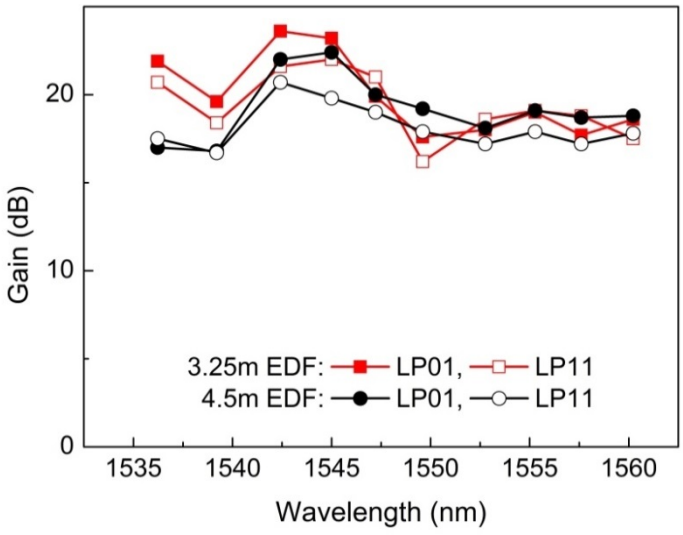

(b)

Fig. 4.17 (a) Mode-dependent gain for different input signal powers per mode at a fixed pump power of 3.6W for 3.25m of fibre, and (b) gain comparison between two different fibre lengths (3.25m and 4.5m) at a fixed pump power of 5.1W.

Figure 4.17 (a) shows the amplifier gain variation for -2.5dBm and -12.5dBm per mode of input signal powers at a randomly chosen fixed pump power of 3.6W. Both spatial modes experienced gain reduction with an increase in input signal power due to amplifier gain saturation. The DMG did not show much dependence on the input signal power and the maximum DMG remains at ~3dB for all the input signal powers investigated. We also investigated the length dependence of 3M-MEFA. Figure 4.17 (b) compares the gain spectra for two different fibre lengths (3.25m and 4.5m), for similar input signal powers (-2.5dBm and -3.3dBm per mode for 3.25m and 4.5m respectively) but at a fixed pump power of 5.1W. It can be seen that 3.25m fibre exhibited about 5dB higher gain in the shorter wavelength region as compared to that of the 4.5m fibre indicating that the gain at shorter wavelength can be increased by optimizing the fibre length. The gain difference at shorter wavelengths was relatively less for 3.6W of pump power.

4.6. Conclusions

A MEF based Er/Yb-doped cladding-pumped amplifier has been demonstrated for a wideband operation covering both C and L band. At first, a C-band cladding-pumped MEFA is presented. A maximum gain of 37dB and corresponding NF of 7.3dB in the C-band has been obtained in the S2 fibre-element with lowest Er concentration for MEF length of 6m at 6.4W of pump power and -23dBm of input signal. Element-to-element gain variation of about 3.5dB was observed at 1545nm with an input signal

of -23dBm. It was due to different doping concentration along the length of the used preform. The cladding-pump MEFA performance for different fibre length, pump power, and cascading configuration was also investigated. The maximum gain of 29dB was obtained for -10dBm input signal at 1605nm using 3- element cascade in 12m of MEF. In addition, a cladding pumped MEFA based broadband amplifier was proposed. It was demonstrated that such an amplifier could provide >17dB gain in 1536-1615nm wavelength region. Furthermore, relatively flat gain of 22±1.5dB was observed across the wavelength band of 1545-1615nm. The performance of the broadband amplifier can be further improved by tailoring the doping concentration in fibre elements. In cladding-pump amplifier, generally the optical pump power required is higher compared to its core-pump counterpart. However, in cladding-pump amplifiers, low-brightness pumps could be used. Furthermore, the pump sharing in cladding-pump MEFA is the main advantage over core-pumped MEFA as it can help reduce the component numbers. This configuration could also be used for power scaling.

Also, the first cladding-pumped few-mode MEFA was successfully demonstrated by combining MEF and FMF technologies. An overall spatial multiplicity of 12 (3 spatial modes × 4 signal fibre-elements) was obtained. An average signal gain of 18.3dB and differential modal gain of ~1-6dB were achieved in the wavelength range of 1542-1560nm. This architecture can be further scaled both in terms of the number of elements and number of modes per-element. Improvements in differential gain between elements and modes can also be envisaged by tailoring the rare-earth doping profiles of the optical fibre.

References

[1] Y. Tsuchida, and R. Sugizaki, "Multicore erbium doped fiber amplifier for space division multiplexing," in IEEE Photonics Summer Topical Meeting 2013, paper TuC3.1

[2] H. Ono, K. Takenaga, K. Ichii, S. Matsuo, T. Takahashi, H. Masuda, and M. Yamada, "12-core double-clad Er/Yb-doped fiber amplifier employing free-space coupling pump/signal combiner module," in European Conf. on Opt. Commun. (ECOC), We.4.A.4 (2013)

[3] Y. Mimura, Y. Tsuchida, K. Maeda, R. Miyabe, K. Aiso, H. Matsuura, and R. Sugizaki, "Batch multicore amplification with cladding-pumped multicore EDF," in European Conf. on Opt. Commun. (ECOC 2012), paper Tu.4.F.1

[4] K. S. Abedin, T. F. Taunay, M. Fishteyn, D. J. DiGiovanni, V. R. Supradeepa, J. M. Fini, M. F. Yan, B. Zhu, E. M. Monberg, and F. V. Dimarcello, "Cladding-pumped erbium-doped multicore fiber amplifier" Opt. Express, 20 (18), 20191, (2012)

[5] S. Takasaka, H. Matsuura, W. Kumagai, M. Tadakuma, Y. Mimura, Y. Tsuchida, K. Maeda, R. Miyabe, K. Aiso, K. Doi, and R. Sugizaki, "Cladding-pumped 7-core EDFA using a multimode pump light coupler," in European Conf. on Opt. Commun. (ECOC 2013), paper We.4.A.5

[6] H. Ono, K. Takenaga, K. Ichii, S. Matsuo, T. Takahashi, H. Masuda, and M. Yamada, "12-core double-clad Er/Yb-doped fiber amplifier employing free-space coupling pump/signal combiner module," in European Conf. on Opt. Commun. (ECOC), We.4.A.4 (2013)

[7] S. U. Alam, A. T. Harkar, R. J. Horley, F. Ghiringhelli, M. P. Varnham, P. W. Turner, and M. N. Zervas, "All-fibre, high power, cladding-pumped 1565nm MOPA using high brightness 1535nm pump sources," in Conference on Lasers and Electro-optics, CWJ4, (2008).

[8] K. H. Yla-Jarkko, C. Codemard, J. Singleton, P. W. Turner, I. Godfrey, S.-U. Alam, J. Nilsson, J. K. Sahu, and A. B. Grudinin, "Low noise intelligent cladding-pump L-band EDFA," in IEEE Photonics Technology Letters, 15(7), 909-911 (2003).

[9] S. Jain, T. C. May-Smith, and J. K. Sahu, "Er/Yb-doped cladding-pumped multi-element fiber amplifier," in Workshop on Specialty Optical Fibers and Their Applications, W5.4, (2013).

[10] S. Jain, V. J. F. Rancaño, T. C. May-Smith, P. Petropoulos, J. K. Sahu, D. J. Richardson, "Multi-element fiber for space-division multiplexing operations," Optics Express, **22**(4), 3787-3796 (2014)

[11] W. J. Miniscalco, "Optical and electronic properties of rare earth ions in glasses," in Rare-earth-doped fiber lasers and amplifiers, ed. M. J. F. Digonnet, Marcel Dekker Inc., 2001

[12] A. K. Srivastava and Y. Sun, "Advances in Erbium-doped fiber amplifiers," in Optical fiber telecommunications IVA: components, ed. I. P. Kamikov, and T. Li, Academic Press, (2002), pp. 174-212

[13] H. Masuda, in Raman amplifiers for telecommunications 2: sub systems and systems, M. N. Islam eds. (Springer, 2004)

[14] K. Rottwitt, "Distributed Raman Amplifiers", in Raman amplification in fiber optical communications systems, C. Headley, and G. P. Agrawal, (Elsevier Academic Press, 2005), pp. 103-168

[15] S. Jain, N. K. Thipparapu, P. Barua, and J. K. Sahu, "Cladding-Pumped Er/Yb-Doped Multi-Element Fiber Amplifier for Wideband Applications," IEEE Photonics Technology Letters, 27 (4), 356 - 358 (2015)

[16] S. Jain, T.C.May-Smith, J.K.Sahu, "Cladding-pumped Er/Yb-doped Multi-Element Fiber Amplifier for C+L band Operations," in Opt. Fiber Commun. (OFC) San Francisco 9-13 Mar, M2J.3, (2014).

[17] D. Qian, E. Ip, M.-F. Huang, M.-J. Li, A. Dogariu, S. Zhang, Y. Shao, Y.-K. Huang, Y. Zhang, X. Cheng, Y. Tian, P. Ji, A. Collier, Y. Geng, J. Linares, C. Montero, V. Moreno, X. Prieto, and T. Wang, "1.05Pb/s transmission with 109b/s/Hz spectral efficiency using hybrid single- and few-mode cores," Frontiers in Optics (FIO2012), PDP FW6C.3 (2012).

[18] R. G. H. van Uden, R. Amezcua Correa, E. Antonio Lopez, F. M. Huijskens, C. Xia, G. Li, A. Schülzgen, H. de Waardt, A. M. J. Koonen, and C. M. Okonkwo "Ultra-high-density spatial division multiplexing with a few-mode multicore fibre," Nature Photonics 8(11), pp. 865-870, (2014)

[19] Y. Sasaki, Y. Amma, K. Takenaga, S. Matsuo, K. Saitoh, and M. Koshiba, "Few-mode multicore fiber with 36 spatial modes (three modes (LP_{01}, LP_{11a}, LP_{11b}) × 12 cores)," Journ. of Lightwave Tech., **33**(5), 964-970 (2015)

[20] S. Jain, Y. Jung, T. C. May-Smith, S. U. Alam, J. K. Sahu, and D. J. Richardson, "Few-mode multi-element fiber amplifier for mode division multiplexing," Optics Express, 22(23), 29031-29036, (2014)

[21] Y.Jung, S. Jain, T.May-Smith, J.Sahu, S-U.Alam, D.J.Richardson, "Few-mode multi-element fiber amplifier for mode division multiplexing," European Conference on Optical Communications (ECOC), Cannes 21-25 Sep, Tu.3.4.4, (2014)

[22] E. L. Lim, Y. Jung, Q. Kang, T. C. May-Smith, N. H. L. Wong, R. Standish, F. Poletti, J. K. Sahu, S. U. Alam, and D. J. Richardson, "First demonstration of cladding pumped few-moded EDFA for mode division multiplexed transmission," in Optical Fiber Communications, M2J.2, San Francisco (2014).

Chapter-5

Passive Multi-element Fibre

5.1. Introduction

The passive SDM fibre as a component offers integration of multiple spatial channels. The passive SDM fibre along with development of passive SDM components could potentially provide huge cost saving. For this, development of SDM transmission fibres has attracted a major investment by research community. In particular, two major technologies, MCF and FMF have gained significant research attention. Data capacity of up to 2.15 Pbit/s has been demonstrated in MCF [1-2]. The review of MCF and FMF is covered in Chapter-2. In this Chapter, development of passive fibres based on MEF technology has been demonstrated. The fabrication parameters and commercial requirements of passive fibres are drastically different from amplifier fibres. In passive fibres, low loss (0.2 dB/km in current SSMFs) is desired, whereas, the background loss of the amplifiers reach up to tens of dB/km, two order of magnitude higher than the losses in passive fibres. Also, the fibre length in passive fibres is in hundreds of kilometre compared to short length of active fibre required in an amplifier. Moreover, the high mechanical strength of the fibre (>100kpsi) is critical in passive fibre to ensure long lifespan after deployment [3]. In this chapter, modification in MEF preform assembly and MEF drawing is considered in order to

meet the telecoms requirement. The proof-test strength and characterisation of loss and transmission performance of developed MEFs is reported. Finally, an SDM experiment involving 3-MEFs and cladding-pump MEFA is demonstrated to show the potential of MEF technology for SDM networks.

5.2. Modified Fabrication for passive MEF

The fabrication of long length of MEFs can be achieved by increasing the volume of glass in individual preform-elements either by increasing their diameter or length. Since the diameter of perform-elements is limited by the diameter of the furnace as explained in section 3.2. The only possible solution was to increase the length of MEF perform assembly which required longer length of stretched preform-elements. However, the length that could be obtained from stretching on GWL decreases as the diameter of preform-elements decreases. This is due to the fact that at low diameter, the preform-element starts to flex due to its weight. This changes the position of the glass in the flame along the length thereby resulting in temperature fluctuation and hence diameter deviation along its length. As discussed in Chapter-3, fluctuation in diameter of preform-elements in MEF assembly could lead to collapsing of the assembly. On the other hand, the maximum preform length that could be fabricated in a single stroke with our tower is 80cm resulting in maximum of 3-km length of 7-MEF with fibre-element diameter of 100µm, if the process explained in section 3.2 is implemented.

Modification in MEF preform assembly was implemented to increase the fabricated MEF lengths, and it is explained in section 5.2.1. Section 5.2.2 discusses the modification in MEF drawing conditions to further improve their strength. The coating system used in the passive MEF fabrication was changed from single coating to dual coating. The advantages of the dual coating system have been explained in section 5.2.2, and subsequently MEFs are proof-tested to show their high strength. The loss and transmission performance of MEFs has been discussed in section 5.3.

5.2.1. Modification of MEF Preform Assembly

In previous work (see Chapter-3), diameter of the preform-elements was limited by dimensions of the restrictor tube in the furnace, 21mm. But, the diameter of the preform-elements can be increased by adapting some changes in the MEF assembly

process. It can be seen from Fig. 5.1, the upper section of the furnace is 34mm and the diameter of the preform-elements can be larger in this section. The MEF preform assembly can be pre-necked on the GWL i.e. the assembly can be tapered and joined to a drop of diameter, φ<18mm, for the drop to pass through the restrictor in order to initiate the MEF drawing process. Through this, the volume of the glass to be drawn could be increased whilst using the same furnace. With this, the size of each preform elements in 3-MEF and 7-MEF preform assembly could be increased to 12mm and 8mm respectively.

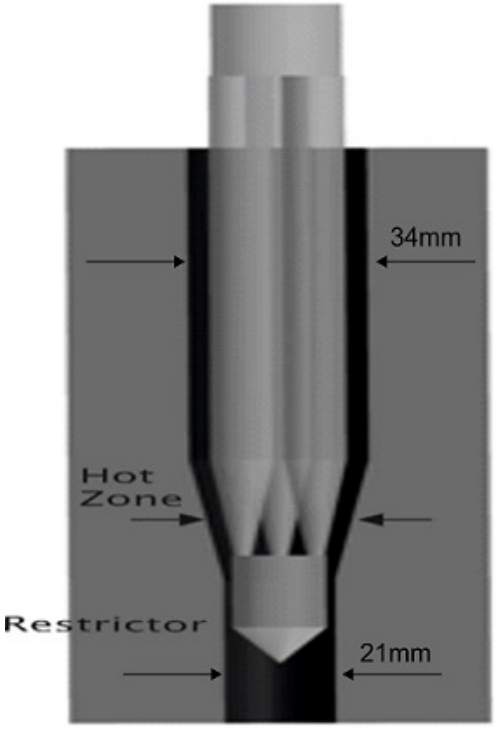

Fig. 5.1 Placement of 3-MEF preform assembly for long length fabrication

A few changes were also made in the MEF preform assembly process to accommodate the new procedure. First, a new jig for 3-MEF with 12mm holes was prepared, and the holes in the jig were made deeper (100mm) than previous case (50mm) to hold the thicker (12mm of 3-MEF and 8mm for 7-MEF) preform elements.

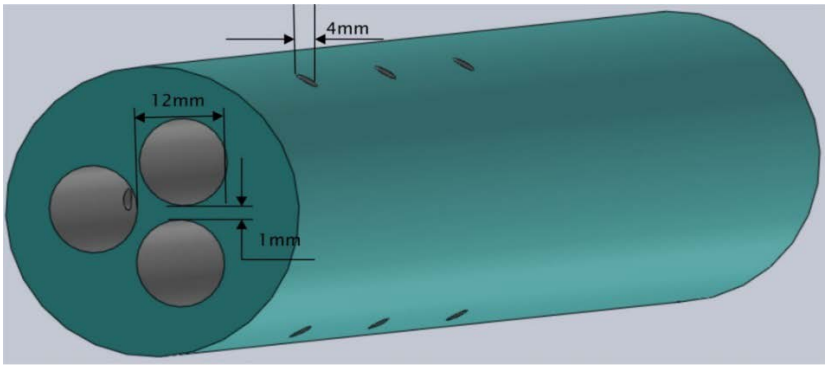

(a)

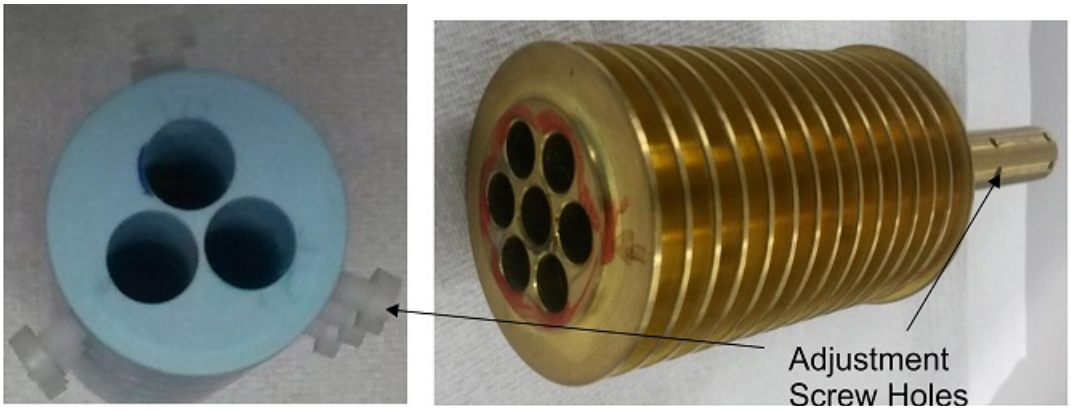

(b) (c)

Fig. 5.2 (a) shows the schematic jig of 3-MEF, and image of (b)-(c) 3-MEF and 7-MEF jigs, respectively, used for passiveMEF assembly with 3-adjustment screw holes for each preform element

Figure 5.2 (a) and (b) shows the schematic diagram and actual jig for 3-MEF with 3 adjustment screws for each preform element on curved surface. The adjustment screws on each hole were used to tightly clamp the preform elements. The screws also allowed some tolerance to the diameter and length precision required during MEF preform assembly. The metal hooks and glass tube (see Fig. 3.4) during handle joint were not required as a result of thicker preform and modified jig ensuring further cleanliness of the assembly procedure. Figure 5.2 (c) shows similar jig for 7-MEF preform assembly. In jig for 7-MEF preform assembly, the central rod was clamped at positions along the length which is different from the positions of outer preform-element clamps. Figure 5.3 (a) shows the 7-MEF jig on the GWL with the 8mm preform elements inserted into it. The end view shows 7 preforms in the hexagonal geometry and uniform separation can be seen in Fig. 5.3 (b). The schematic procedure for 3-MEF preform assembly is shown in Fig. 5.4 (a)-(e).

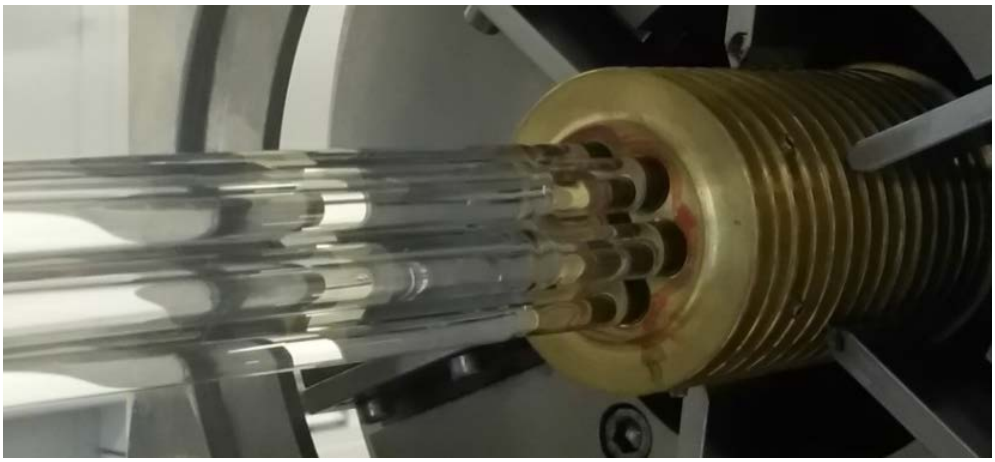

(a)

(b)

Fig. 5.3 (a) Side and (b) end view of the 7-MEF preform assembly on GWL showing the separation of preform-elements

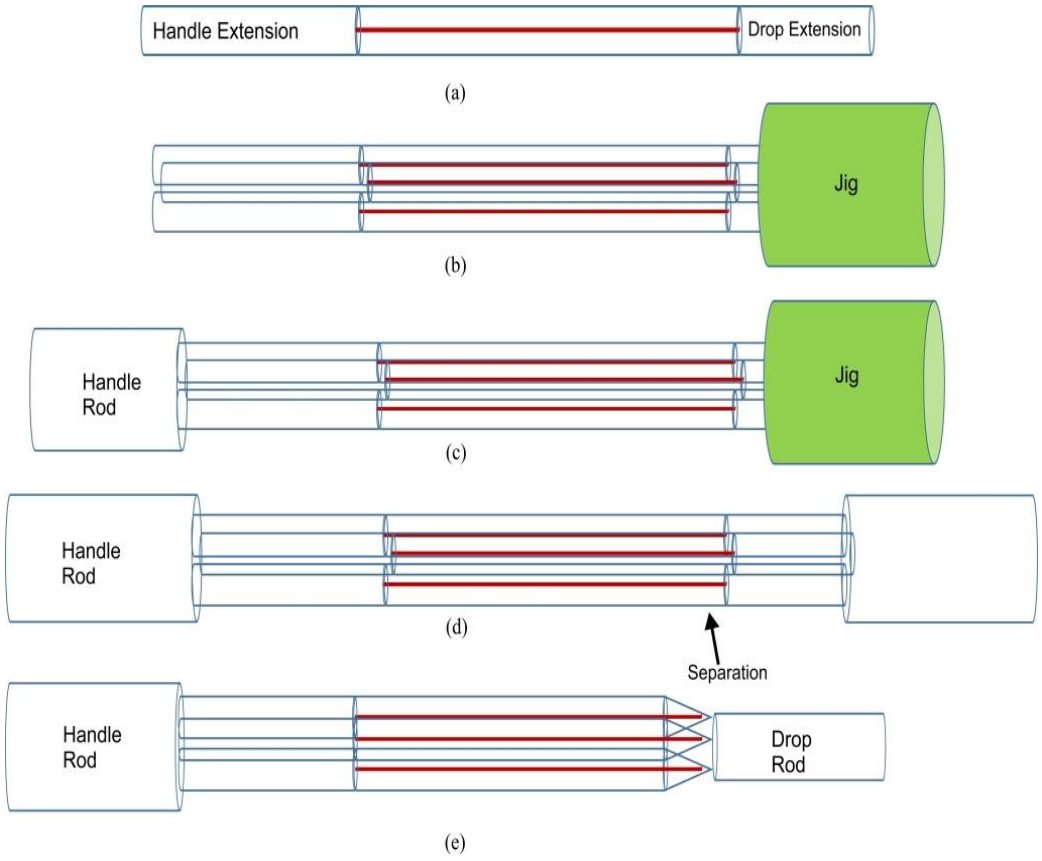

Fig. 5.4 (a)-(e)Schematic steps of 3-MEF assembly

The fluctuation in the furnace gas flows during the fibre fabrication could result in the diameter variation in the fibre and even fibre break. One such fluctuation might arise when the handle joint enters the furnace through iris. As shown in Fig. 5.4(a), the handle extension rod of 200mm length was used on each preform element to prevent the perturbation of furnace gas flows via handle joint. The length of handle extension rod chosen to be the same size as the distance of the iris from the hot zone in the

furnace, and its diameter is same as the diameter of preform elements. As shown in Fig. 5.4 (a), the drop extension rods on other side of the preform was also used to ensure that the actual preform is not touched with hand during assembly and cleanliness of the preforms is maintained. Cleanliness of the preform is critical to fibre fabrication procedure [4]. The preform elements are then inserted into the jig from drop extension side as shown in Fig. 5.4 (b). The MEF preform assembly is then joined to a 25mm handle rod on other side (see Fig. 5.4 (c)), and the actual image of joint handle can be seen in Fig. 5.5. Next, the jig is removed from the other side, and another rod is attached on the other side as shown in Fig. 5.4 (d). The drop extension rods are then separated using flame which results in pointed tips (see Fig. 5.3 (b)). After this, these tips at the end are bent inwards using hand torch to ensure that they touch the drop rod.

Fig. 5.5 Handle joint of 7-MEF assembly

Finally, the preform assembly with the bent tips is joined to the drop rod of diameter <18mm as shown in Fig. 5.4(e). Fig. 5.6 shows the bent tips joined to the 16mm drop in the finished assembly.

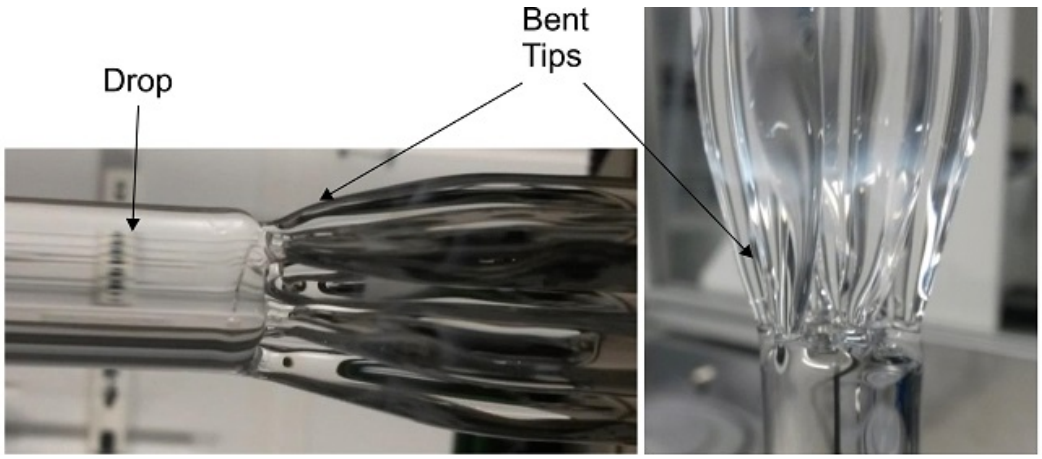

(a) (b)

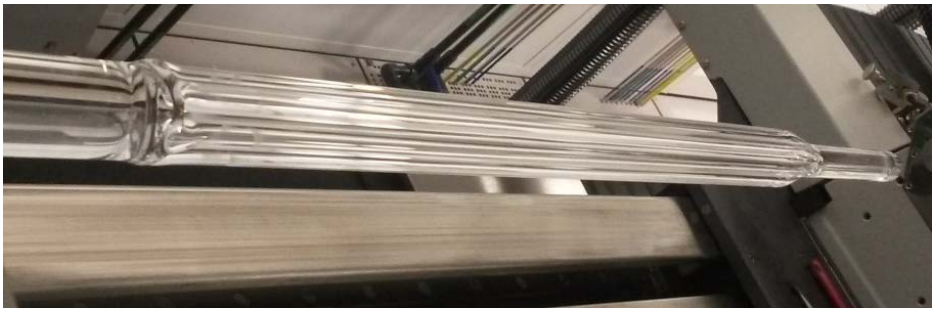

(c)

Fig. 5.6 (a)-(b) Images of MEF assembly with bent tips of preform elements that are joined to 16mm drop, and (c) Completed MEF assembly.

It should be noted that in a commercial environment, the assembly process could altogether be eliminated. A jig could be fabricated which can allow to stack the preforms on the drawing tower. One such example of a jig is shown in Fig. 5.7 which allows 12mm preforms to be stacked on the fabrication tower and also incorporates water cooling. Water cooling is to prevent the jig from expanding which might result in loose grip of the preform elements. Multiple furnaces close to each other could also be used with each using thick preforms which would ease the stringent requirement of MEF assembly faced in our research conditions.

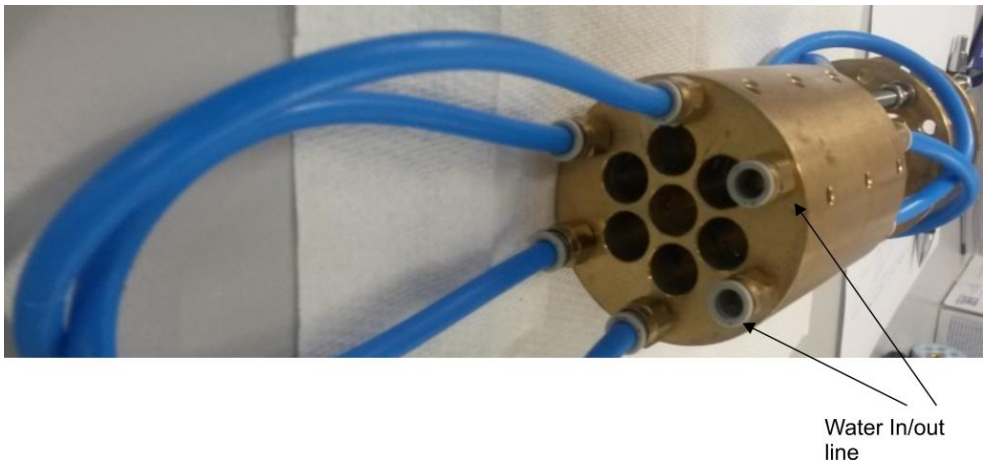

Fig. 5. 7 Image of 7-MEF jig for 12mm preform with water cooling

5.2.2. Modification of MEF Fabrication

While modification in the assembly enabled larger MEF fabrication length, the strength was improved by changing the coating system from single coating to dual coating. Dual coating consists of an inner coating referred to as primary coating, and an outer coating referred to as secondary coating. Both primary (DSM DP-1004) and secondary (DSM DS-2015) coatings used for passive MEFs were high index with respect to silica cladding. It should be noted that commercial passive fibres conventionally use the dual coating system to mitigate the microbending loss. The

primary coating is soft with low elastic modulus which acts as a cushion for the fibre whereas secondary coating protects the fibre from the environment.

Table 5.1 Viscosity and modulus of the high-index coatings used for passive MEF fabrication.

	DSM-3471-314 (Single coating)	DP-1004 (Primary Coating)	DS-2015 (Secondary Coating)
Viscosity @25^{0}C (mPa.sec)	10,000	4300	5900
Modulus (MPa)	35	1.3	950

In MEF, the viscosity of primary coating was much lower than the secondary coating as well as high-index and low-index single coatings used in the previous cases for fabrication of Er-doped active MEFs. Table 5.1 lists the supplier specified modulus and viscosity of the high-index coatings used for the fabrication [5]. The coating dies plays even more important role in the fabrication of the MEF as compared to conventional fibre drawing. The primary coating die acts as a restrictor to the fibre coming to the coating applicator which in turns decides the total diameter and hence the compactness of the MEF.

In MEF, the dual coating system provided additional advantage that the low viscosity of primary coating did not make the MEF grouping unstable as opposed to the case of single coating system, in which asymmetry in the fibre alignment destroyed the symmetric grouping. Previously, in a single coating, the MEF preform assembly was rotated during the MEF drawing to make the grouping stable. Whereas, the rotation of preform assembly was not necessary to keep the fibre-element geometry stable in coating cup during MEF fabrication. The stability of MEF coating procedure becomes critical as the number of elements are increased from 3 to 7. The use of dual coating system was implemented with wet-on-wet coating application as opposed to conventional wet-on-dry [6] application due to limitation of the height of tower. This made the position of fibre-elements in the coating sensitive to manual die alignment in MEF fabrication. Figure 5.8 shows the primary and secondary coating die assembly of the applicator provided by SG Controls. These assemblies are manually aligned to each other with the help of a microscope.

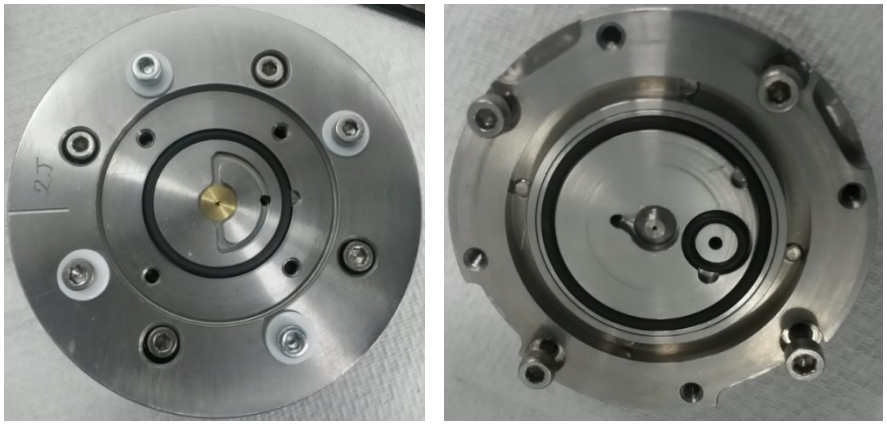

(a) (b)

Fig. 5.8 (a) Primary, and (b) secondary die assemblies of the dual coating system.

The use of dual coating system also eliminated the potential air gaps between the elements in MEF with single coating as seen in Fig. 3.1. Though air gaps are not believed to be critical issue as far as passive MEF and core-pump MEF is concerned but in cladding-pump configuration it can lead to variation in pump-signal coupling. It was believed that the dual index coating would provide better strength to the MEFs due to the stability of the fibre geometry attained in coating applicator die. This was confirmed with the MEF strength tests, as demonstrated in section 5.3.

5.3. Passive MEF Characterisation

5.3.1. Proof-Test

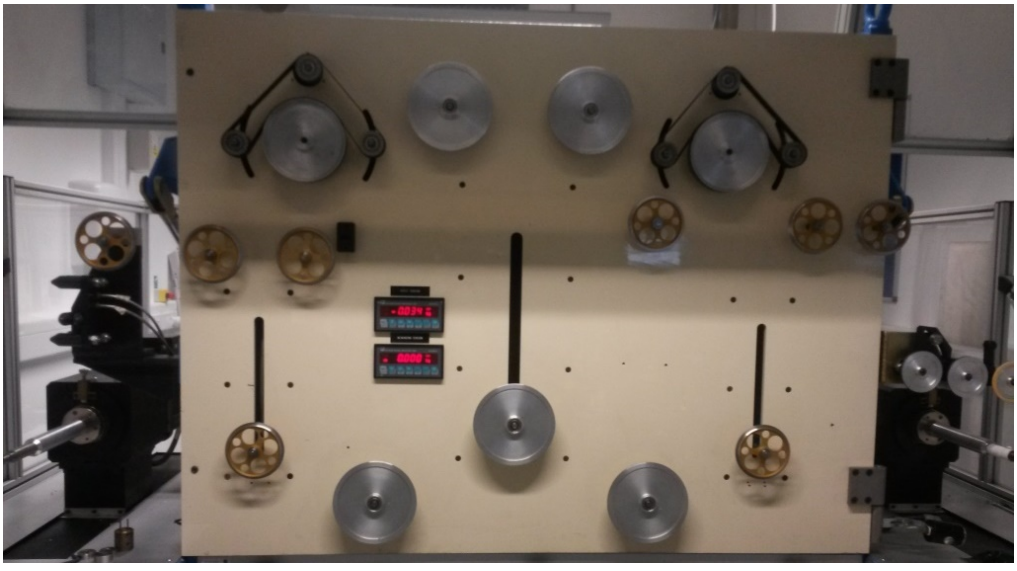

Fig. 5.9 Proof-test and rewinding machine

Proof testing is a well-established method to verify the strength of the fibre by applying stress to it. Figure 5.9 shows the proof test machine used for the

measurement. Multiple 3-MEF and 7-MEF preform assembly were made using clear fused quartz (CFQ) test rods as preform elements, and MEFs with different element diameters were fabricated from it using the modified fabrication and dual coating system. These MEFs were then proof tested. The weight required for proof testing was calculated using the equation given below.

$$W = nW_o\left(\frac{d_i}{d_o}\right)^2 \tag{5.1}$$

Where, W_o, d_i, d_o and n are weight required for standard fibre, diameter of each element of MEF, diameter of standard fibre and number of fibre-elements in MEF respectively. The standard weight corresponding to 100 kilo-pounds per square inch (kpsi) (1% proof strength) for a fibre with the outer diameter of 125μm is 0.86kg.

Table 5.2 Proof-test of different MEFs

Fibre No.	Fibre Type	Element-to-element spacing (μm)	Element Diameter (μm)	Primary Die (μm)	Proof Test Strength (Kpsi)
A0327	3-MEF	95	80	300	400
A0330	3-MEF	55	80	250	400
A0356	3-MEF	No (Compact)	80	190	˜100
A0316	3-MEF	95-100	60	250	>500
A0496	7-MEF	25-40	80	340	>250
A0711	7-MEF	20-60	60	300	>430

Several test draws of compact and non-compact 3-MEF geometries with different element sizes (80 and 60 μm) and element-to-element spacing were made using CFQ rods. This was to establish the 3-MEF fabrication parameters that are suitable for the manufacturing of long lengths of fiber while keeping its mechanical strength. It was observed that the strength of MEFs increased with decrease in their fibre-element diameter. Table 5.2 summarise the results of proof test on various MEFs that were fabricated with different fibre-element spacing. Different fibre-element spacing was achieved by using different primary dies as shown in table 5.2. For 80μm fibre-elements diameter, the MEFs in which fibre-elements were not touching each other showed similar proof-test strength (400 kpsi), whereas strength of compact MEF was reduced (100kpsi). It was established that in order to maintain higher strength in MEFs, the fibre-elements should not touch each other. It is worth noting that the same

fiber drawing conditions as obtained from the test draws of non-compact 3-MEF with 95μm element spacing and compact (no-spacing) were utilized to draw germanium (Ge)-doped non-compact (Fig 5.10(a)) and compact (Fig. 5.10(b)) 3-MEFs respectively.

Table 5.3 List of fabricated passive fibres (: from commercial low loss preform, **: from CFQ rods)*

Fibre No.	Fibre Type	Primary Die (μm)	Diameter (μm)	Length (km)	Coating system	Temp. (°C)	Draw Speed (m/min)
A0292	7-MEF	--	100	1.2	Single	2025	10
A0298	Single Fibre	--	100	1.2	Single	2025	20
A0286	7-MEF**	--	60-100	N/A	Single	2025	10
A0316	3-MEF**	250	60	N/A	Dual	2030	10
A0317	3-MEF	250	60	2.5	Dual	2030	10
A0322	3-MEF**	300	80	N/A	Dual	2030	10-20
A0327	3-MEF**	300	80	N/A	Dual	2030	10-30
A0328	Single Fibre	190	60	7	Dual	2030	30
A0330	3-MEF	300	80	9.5	Dual	2030	30
A0351	3-MEF**	190	60-80	N/A	Dual	2030	10
A0356	3-MEF**	190	80	N/A	Dual	2030	30
A0360	3-MEF	190	80	3.07	Dual	2030	20
A0396	3-MEF	250	80	4.5	Dual	2030	20
A0408	7-MEF**	250-300	80	N/A	Dual	2000-2030	10
A0419	7-MEF**	300	80	N/A	Dual	2030	10-30
A0496	7-MEF**	340	80	N/A	Dual	2020-1970	20
A0504	7-MEF	340	80	2.7	Dual	1990	20
A0640	Single*	170	80	2	Dual	2010	20
A0656	7-MEF*	340	80	0.91	Dual	2000	10
A0711	7-MEF**	300	60	N/A	Dual	2000	10
A0725	7-MEF*	300	60	3.5	Dual	2000	10

Several passive MEFs were fabricated from a Ge-Si preform, with NA, core and outer diameter of 0.12, 10mm and 15mm respectively. The preform was sleeved multiple times by Dr. T. C. May-Smith to obtain the core/cladding ratio corresponding to the cut-off wavelength, 1250-1300nm. Before each fabrication, the corresponding parameters were obtained by performing multiple test draws using CFQ MEF preform

assembly. Table 5.3 lists the passive and test fibres that were fabricated from above mentioned preform, CFQ rods**, and low loss commercial preform*.

5.3.2. Loss Measurement

3-MEF

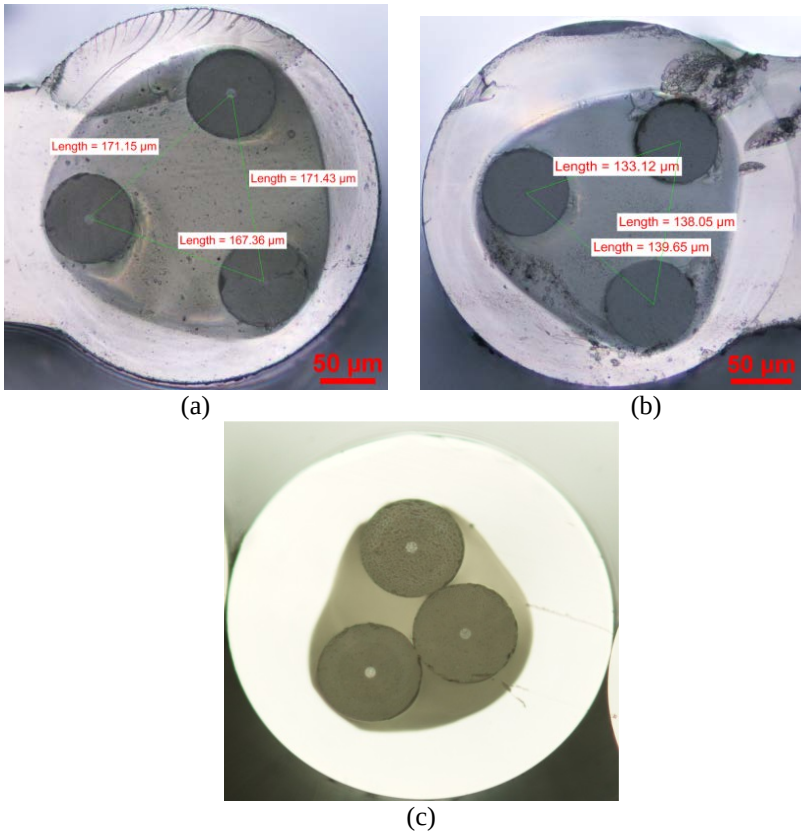

(a) (b)

(c)

Fig. 5.10 Microscope images of non-compact with element to element separation (a) 90-95µm, (b) 50-55µm, and (c) compact passive 3-MEF fabricated from Ge-doped preform

Figures 5.10 (a)-(c) show microscope images of the cross-section of 3-MEFs that were fabricated with different element-to-element spacing using primary coating die size of 300µm, 250µm and 190µm respectively (A0330, A0360 and A0396) [7]. Using the conditions obtained from the test draws, first, a non-compact 3-MEF preform was assembled from a Ge-doped silica preform with a step index difference (Δn) of 0.0055, and 9.5 km of 3-MEF (A0330) was fabricated with fibre-element cladding and core diameters of ~80µm and 8.5µm respectively. The overall coated diameter was 340µm and separation of 90-95µm as shown in Fig. 5.10 (a). As shown before in active MEFs, the coating in passive MEFs also can be simply stripped off which provides the access to each fibre-elements. These fibre-elements could then be used as conventional fibres. Figure 5.11 shows the 3-MEF preform assembly from Ge-doped preform and

corresponding fibre-sample respectively where coating is removed from the ends of a MEF sample to show fibre-elements fanning out [7]. Similarly, the coating was stripped at each of the drawn MEFs and single mode pigtails were spliced to the each fibre-element at both end using standard fusion splicing.

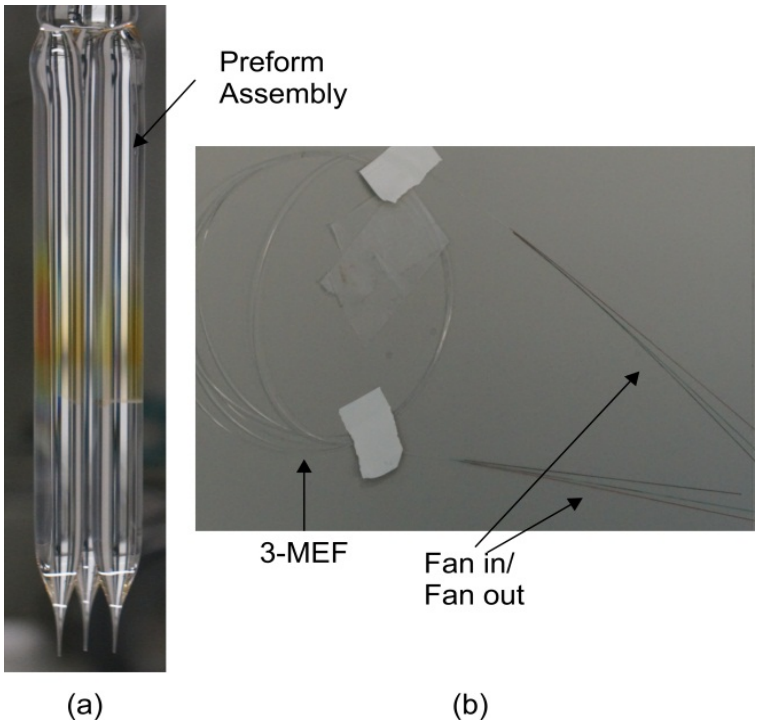

Fig. 5. 11 (a) 3-MEF preform assembly and (b) 3-MEF with fibre-elements fanning out at each end [5]

The cut-off wavelength of fibre-elements was measured to be approximately 1250nm. The dispersion at 1550 nm was measured by Dr. Victor Rancano, and it was 18-ps/nm/km respectively. The loss measured at 1550nm with an Exfo-FTB-7300E optical time-domain reflectometer (OTDR) was 0.6dB/km [7]. Similar loss was measured in a single fibre, A0298, drawn from the same Ge-doped preform with single mode core and cladding diameter of 100μm. Fig. 5.12 compares the OTDR loss for one of the fibre-elements of A0330, 9.5km, with the complete channel length obtained by looping back the fibre-elements [7]. The loss profile along the length of the MEF was similar for all the fibre-elements. Also, the crosstalk in the MEF was also measured by launching the signal in one fibre-element and detecting the level of output in other fibre-elements. As expected, no crosstalk (down to the level of -80 dB) was observed between the different fibre-elements when measured using a laser source at 1550nm.

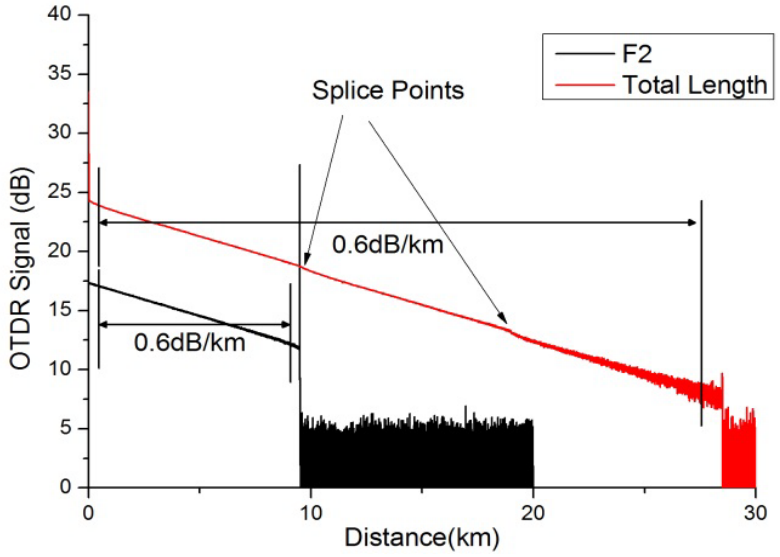

Fig. 5. 12 OTDR loss for one of the fibre-element of 3-MEF and fibre-elements in loop-back

After that, a compact 3-MEF (A0360) was fabricated. The cross-section image of the corresponding MEF is shown in Fig. 5.10 (c). No crosstalk was observed in compact 3-MEF as well. However, the loss of the compact 3-MEF was significantly higher for two of the fiber-elements than it was in the third (2.5dB/km as compared to ~0.7dB/km at a wavelength of 1550nm) [7].

Table 5.4 OTDR loss of non-compact and compact Ge-doped passive 3-MEF

3-MEF (80 µm element diameter)	Length (km)	Loss at 1310nm (dB/km)	Loss at 1550nm (dB/km)	Loss at 1650nm (dB/km)
95µm spacing	9.5	1.6	0.6	0.7
No spacing	3.07	2(1-element) ~3.5(remaining elements)	0.7(1-element) ~2.5 (remaining elements)	0.95(1-element) ~3.5 (remaining elements)

Table 5.4 lists the loss variation of the fibre elements in compact and non-compact MEF [8]. The loss in the fibre-elements of compact 3-MEF was higher compared to non-compact 3-MEF, A0330. This was due to imperfect coating with the primary polymer, resulting from the limited choice of primary coating dye sizes that were available in the laboratory. A 190µm primary dye was used for the compact 3-MEF fabrication. The size of the die was comparable to a notional triangular geometry fibre diameter of 173µm. As seen in Fig. 5.10 (c), the fibre-elements were positioned off-centred with respect to the outer coating, and also touching each other. This also resulted in loss increment in fibre-elements of compact MEF.

Following this, a 4.5km length of Ge-doped 3-MEF, A0396, with an element separation of about 55 µm (cross-section image in Fig. 5.10 (b)) was fabricated. This MEF exhibited a similar loss profile for all three fiber-elements as that of the non-compact 3-MEF with element separation of 95µm, confirming the scope of a dense packing of the fiber-elements in MEF. It was concluded that a minimum separation between the fibre-elements is required to ensure that the strength of MEF is maintained as well as there is no degradation in the performance.

7-MEF

After the fabrication and characterisation of passive 3-MEFs, the MEF fabrication was scaled to 7 fibre-elements. It was observed that parameters became harder to control as the number of elements increased and the separation between the fibre-elements decreased. Test draws were performed to observe the effect of drawing tension, controlled through furnace temperature and MEF drawing speed, on the fibre-element geometry inside the coating of MEF. The temperature was taken down and fibre cross-section was inspected. In general, the tension in the fibre could be increased by either reducing the furnace temperature or increasing the draw speed [4]. Moreover, temperature has a more significant effect on the tension as compared to drawing speed. Due to height of the tower and to avoid the wastage of preform during ramp-up the maximum draw speed was kept to be 20m/min and temperature was reduced.

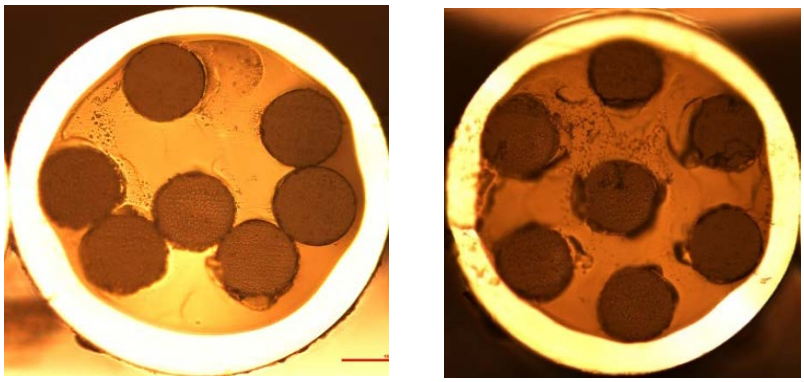

(a) (b)

Fig. 5. 13 Cross-section image of 7-MEF at different drawing temperature for (a) low, and (b) high drawing tension per fibre-element

It was observed that the fibre-elements came into the desired geometry when the furnace temperature was reduced below 1995^{o}C (A0496) corresponding to about 60 grams of tension per fibre-element with fibre-element diameter of 80µm. Figure 5.13 (a) and (b) shows the cross-section image of 7-MEFs at 2020^{o}C and at 1990^{o}C (60-

80gm/ fibre-element). Note that, due to the limitation of tension gauge which could measure tension up to only 240 gm. The tension at different temperature and drawing speed was measured during the single fibre draw with same fibre diameter as that of each fibre-element. The drawing tension in MEF is expected to multiply by number of fibre-elements. It can be clearly seen that at low tension (higher temperature), the fibre-elements were randomly arranged in the coating, whereas, higher tension (lower temperature) provided stable coating conditions. However, it should be noted that in industrial environment the fibre fabrication speed are of the order of kms per min with furnace temperature well above 2000^{o}C. The corresponding tension in the standard fibre is also kept around 50gms during commercial fabrication [4]. The low temperature fabrication requirement in our draw further restricted the fabrication tolerance in 7-MEF and frequent failures at low temperature were observed during the MEF draw which was not favourable for long length fabrication. The 7-MEF test fibres fabricated with fibre-element cladding diameter of 60µm (A0711) and 80µm (A0496) using CFQ rods were then proof tested which successfully passed 430kpsi and 250kpsi of proof test strength (see Table 5.2). It should be noted that the load corresponding to these measurement was the maximum load that the proof test machine could bear, and 7-MEFs is expected to have higher strength.

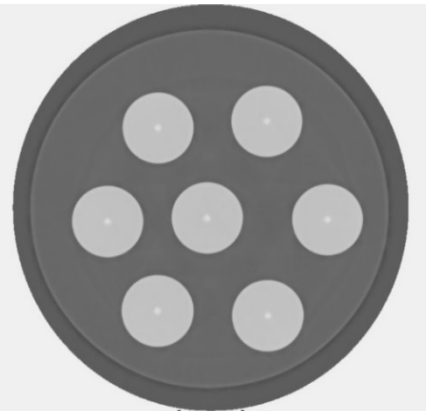

Fig. 5.14 X-ray coherence tomographic (XCT)-Scan image of 7-MEF from Ge-doped preform [7]

After this, a 2.7km of 7-MEF, A0504, was fabricated using the same preform as used before for 3-MEFs. The cross-section image using x-ray coherence tomographic (XCT)-scan taken by Reza Sandoghchi is shown in Fig. 5.14 [9]. In XCT-scan, multiple images of a sample are captured from different angle which are then stitched together to obtain a 3-D image of the sample. The spacing between the fibre-elements were between 25-40µm. The loss of all the fibre-elements was found to be about 0.6

dB/km which was equal to the losses observed in non-compact 3-MEFs and the single fibre, A0298, drawn from same preform.

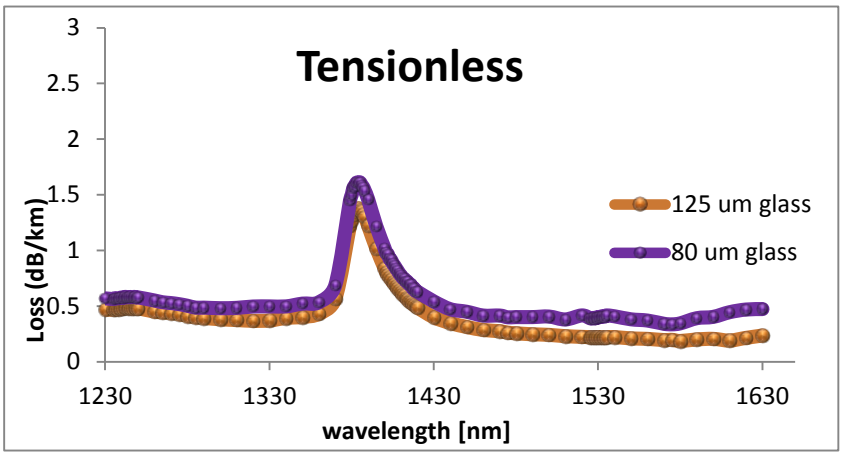

(a)

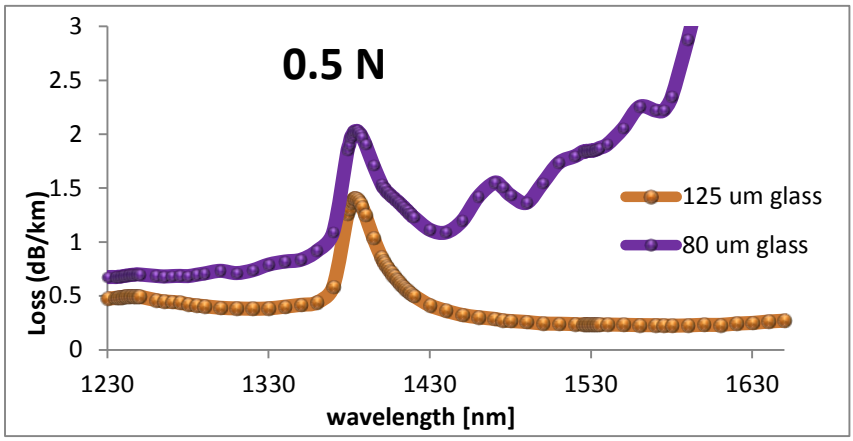

(b)

Fig. 5.15 Loss measurement in 125µm and 80µm single core fibre with (a) minimum tension and (b) 0.5N tension

To further establish that the higher losses observed in the passive MEFs were not due to the MEF geometry, single fibres were fabricated using commercially available low loss preform. The corresponding fibres from this preform are marked with * in table 5.3. Single fibres consisting of similar core size and NA as used in previous cases were fabricated with cladding diameter of 125µm and 80µm (A0640). The fabricated fibres were sent to the preform supplier for testing and it was observed that the rewinding tension in the 80µm had significant impact on the fibre loss as shown in Fig. 5.15. The results of the fibres fabricated at Optoelectronics Research Centre (ORC) and at suppliers premises produced nearly identical results. As the tension was increased to 0.5N (50grams), the loss in 80µm increased significantly compared to the loss in 125µm fibre due to microbending effect in single core fibre. Whereas, both showed similar loss when measured in tensionless condition (see Fig. 5.15).

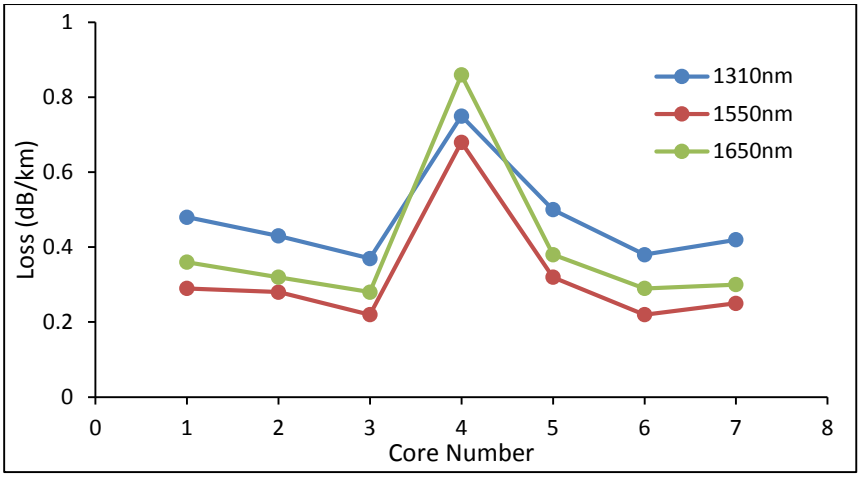

Fig. 5.16 Loss measurement in fibre-elements of 7-MEF fabricated from low-loss preform (Commercial)

Subsequently, a 7-MEF, A0656, with the same low-loss commercial preform corresponding to 80µm of fibre-element diameter was used to fabricate the fibre (see table 5.3). The fibre was drawn at 2000^0C instead of desired <1990^0C in order prevent fibre break during due to fragility at lower temperature. Thus, the resulting MEF geometry was not perfectly hexagonal due to low tension. The loss of the fibre-elements at 1550nm was observed to be <0.3 dB/km for 5 of the fibre-elements whereas the remaining two showed 0.35dB/km and 0.75dB/km of loss respectively. The loss variation at 1310nm, 1550nm and 1650nm for all the fibre-elements is shown in Fig. 5.16. It can be seen from Fig. 5.17(a) that some of the fibre-elements came close to each other which is likely to cause higher losses. However, there was no significant increase in the loss as the rewind tension was increased to 90gms as opposed to increased loss effect observed in 80µm single fibre, A0640, drawn from same preform.

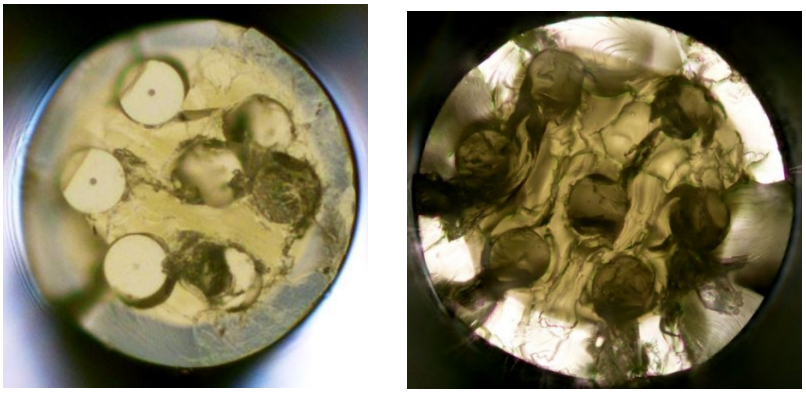

(a) (b)

Fig. 5. 17 Cross-sectional image of 7-MEF with fibre-element diameter of (a) 80µm, and (b) 60µm

Recently, a 7-MEF, A0725, with element diameter of 60µm has been fabricated. The cross-sectional image is shown in Fig. 5.17 (b). This MEF was characterised by

Miguel Nunez. In this MEF, the loss at 1310nm has been checked in one of the fibre-element and is about 0.46dB/km whereas the loss at 1550nm and 1650nm is significantly higher. Owing to difficulties in splicing 60µm fibre-element with SMF pigtail, the losses in other fibre-elements has not yet been measured. The effect of tension on the loss in this fibre-element was comparatively severe at 1650nm whereas at 1310nm no significant change was observed in 7-MEF (60µm).

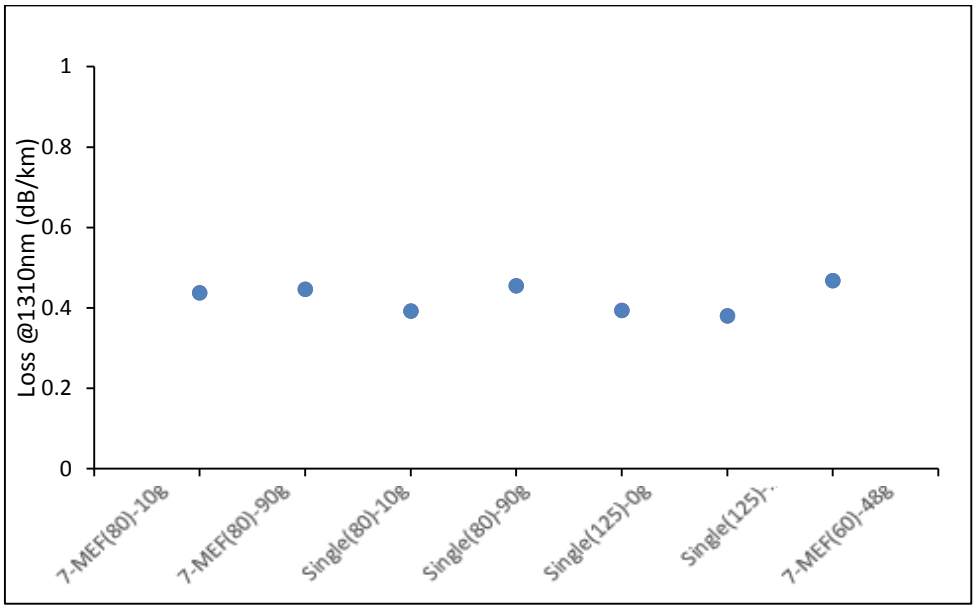

Fig. 5.18 1310nm Loss in different fibres with varying tension.

Figure 5.18 shows the comparison of tension dependent loss at 1310nm in single fibres with 80µm and 125µm outer diameter, 7-MEF (80) and 7-MEF (60), all drawn from same preform and having same core size. The results suggest that the bending losses at operating wavelengths away from the cut-off wavelength become significant as the diameter is reduced. However, the cut-off can be kept close to the operating band in order to maintain lower loss as observed in 7-MEF (60) at 1310nm. The cut-off in 7-MEF (60) was around 1270nm.

5.3.3. Transmission Experiment

A transmission experiment was performed using 3-MEFs with the help of Victor Rancano in ORC Transmission Group. The experiment experimental setup is shown in Fig. 5.19 [7]. F1, F2 and F3 represent the three different fibre-elements of the 3-MEF. Twenty one 10-Gbps-on/off keying (OOK) or intensity modulated (IM)channels, two 40-Gbps-binary phase-shift keying (BPSK) channels, and two 24-Gbps-quadrature phase-shift keying (QPSK) channels were wavelength multiplexed into the fibre using an array wave guide grating (AWG) resulting in a data rate of

338Gbps per fibre-element and an overall transmission rate of 1014 Gbps. Prior to retrieving the channels at the output, dispersion compensating fibre (DCF) was used. Due to the limited choice of tailored DCF modules in our lab, 120-ps/nm of dispersion was left uncompensated. A variable optical attenuator (VOA) and a constant power amplifier was used before the receiver, Rx, to measure the bit-error-rate (BER).

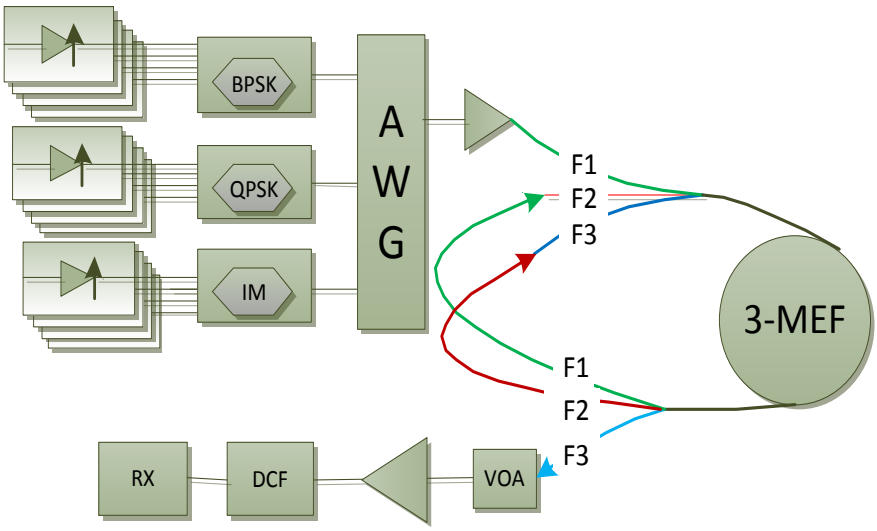

Fig. 5.19 Schematic setup for BER measurement

All the channels were detected to be error-free at the output. Indicatively, the BER vs. OSNR curves for three of the transmitted signals (one for each modulation format) are shown in Figs. 5.20 (a)-(c) [7]. For reference, the wavelengths of the BPSK, OOK and QPSK channels shown in the figure were 1555.710nm, 1541.804nm and 1551.562nm respectively. A slight difference in slope due to incomplete dispersion compensation is evident for higher baud rate signal (BPSK) as compared to QPSK. It can be seen from Fig. 5.20 (d) that the input and attenuation compensated output spectra of the channels launched in the MEF overlapped, indicating no OSNR degradation. The loss was also similar for the complete wavelength band. Similar experiments were performed on a 3.07-km length of compact 3-MEF with an overall coated diameter of 297μm, which was fabricated from the same preform to increase the element density. Fig. 5.10 (b) shows the cross-section image of the compact 3-MEF. The compact 3-MEF was also measured to be free from any crosstalk, and its performance was again confirmed by performing BER measurements. The same setup of Fig. 5.19 was used and this time the overall loop-back length was 9.21 km.

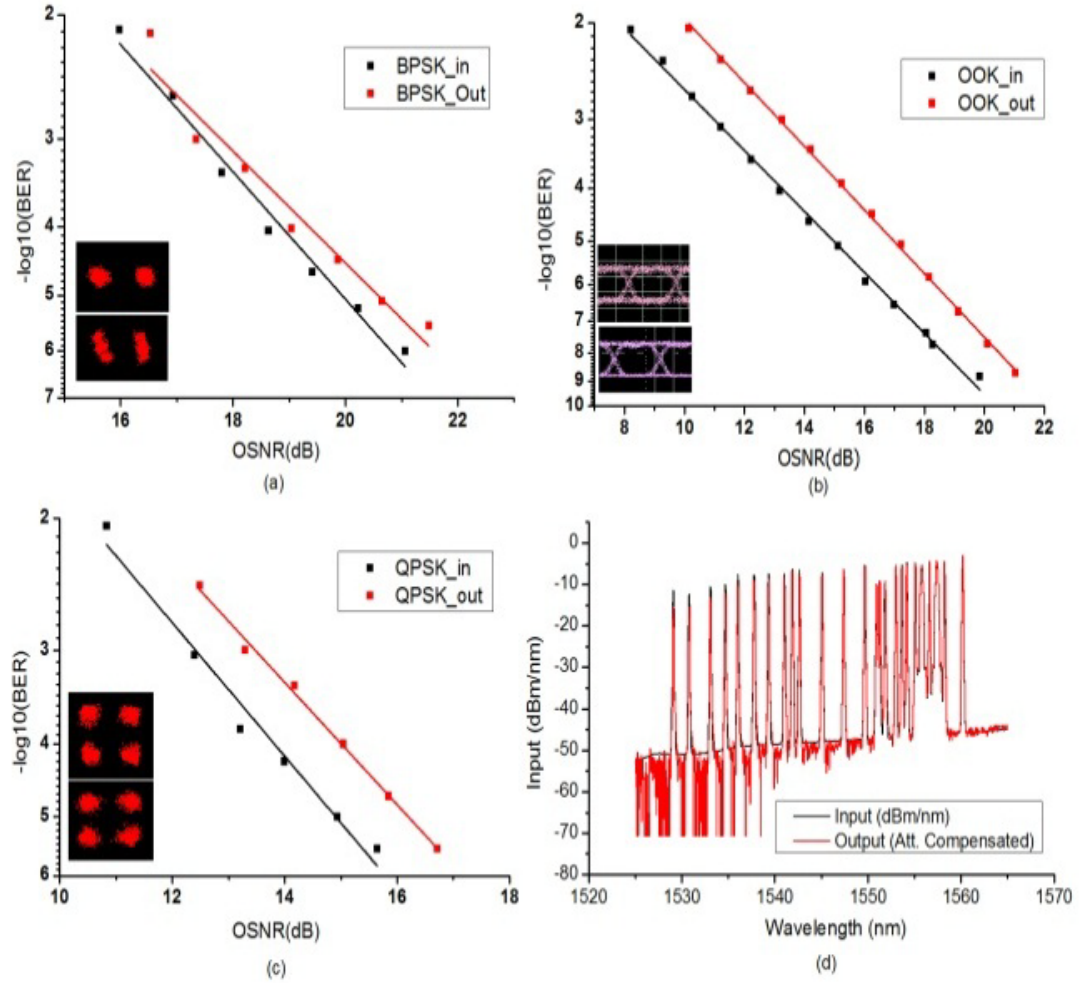

Fig. 5.20 BER vs. OSNR plots for a) 40-Gbps-BPSK, b) 10-Gbps-OOK, and c) 24-Gbps-QPSK channels. Inset shows constellation/eye diagrams at the input (top) and output (bottom), respectively; d) input and output spectra (attenuation-compensated) for all the channels [5]

SDM System Demonstration

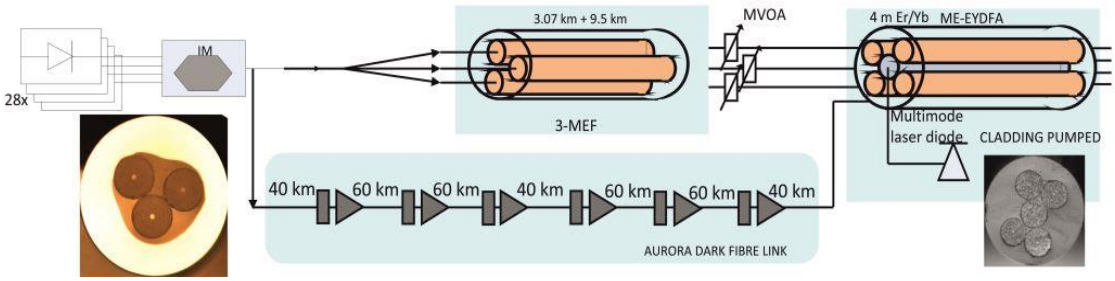

Fig. 5.21 Experimental set-up and cross-section of the MEF [7] and ME-EYDFA [10, 11].

A transmission experiment using the two passive 3-MEFs (the Non-compact MEFs, 95µm spacing, and the Compact MEF) and cladding-pump ME-EYDFA (or MEFA) was set up to emulate a hypothetical scenario of a smooth system upgrade from a single-mode WDM system to an MEF-based SDM one [12, 13]. The schematic of experimental setup is shown in Fig. 5.21. The transmitter comprised of 28 channels in the range 1535nm to 1562nm, which were modulated using a 10Gbit/s 2^{31}-1 NRZ

OOK bit sequence. The transmission line in the setup comprised four parallel paths, three of which were formed in the corresponding elements of a 3-MEF, whereas the fourth was a 400km dark fiber link (installed as part of the UK's AURORA network and ranging the distance from Southampton to London (Telehouse) and back). The total length of the 3-MEF was 12.57km and was made up of the two fiber lengths presented above, non-compact MEF (95μm spacing) and compact MEF, with respective lengths of 9.5km and 3.07km. As described previously, in order to connect the two MEFs sections together, their individual fiber-elements were simply stripped out of their protective coating at the fiber tips and spliced to standard SMF connectors using a conventional fiber splicer. The outputs of the four transmission paths with an aggregate data rate of 1120 Gbit/s were connected to the four signal fiber-elements of the 5-MEFA: the three elements of the MEF were connected to three of the input ports of the MEFA, the fourth port of which was connected to the dark fiber link (see Fig. 5.20). Three manual variable optical attenuators (MVOA) were installed at the input ports of the MEFA to compensate for any differences in both the attenuation of the different MEF elements and the gain of the various MEFA elements. It should be noted that the MEFA did not include any isolators or gain flattening elements (as opposed to what would be considered as normal for an amplifier used in a transmission link).

Fig. 5.22 (a) and 5.22 (b) shows the input from dark fiber link and MEF to the MEFA and their corresponding output after MEFA, respectively [12, 13]. The BER of all channels propagating through the four elements of the MEFA was assessed at the output of the amplifier and error-free transmission (BER<10^{-9}) was verified for both the MEF and the dark fiber paths.

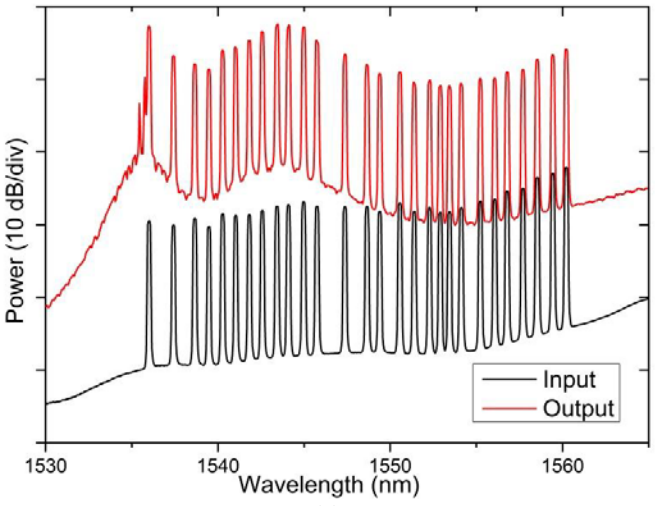

(a)

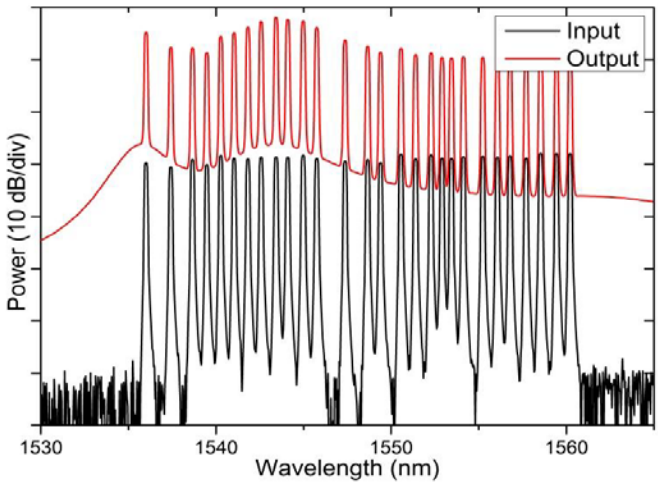

(b)

Fig. 5.22 Input spectra form dark fiber link, and output spectra before and afterMEFA respectively in (a) Drak fibre line, and (b) one of the passive MEF fibre-element line

An example of the BER performance of the system including the MEFA for both types of paths is displayed in Fig. 5.23 (as measured for the channel operating at a wavelength of 1542nm) [12, 13]. The black curve shows the BER spectra of the input signal (B2B), and it was same at the output of any of the passive MEF whereas red curve corresponds to the BER values after the dark fibre link. The OSNR degradation in MEF and dark fiber link channel was about 2dB and 1dB respectively. Higher degradation in MEF link was due to the first instance of amplification whereas the dark fibre link consisted of multiple amplifiers in the link.

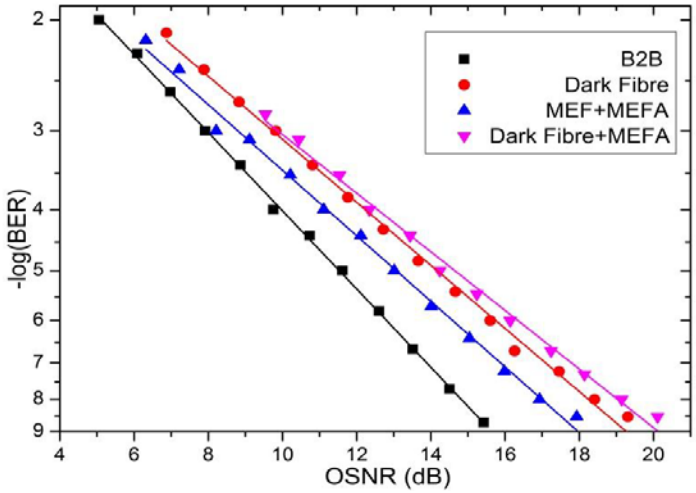

Fig. 5. 23 BER curves for the single amplification experiment.

Amplifier Crosstalk measurement using transmission setup

As discussed in Chapter-4, the crosstalk in the MEFA was not measurable due to ASE. In order to further verify that no crosstalk occurred in the MEFA, the signals at each of the MEFA output ports were characterized while the remaining fiber amplifier

elements were either fed with the data signals on or off at their inputs. The OSNR of the signals was adjusted traversing one element of the MEFA in order to achieve a BER level of 10^{-8} at the output. The deviation from this BER value was then measured while successively turning on the signals in the remaining fiber elements. No change in the detected signal power and no measurable degradation in the BER of any of the assessed channels were observed, irrespective of the number of elements of the MEFA used in parallel, or their input powers, thus confirming that the various elements were completely independent from one another in terms of crosstalk, and/or cross-gain modulation effects.

Verification of Gain Profiling Capabilities of Cladding-Pump MEFA

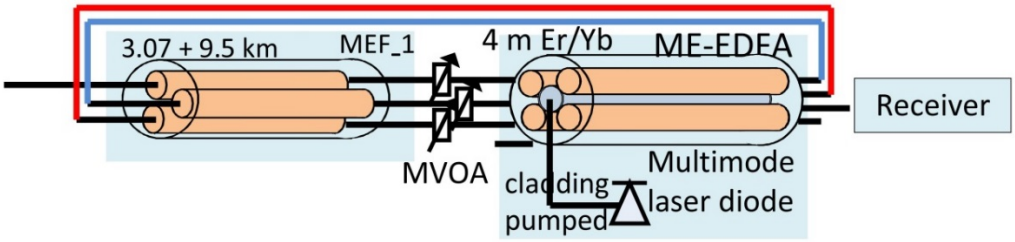

Fig. 5.24 Schematic of the cascaded chain consisting of passive and active MEF in each span [5]

Subsequently, in order to assess the performance of a chain of MEFAs, the transmission path was changed so that pairs of MEFs and MEFA spans were connected in succession, as shown in the Fig. 5.24. Figure 5.25 shows the output after each span. The accumulated spectral gain ripple of the MEFA led to a gain variation of up to 15dB between the transmitted WDM channels, leading to compromised data transmission at wavelengths away from the 1545nm peak gain region.

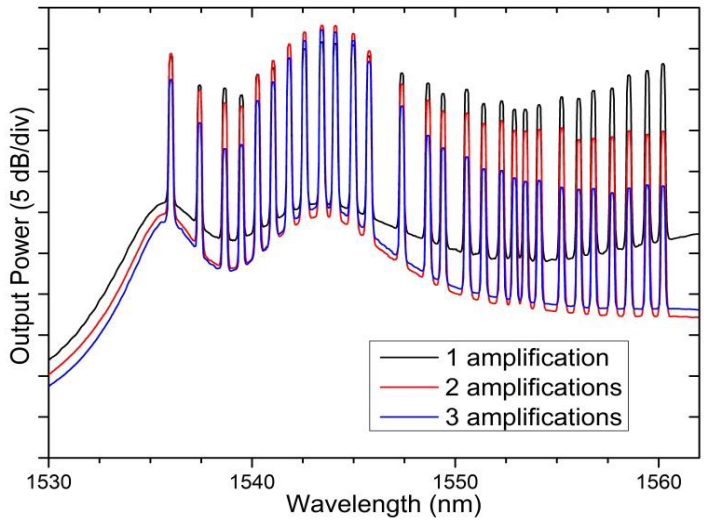

Fig. 5.25 Spectra after each amplification with three single-stage ME-EYDFA

In order to demonstrate the improved performance that might be achieved by optimizing the amplifier length and also the tuneability of the cladding-pump MEFA, the set-up was modified to exploit the gain profiling capacity of the amplifier. The second stage of amplification was made up by cascading two elements of the MEFA with co-propagating pump (see green path in Fig.5.26). The result is presented in Fig. 5.27, and expectedly the gain shifts to longer wavelengths and shows a better gain equalized performance. It was verified that by using this configuration that it was possible to achieve error-free performance for all channels beyond a wavelengths of 1540nm, indicating that important performance benefits can be gained from an optimized amplifier design.

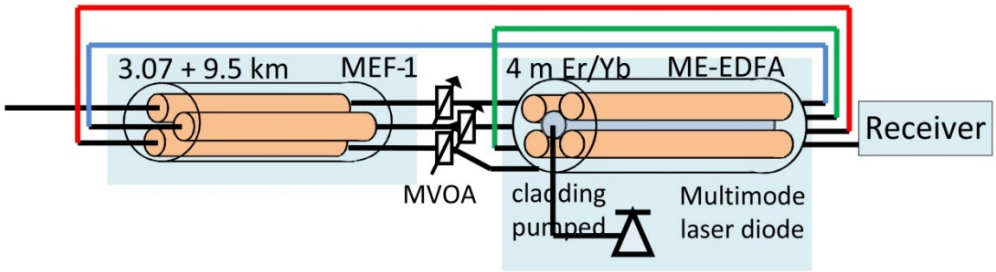

Fig. 5.26 Schematic of the cascaded chain consisting of 2-cascade (dual stage) MEFA in 2nd chain.

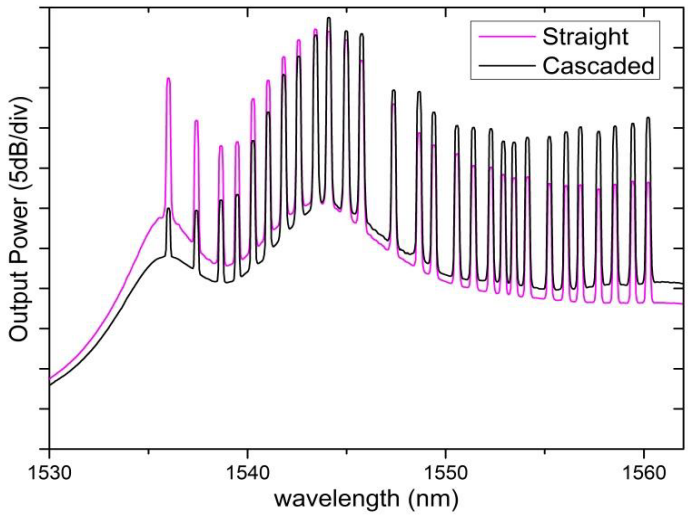

Fig. 5.27 Comparison of spectra with two single stage amplifiers and a dual-stage amplifier.

5.4. Conclusions

Modified MEF fabrication was demonstrated to accommodate the passive fibre requirements. In spatial density, MEF cable lies between MCF and conventional SMF cables. Furthermore, it was shown that the MEFs exhibit crosstalk-free operation, compatibility with conventional WDM systems and do not require the development of any special multiplexing components. MEF technology enables multiple fibers to be

drawn together within a common coating, and can be applied to the manufacturing of passive transmission fibers. Various 3-MEFs and 7-MEFs were fabricated and tested for their strength and loss. It was observed that fibre-element should not touch each other in order to ensure that the strength as well as loss characteristics of MEF does not degrade. It was shown that the technology could be scaled to incorporate higher number of elements without incurring additional losses due to the geometry. We demonstrated the feasibility of this approach by fabricating and characterizing 9.5 km and 3.07 km lengths of a passive 3-MEF from a Ge-doped preform. Error-free 1014Gbps data transmission over the lengths of MEF was demonstrated, highlighting the crosstalk-free operation offered. Finally, the first implementation of an amplified MEF-based SDM transmission system including both passive and active SDM components was experimentally demonstrated. The MEF technology shows full compatibility with existing WDM systems and sufficient flexibility to be considered as a contender for the implementation of fully functional SDM systems. In cladding-pump MEFAs crosstalk free operation and tuneability through cascading was also checked in the transmission networks thereby further confirming the results of Ch-4.

References

[1] B. J. Puttnam, R. S. Luís, W. Klaus, J. Sakaguchi, J.-M. Delgado Mendinueta, Y. Awaji, N. Wada, Y. Tamura , T. Hayashi, M. Hirano, and J. Marciante, "2.15 Pb/s Transmission Using a 22 Core Homogeneous SingleMode Multi-Core Fiber and Wideband Optical Comb, " in European Conf. on Optical Communication (ECOC 2015), PDP.3.1 (2015)

[2] D. Soma, K. Igarashi, Y. Wakayama, K. Takeshima, Y. Kawaguchi, N. Yoshikane, T. Tsuritani, I. Morita, and M. Suzuki, "2.05 Peta-bit/s Super-Nyquist-WDM SDM Transmission Using 9.8-km 6-mode 19-core Fiber in Full C band," in European Conf. on Optical Communication (ECOC 2015), PDP.3.2 (2015)

[3] https://www.corning.com/media/worldwide/coc/documents/Fiber/SMF-28%20Ultra.pdf

[4] F. V. DiMarcello, C. R. Kurkjian, and J. C. Williams, "Fiber drawing and strength properties," in Optical Fiber Communications Vol. 1, ed. Tingye Li, Academic Press Inc., (1985).

[5] http://www.dsm.com/markets/paint/en_US/home.html?WT.srch=1&WT.mc_id=CoatingResins_Branding_SEA_Google

[6] S.R. Schmid, and A, F. Toussaint, "Optical fiber Coatings," in Specialty Optical Fibers Handbook, ed. A. Mendez and T. F. Morse, Elsevier Inc., (2007).

[7] S. Jain, T. C. May-Smith, V. J. F. Rancaño, P. Petropoulos, D. J. Richardson, and J. K. Sahu, "Multi-element fibre for space-division multiplexed transmission, " in European Conf. on Optical Comm. (ECOC), London 22-26 Sep, Mo.4.A.2, (2013)

[8] J. K. Sahu, S. Jain, V. J. F. Rancaño, T. C. May-Smith, A. Webb, P. Petropoulos, and D. J. Richardson, "Multi-element fiber for space-division multiplexing," SPIE Photonics West San Francisco 1-6 Feb, 9009, (2014)

[9] S. R. Sandoghchi, G. T. Jasion, N. V. Wheeler, S. Jain, Z. Lian, J. P. Wooler, R. P. Boardman, N. Baddela, Y. Chen, J. Hayes, E. N. Fokoua, T. Bradley, D. R. Gray, S. M. Mousavi, M. Petrovich, F. Poletti, D. J. Richardson, "X-ray tomography for structural analysis of microstructured and multimaterial optical fibers and preforms," Opt Express, 22 (21), 26181-26192, (2014)

[10] S. Jain, N. K. Thipparapu, P. Barua, and J. K. Sahu, "Cladding-Pumped Er/Yb-doped multi-element fiber amplifier for wideband applications," IEEE Photonics Technology Letters, 27 (4), 356 - 358 (2015)

[11] S. Jain, T. C. May-Smith, and J. K. Sahu, "Cladding-pumped Er/Yb-doped multi-element fiber amplifier," in Workshop on Speciality Optical Fibers and their Applications (WSOF 2013), 5.4, (2013)

[12] V. J. F. Rancaño, S. Jain, T. C. May-Smith, J. K. Sahu, P. Petropoulos, and D. J. Richardson, "First demonstration of an amplified transmission line based on multi-element fibre technology," in European Conf. on Optical Comm. (ECOC), London 22-26 Sep, PD1.C.2, (2013)

[13] S. Jain, V. J. F. Rancaño, T. C. May-Smith, P. Petropoulos, J. K. Sahu, D. J. Richardson, "Multi-element fiber for space-division multiplexing operations," Optics Express, 22(4), 3787-3796, (2014).

Chapter-6

Conclusions and Outlook

6.1. Conclusions

In the thesis, a novel MEF technology has been demonstrated for implementing SDM in optical fibres. The fabrication aspects of MEF have been discussed for both, core and cladding pumped amplifier. In the first demonstration of the technology, core-pumped SDM amplifiers, Er-doped 3-MEFA and 7-MEFA were fabricated and characterized for their amplification performance. All fibre-elements in the 3-MEF and 7-MEF provided similar performance. An average gain of 33dB and a NF <5dB was achieved per fibre-element using -23dBm of an input signal at a wavelength of 1530nm. The fabrication of core-pump MEFA was shown to be tolerant to imperfections in the MEF geometry as opposed to MCF based amplifiers. This is due to that fact that conventional splicing technique could be employed in MEFs and precision alignment to cores was not required. It was shown that the MEF fabrication meets the criteria of practical rigor, and could be used to fabricate long lengths of fibres. Moreover, there was no measurable crosstalk between the signals in the fiber-elements of core-pumped MEFA, i.e. fibre-elements of core-pumped MEFAs were shown behave as individual EDFAs in isolation. This was expected as at the

minimum fibre-element diameter was 100μm in core-pumped MEFAs. It was shown that the added flexibility in changing the length of amplifier fibre through cascading of the fibre-elements could help to tune the gain profile of the amplifier. It can also be exploited to develop a broadband amplifier in split-band configuration. Such an amplifier was proposed to provide an overall gain of >20dB in a wideband covering wavelength region of 1520-1595nm.

The approach was also extended to develop a novel cladding pump MEFA. A cladding pump based 5-MEFA was developed. Cladding-pumped 5-MEFA consisted of a pump fibre-element and 4 surrounding signal fibre-elements. The cladding-pumped MEFA enabled easy side pump coupling scheme which eliminates the need for a pump/signal combiner. At first, a C-band MEFA was developed. A maximum of 37dB gain and 7.3dB of corresponding NF was obtained in the fibre-element with lower Er/Yb concentration. Element-to-element gain variation of about 3.5dB was observed at 1545nm with an input signal of -23dBm. This was mainly due to the variation of the concentration along the length of the preform. It is expected to improve with the use of uniform preforms. Improvements in NF should also be achieved by reducing the signal loss at the input section of the fibre-elements. The initial stripped section in cladding-pumped MEFA was unpumped which directly translates to increase in the NF. However, this section can be recoated to prevent to improve the performance of the amplifier. Similar to core-pump MEFA, it was demonstrated that amplifier gain profile could be tuned by cascading fibre-elements of cladding-pumped MEFA. It was shown that a broadband amplifier could be developed using cladding-pumped MEFA which would require single pump as opposed to conventional split band amplifier. Such an amplifier could provide relatively flat gain of 22±1.5dB in the wavelength band of 1545-1615nm.

Furthermore, a first SDM amplifier was demonstrated which incorporated two SDM technologies, MEF and FMF, with a spatial multiplicity of 12. An average signal gain of 18.3dB and differential modal gain of ~1-6dB were achieved in the wavelength range of 1542-1560nm. The DMG variation was due to un-optimised RIP of the core of fibre-elements. The DMG is expected to reduce by tailoring the rare-earth doping profiles of the optical fiber. The number of fibre-elements and modes in the amplifier could further be increased to obtain higher spatial multiplicity.

In the MEF for transmission channel, modification in fabrication procedure was

demonstrated to accommodate the stringent demand of a transmission fibre in terms of the loss and mechanical reliability and dual coating system was used. At first, various 3-MEFs with different element-to-element separation was fabricated and characterized. The loss in fibre-elements of non-compact 3-MEF was similar to the single fibre drawn from the same preform, and it was 0.6dB/km. The MEFs in which fibre-elements were not touching each other were shown to have >400kpsi of proof-test strength. The compact MEF showed lower strength and higher losses. It was concluded that the higher strength and lower losses could be maintained in MEFs, provided the fibre-elements does not touch each other. The fabrication procedure was then scaled to 7-MEF.A 7-MEF with fibre-element diameter of 80μm was fabricated using commercial low loss preforms, and it was shown that the low losses could be maintain in MEFs. Moreover, it was shown that the loss in 7-MEF was more tolerant to rewinding tension as compared to an 80μm single fibre. Transmission tests were also performed with passive 3-MEFs. Error-free 1014Gbps data transmission over the lengths of MEF was demonstrated, highlighting the crosstalk-free operation offered. Finally, the first implementation of an amplified MEF-based SDM transmission system including both passive and active SDM components was experimentally demonstrated. The MEF technology showed full compatibility with existing WDM systems and sufficient flexibility to be considered as a contender for the implementation of fully functional SDM systems.

6.2. Future Work

MEF based SDM technology has a great potential towards substantial capacity growth of telecommunication. MEF technology could boost the development of dense cable which is in coherence with the commercial development. In commercial development, efforts are being made to reduce the coating of individual fibres from 250μm to 200μm, and reduce the thickness of the cables. The MEF further allows the sharing of the coating among multiple fibres without compromising the flexibility of current SSMF networks. In MEF, the effect of micro-bending loss can be further depreciated in MEF with fibre-element diameter of 60μm, by keeping the cut-off closer to the wavelength band of operation. The number of fibre-elements can be increased to enhance the spatial channel density. To achieve even higher capacity, several SDM technologies could be implemented simultaneously, thanks to their

compatibility with each other. Apart from improvement in MEF, the next direction in SDM fibres would be incorporate MCF and FMF technologies along with the MEF technology. For example, to achieve a spatial multiplicity of 21 using one of the technology alone would add complexity either in terms of fabrication or operation. However, a 7-MEF with each element containing 3 cores would enable the spatial multiplicity of 21. The same could also be achieved by incorporating 2 mode cores in 7-MEF (3 (LP_{01}, LP_{11a} and LP_{11b}) x7=21).